

Computational Chemistry Study of Solvents for Carbon Dioxide Absorption

Eirik Falck da Silva

Doctoral Thesis

Norwegian University of
Science and Technology

Fakultet for Naturvitenskap og Teknologi
Institutt for Kjemisk Prosessteknologi
Trondheim, August 2005

Contents

List of Papers	5
Abstract	7
Acknowledgements	9
1 Introduction	11
1.1 Purpose.....	11
1.2 Global Warming.....	12
1.3 Mitigation.....	13
1.3.1 Background.....	13
1.3.2 CO ₂ Capture and Storage.....	13
2 CO₂ Absorption	17
2.1 Introduction.....	17
2.2 Solvents.....	19
2.3 Challenges.....	20
2.4 Current Understanding of the CO ₂ Absorption Process.....	21
3 Computational Chemistry	25
3.1 Introduction.....	25
3.2 Quantum Mechanics	26
3.2.1 Introduction.....	26
3.2.2 The Born-Oppenheimer Approximation.....	28
3.2.3 Hartree-Fock Self-Consistent Field Method.....	28
3.2.4 Post-HF Methods	28
3.2.5 Density Functional Theory.....	29
3.2.6 Basis Sets	30
3.2.7 Basis Set Superposition Error	31
3.2.8 Temperature	32
3.2.9 Performance	32
3.3 Molecular Mechanics.....	33
3.3.1 Introduction.....	33
3.3.2 Force Field Parameterization.....	35
3.3.3 Atomic Charges.....	36
3.3.4 Polarizable Force Fields.....	38
3.4 Simulations	39
3.4.1 Introduction.....	39
3.4.2 Free Energy Perturbations.....	41
3.5 QM/MM.....	43
3.6 Computational Chemistry and Experiment.....	43
3.7 Review of Computational Chemistry Work on CO ₂ Absorption.....	45
4 Modeling of Solvation Energy	47
4.1 Introduction.....	47
4.2 The liquid state.....	48

4.3	Statistical Mechanics	49
4.4	Models to Calculate the Free Energy of Solution	52
4.4.1	Introduction.....	52
4.4.2	Equation of State and Lattice Models.....	53
4.4.3	Continuum Models.....	56
4.4.4	Molecular Simulation.....	62
4.4.5	RISM and RISM-SCF	63
4.4.6	Supermolecule Approach.....	64
4.4.7	Hybrids of Computational Chemistry approaches.....	65
4.4.8	Descriptor Models.....	66
4.4.9	Other Models.....	67
4.4.10	Hybridization of Gibbs Energy Models and Computational Chemistry Based Models	68
4.5	Comparison of Methods to Calculate the Free Energy of Solution	69
4.5.1	Methods.....	69
4.5.2	The Basicity	71
4.5.3	Amines	72
4.5.4	Results.....	73
4.5.5	Conclusion	79
5	Reaction Mechanisms and Equilibrium.....	81
5.1	Introduction.....	81
5.2	Reaction Mechanisms	81
5.2.1	Introduction.....	81
5.2.2	Bicarbonate Formation.....	82
5.2.3	Carbamate formation.....	84
5.2.4	Bases	87
5.2.5	Alcohol-Group Bonding to CO ₂	87
5.2.6	Carbamate as Reaction Intermediate.....	88
5.2.7	Molecules with Multiple Amine Functionalities	89
5.2.8	Shuttle Mechanism.....	91
5.2.9	Summary and Conclusion	92
5.3	Determining Equilibrium	94
5.3.1	Equilibrium and Kinetics	94
5.3.2	Temperature Dependency of Equilibrium Constants.....	95
5.3.3	Activity Coefficients.....	96
5.3.4	Process Energy Consumption	97
5.3.5	Summary	98
6	Other Solvent Properties.....	99
6.1	Introduction.....	99
6.2	Solubility in Water	99
6.3	Solvent Degradation.....	100
6.4	Corrosion.....	101

6.5	Foaming	102
6.6	Toxicology	103
6.7	Cost	103
6.8	Precipitations.....	104
7	Present and Potential Solvents.....	105
7.1	Introduction.....	105
7.2	Solvents in Use	105
7.2.1	Ethanolamine	105
7.2.2	Tertiary Amines	106
7.2.3	Sterically Hindered Amines.....	106
7.2.4	Multiple Amine Functionalities	107
7.2.5	Ionic solvents	107
7.2.6	Patented Solvents	107
7.3	Ideal Solvent Properties	108
7.3.1	Equilibrium Constants	108
7.3.2	Other Properties	110
7.4	Comparison with Ethanolamine.....	111
7.5	Conclusion	111
8	Future Work.....	113
8.1	Continuation of the Present Research	113
8.2	Other Applications of Present Work.....	113
8.3	Beyond Amines.....	114
	References.....	115

List of Papers

- I. da Silva, E. F. and Svendsen, H. F. (2003) Prediction of the pK_a Values of Amines Using ab Initio Methods and Free Energy Perturbations *Ind. Eng. Chem. Res.* 42, 4414-4421.
- II. da Silva, E. F. and Svendsen, H. F. (2004) Ab Initio study of the reaction of carbamate formation from CO₂ and alkanolamines *Ind. Eng. Chem. Res.* 43, 3413-3418.
- III. da Silva, E. F. (2004) Use of Free Energy Simulations to predict Infinite Dilution Activity Coefficients *Fluid Phase Eq.* 221, 15-24.
- IV. da Silva, E. F. (2005) Comparison of Quantum Mechanical and Experimental Gas Phase Basicities of Amines *J. Phys. Chem. A* 109, 1603-1607.
- V. da Silva, E. F. and Svendsen, H. F. (2005) Study of the Carbamate Stability of Amines Using ab Initio Methods and Free-Energy Perturbations, Accepted in *Ind. Eng. Chem. Res.*
- VI. da Silva, E. F., Kuznetsova, T. and Kvamme, B. (2005) Molecular Dynamics Study of Ethanolamine as a Pure Liquid and in Aqueous Solution.
- VII. da Silva, E. F., Yamazaki, T. and Hirata, F. (2005) Comparison of Solvation Models in the Calculation of Amine Basicity.

Abstract

Absorption with aqueous amine solvents is at present the most viable technology for CO₂ capture. While this is a proven technology, efforts are ongoing to improve it in order to make it a more attractive technology for large scale use to reduce CO₂ emissions. Finding solvents with better properties is one approach to improving the technology.

In this thesis methods in computational chemistry are used to improve the understanding of the chemistry of CO₂ absorption in amine-water systems. The work is also intended to provide models that can be used to predict the performance of new solvents. Such predictive models are intended to facilitate the screening for new solvents.

The main focus of the computational chemistry work has been to model solvent effects. Most of the work has been based on use of quantum mechanical calculations to determine gas phase properties and different models to determine the solvation energy. Most of the solvation energy calculations have been based on molecular simulations and continuum models. In addition solvation energies calculated with the RISM-SCF model have been studied.

The reaction mechanisms of the process have been studied in detail. Calculations have been used to attempt to resolve uncertainties regarding mechanisms. The work is in most cases in agreement with the consensus in the literature, but it is concluded that carbamate formation is most likely to be a single-step mechanism. From the study of reaction mechanisms it is concluded that the reactivity of an amine solvent with CO₂ is governed by two equilibrium constants: the base stability and carbamate stability.

These two equilibrium constants have been modeled with gas phase quantum mechanical calculations and different solvation models. Comparison with experimental data suggests that both equilibrium constants can be modeled with a

semi-quantitative accuracy. The models are not entirely accurate but do mostly capture trends observed in experimental data.

In addition to the equilibrium constants there are other properties that may affect the overall performance and viability of a solvent in large scale industrial use. These properties are also discussed and the possibility of modeling them is assessed.

The ideal values for the main equilibrium constants are unknown and the present work does therefore not reach any specific conclusions on what the ideal solvent is. This thesis does however offer a fairly detailed plan of how to find optimal solvents and tools to carry out the screening.

Acknowledgements

I would like to express my gratitude to all those people that in different ways have helped me with my work on this doctor thesis.

First of all I would like to thank Professor Hallvard Svendsen for giving me the opportunity to do this work. I am also grateful to him for continuous support, interesting discussions and giving me freedom in choosing how to approach different issues. I would also like to thank people in the Department of Chemical Engineering, in particular in the reactor technology group, for providing a good working environment. Special thank goes to Karl Anders Hoff and Jana Poplsteinova Jakobsen for helping to introduce me to the field of gas processing.

My own work has been based on theory and models not studied in the chemical engineering department. I have therefore often relied on help from researchers at other groups and institutions.

At NTNU I would especially thank Professor Per-Olof Åstrand at the Department of Chemistry for insight and discussions on computational chemistry.

Professor Bjørn Kvamme and Tatyana Kuznetsova at the University of Bergen have been of great help in understanding, and working with, molecular simulation.

Professor Fumio Hirata and Takeshi Yamazaki at the Institute for Molecular Science in Okazaki, Japan, have helped me with use and understanding of RISM models. I am also grateful to Professor Hirata for being a very good host during my visit to the Institute for Molecular Science.

I should also like to thank Professor Bjørn Hafskjold and Yasuo Oishi for first introducing me to computational chemistry.

I am also grateful to numerous reviewers that have often provided constructive criticism of my work.

Finally I would like to express special thanks to Mami, for love and support.

1 Introduction

Considering these and many other major and still growing impacts of human activities on earth and atmosphere, and at all, including global, scales, it seems to us more than appropriate to emphasize the central role of mankind in geology and ecology by proposing to use the term 'anthropocene' for the current geological epoch.

Paul J. Crutzen and Eugene F. Storer

1.1 Purpose

The main aim of my thesis has been to contribute to the selection of optimal solvents for CO₂ capture from exhaust gases. The main tools of the work have been various forms of computational chemistry. Selection of solvents for CO₂ capture is not a simple task. There are a number of properties that contribute to determine if a solvent can be applied economically at an industrial scale. At the same time it is not a priori given what the ideal properties are. Extensive and time-consuming experimental work is also required to draw confident conclusions on the viability of a given solvent. The process of solvent selection or design can perhaps in some ways be compared to the process of drug design.

Computational chemistry has come to play a significant role in drug design, and my ambition with this work has been to apply computational chemistry in a similar fashion in CO₂ capture. This work can not resolve all issues regarding solvent selection, rather it is a part of a larger project where different modeling and experimental tools are applied together. I have attempted to focus my work on the central issues where computational chemistry can contribute the most to the process or solvent selection. Part of the work has gone into making predictions of properties that can be used to find promising solvent molecules. Another part of the

1 Introduction

work has been to contribute to the general understanding of the chemistry of the systems.

This thesis has three main parts. The first chapters deal with the how-and-why of this work. First the issue of global warming and mitigation is briefly presented in the present chapter. An introduction is then given to amine-based CO₂ absorption, the technology which is the topic of the present work. Then computational chemistry is presented, with special attention given to issue of modeling energies in solution.

The second part is a set of chapters drawing conclusions from the present work and looking at remaining issues. At the end is included the papers with the results of research carried out as a part of this thesis. Most of the actual research findings are in the papers.

1.2 Global Warming

The United Nations Panel on Climate Change has concluded that if no steps are taken, human emissions of greenhouse-gases are likely to result in a warming of 1.4 to 5.8 °C over the next 100 years (IPCC 2001a). Human emissions are already believed to be affecting the climate, and to have been the main cause of observed warming during the last century. While it is almost certain that our emissions of greenhouse-gases will result in the planet becoming warmer, the specific consequences for life on our planet are more difficult to predict. It has been observed by some that what we are doing amounts to carrying out a laboratory experiment with our entire planet. Some of the more likely consequences are stronger heat-waves, changing precipitation patterns, disappearing glaciers, loss of biodiversity and rising sea levels (IPCC 2001b). More recent work such as the Arctic Climate Impact Assessment Report (ACIA 2004) strengthens these conclusions.

1.3 Mitigation

1.3.1 Background

The issue of anthropogenic global warming leads us to the question of what, if anything, we can do to combat it. The answer is to reduce our emissions of greenhouse gases. While the answer is simple there is a significant challenge involved in carrying out such reductions. Consumption of fossil fuels is at present a necessity in the industrialized world. Use of fossil fuels inevitably leads to carbon dioxide (CO₂) being formed and CO₂ is the greenhouse gas responsible for most of the anthropogenic global warming (IPCC 2001a). As new countries develop, their consumption of energy and CO₂ emissions are expected to increase.

There are three main alternatives to reducing our CO₂ emissions without hampering economic growth (Haug 2004). One is to use energy more efficiently, thereby reducing the energy consumption. The second option is to change to consumption of renewable energy sources and the final option is to burn fossil fuels while capturing and storing the CO₂ instead of releasing it unto the atmosphere. None of these options are by themselves likely to be enough to stabilize our emissions of CO₂ and the viable way forward is therefore likely to be a combination of these approaches (IPCC 2001c, Herzog et al. 2000 and Kuuskra et al. 2004). The option of burning fossil fuels while storing the CO₂ instead of releasing it unto the atmosphere is referred to as “CO₂ capture and storage”, “Carbon capture and storage” or “CO₂ sequestration”.

1.3.2 CO₂ Capture and Storage

Combustion of fossil fuels takes place as a set of reactions between oxygen and hydrocarbons with CO₂ as one of the products. Usually the reaction is carried out, not with pure oxygen, but with air as a reactant. The exhaust gas that is produced resembles air but with a higher concentration of CO₂. The total amount of exhaust

1 Introduction

gas produced is very large and to store all of it is not an option (Thambimuthu and Davidson 2004). The CO_2 must therefore be separated from the other exhaust gas components. Once the CO_2 has been isolated it can be transported and stored. The main option for storage being explored at present is geological storage, i.e. to pump the CO_2 in to geological formations below the earth's surface (Hepple and Benson 2005). The most demanding part of this approach is the capture, how to separate the CO_2 from other exhaust gas components. Other aspects such as compression of the gas and transport do however also contribute to the overall cost.

There are a number of technologies available for capturing CO_2 . The technologies vary in complexity, degree of maturity and cost. The technologies can be separated into different categories (Thambimuthu and Davidson 2004 and Bolland 2004), a overview is given in Figure 1.1.

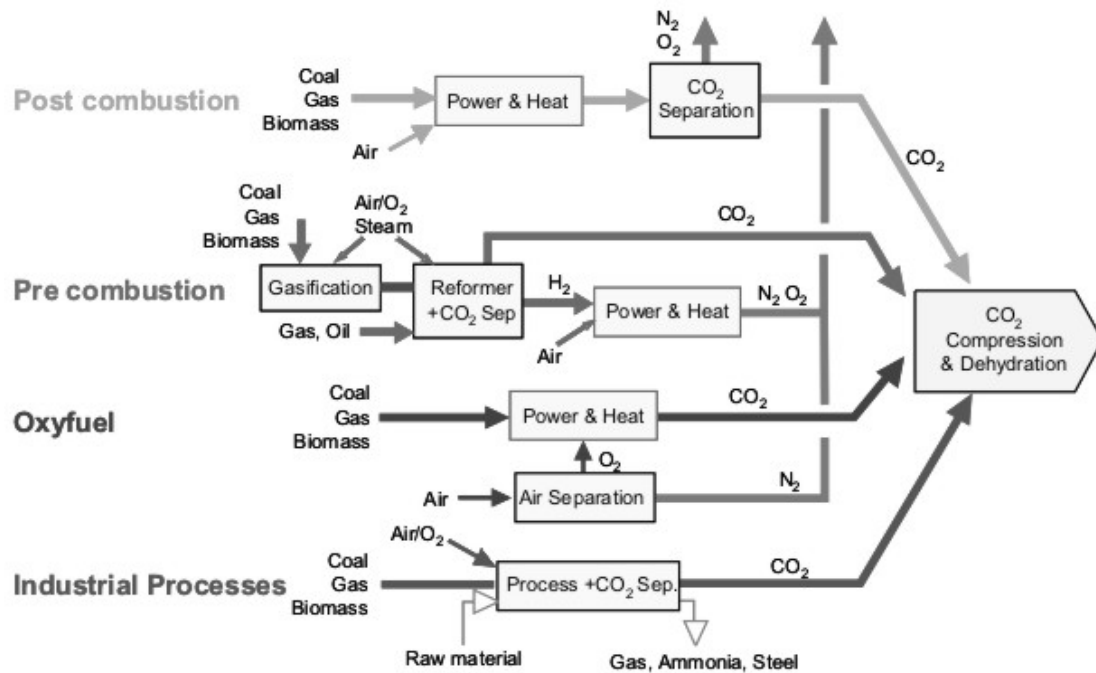


Figure 1.1 Technologies for CO_2 capture (Bolland 2004).

1 Introduction

Technologies based on capturing the CO₂ from the exhaust gas are referred to as post-combustion technologies. Technologies based on using pure oxygen as a fuel are called oxyfuel processes. Finally there are technologies based on converting hydrocarbons to hydrogen and CO₂. This approach is called pre-combustion. Another classification of separation technologies is presented in Figure 1.2.

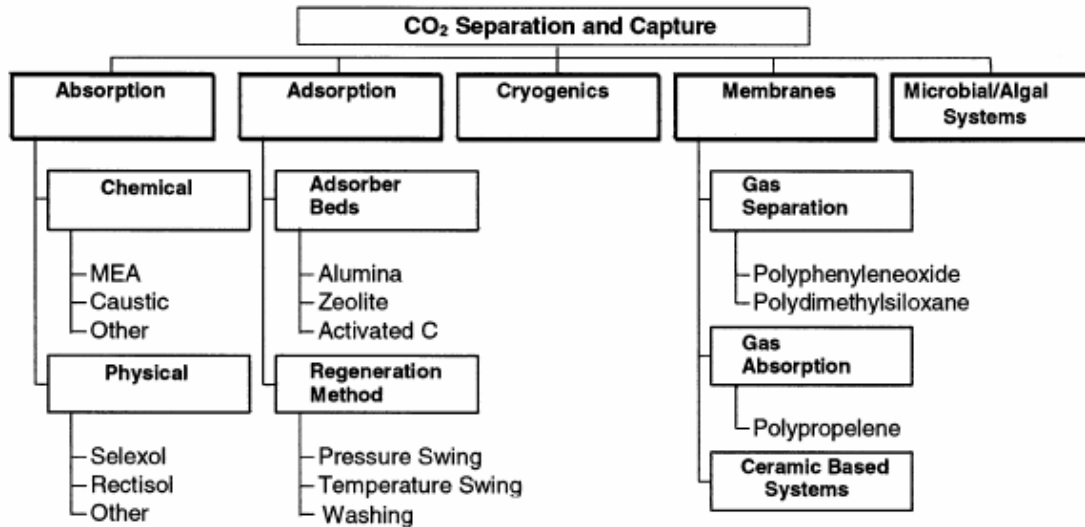


Figure 1.2 Technologies for CO₂ capture (Rao and Rubin 2002).

The present thesis deals with chemical absorption of CO₂, this technology is today the most important post-combustion CO₂ capture technology. Of all the available CO₂ capture technologies this also represents at present the most efficient technology for capturing CO₂. This in part reflects technological maturity, the technology having been patented for natural gas sweetening as early as 1930 (Kohl and Nielsen 1997). It has also been used in small-scale removal of CO₂ from exhaust gas (Reddy et al. 2003 and Yagi et al. 2004). Chemical absorption is also a technology that can be fairly easily installed. Existing power-plants can be retrofitted with equipment for chemical absorption (Thambimuthu and Davidson 2004); whereas many other technologies involve new forms of power plant technology. Research is being carried out to improve the different technologies,

1 Introduction

and improvements are likely to change the relative performance of different technologies. Recent investigations (Kvamsdal et al. 2004 and de Koeijer 2004) have however suggested that chemical absorption of CO₂ is likely to remain a highly competitive technology for CO₂ capture in the future.

2 CO₂ Absorption

We've learned from experience that the truth will come out. Other experimenters will repeat your experiment and find out whether you were wrong or right. Nature's phenomena will agree or they'll disagree with your theory. And, although you may gain some temporary fame and excitement, you will not gain a good reputation as a scientist if you haven't tried to be very careful in this kind of work.

Richard P. Feynman

2.1 Introduction

In the present chapter a general presentation will be made of the CO₂ capture technology and the nature of available experimental data for the process will be summarized. Where nothing else is indicated the material is drawn from the textbook “Gas Purification” (Kohl and Nielsen 1997). Figure 2.1 illustrates the apparatus commonly used for CO₂ capture.

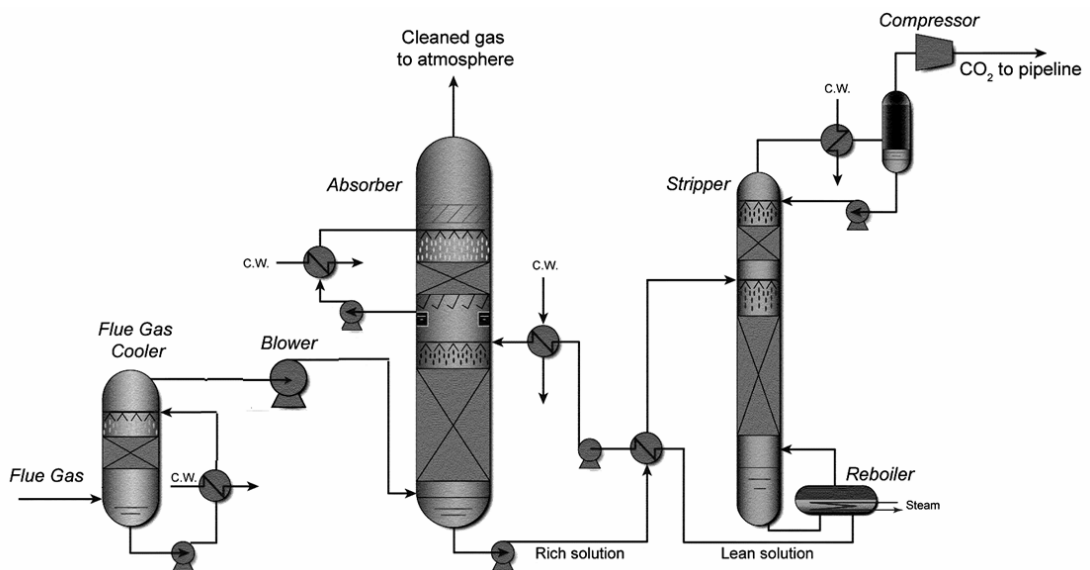


Figure 2.1 CO₂ Absorber columns.

2 CO₂ Absorption

A cooled exhaust gas is led into the bottom of the absorber column. The gas rises through the column meeting a counter-current liquid stream. The CO₂ absorbs and reacts with components in the liquid, and the gas stream gradually loses its CO₂ while moving up the column.

At the top the gas with low CO₂ content is released into the atmosphere. The CO₂ content of the liquid increases as the liquid moves down the column. The liquid stream is typically at 90-95% of equilibrium with incoming exhaust gas at the column bottom. At the bottom the liquid is taken out and is pumped to the top of a second column, the stripper (also called desorber). In the stripper the temperature and/or pressure are set so that the chemical equilibrium in the liquid are reversed and the CO₂ is released into the gas phase. Pressure release is very common in natural gas applications whereas changing the temperature is the most common approach for exhaust gas treatment. Change in temperature is usually achieved by adding heat as steam in the reboiler below the stripper column. A gas phase consisting only of CO₂ and steam is taken out at the top of the column. The steam is separated from CO₂ in the overhead condenser and the CO₂ can be compressed and sent to storage. The liquid at the bottom of the stripper column will have a low concentration of CO₂; and is again ready to be used for CO₂ absorption. It is sent back to the top of the absorber column. The liquid keeps circulating between absorber and stripping column, transporting the CO₂ between the columns. In an industrial process the absorber will often be operated at temperatures around 40-55 °C while the stripper will be operating at around 120 °C.

Exhaust gas pressure is usually much lower than encountered in natural gas processing. The Sleipner natural gas sweetening process is for example operated at a 100 bar (de Koeijer and Solbraa 2004) while exhaust gas is usually at atmospheric pressure. This means that while the technology for CO₂ removal from natural gas removal can be applied for exhaust gas treatment, optimal operating conditions and solvents are quite different.

2 CO₂ Absorption

The concentration of CO₂ in the exhaust gases will vary with the nature of the fossil fuel used. Typically a coal fired power station will have an exhaust containing 10-12 volume percent CO₂ (Rao and Rubin 2001), whereas a natural gas fired power station can produce an exhaust gas with a CO₂ concentration as low as 3 volume percent (Reddy et al. 2003). This means that even for different exhaust gases optimal process settings may vary.

2.2 Solvents

There are a number of different solvents that are, and have been, applied in CO₂ absorption. Most solvents are mixtures of water and base molecules. The bases can either be organic or inorganic compounds. Almost all organic bases are amine molecules, and such amine solvents are the topic of the present thesis.

The standard amine solvent for exhaust gases is ethanolamine; this molecule is shown in the Figure 2.2. Most of the other common solvents are also alkanolamines, i.e. molecules with both amino and hydroxyl functional groups. Different amines vary significantly in how they react with CO₂. Ethanolamine is a particularly important solvent because it is the most widely used at present, and it represents the benchmark that new solvents will be compared with. Amines can be classified into different groups depending on the number of carbon atoms directly bonding to the nitrogen atom; there are primary, secondary and tertiary amines. Tertiary amines differ from the others in how they can react with CO₂. I will return to the various amines and reaction mechanisms in later chapters.

2 CO₂ Absorption

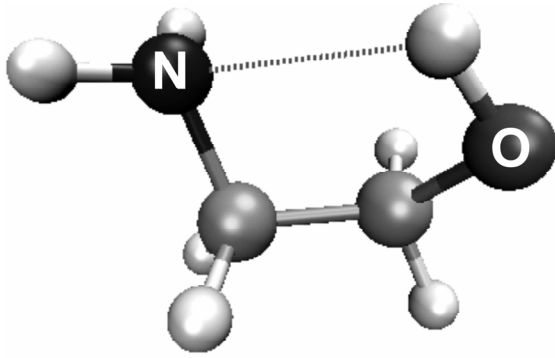


Figure 2.2 Ethanolamine.

In addition to solvents that react chemically with CO₂ there are other solvents that have a capacity to absorb CO₂ without reacting, these are called physical solvents. There is to my knowledge no physical solvent that is being considered for the treatment of exhaust gases and chemical absorption is believed to be the viable option. Solvents with some degree of both chemical and physical absorption might however be an interesting option. An example of a physical solvent that can be applied in such a way is Sulfolane (Jenab et al. 2005).

2.3 Challenges

The CO₂ absorption process is an established and proven technology, the overall challenge is to bring the costs down to the point where it becomes an attractive option in mitigation of global warming. The cost of the process stems from several components. There is the cost of building the plant and purchasing the solvents. There are also the operational costs, in particular the energy required to run the process. Thermal energy is required to heat the solvent entering the stripper, to generate the heat required to release the CO₂ and to generate steam for dilution in the stripper (Erga, Juliussen and Lidal 1995). In addition electric energy is required for blowing the exhaust gas through the absorber and for solvent pumping.

One approach to making the process more efficient is to find solvents with more favorable characteristics than the ones presently in use. This is the topic of the

2 CO₂ Absorption

present thesis. The performance of the process can also be improved in other ways; a better design can be proposed or the conditions under which the process is run may be optimized.

There are other solvent properties besides the reactivity towards CO₂ that are of importance for the overall economy of the process. The solvent may be corrosive, and the effect on the equipment must be considered. The solvent can also degrade over time as a consequence of undesired reactions taking place. If the solvent has a high vapor-pressure it will also evaporate in the absorber and in the stripper. Water washes are for this reason mounted on the absorber and stripper to recover the solvent. A recent study has suggested that the water wash operation significantly affects the overall system performance (Tobiesen, Svendsen and Hoff 2005). The cost of producing the solvent is also a factor to be considered, particularly if the solvent has a high degradation rate and must be replaced often. It is also of great importance that a solvent to be utilized in large quantities in an industrial process is not toxic. I will return to the various solvent characteristics in a later chapter.

2.4 Current Understanding of the CO₂ Absorption Process

The foundation for my work lies in the current level of understanding of the CO₂ absorption process. The nature, quality and quantity of experimental data available is therefore of importance. I have already noted that the CO₂ absorption technology is quite mature, it does however not necessarily follow that the process is well understood. A lot of experimental work has been published on various aspects of the absorption process. Here I will briefly go through the nature of published data.

A number of studies deal with the gas-liquid equilibrium of CO₂-amine-water systems. In such equilibrium experiments the system pressure and temperature is set. The CO₂ partial pressure and CO₂ concentration in the liquid is then

2 CO₂ Absorption

determined. Results from such experiments can be used to generate plots as the one shown in Figure 2.3.

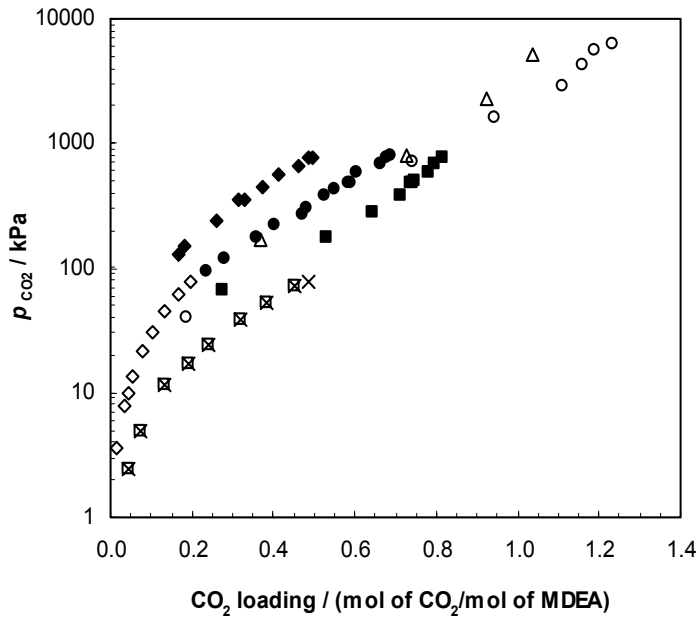


Figure 2.3 Plot from Ma'mun, Nilsen and Svendsen (2005).

Another important form of experiment is study of the kinetics. The experimental setup for kinetics studies varies significantly but the general approach is to measure the rate of CO₂ uptake in the liquid at a given set of conditions. The conditions set are usually temperature, pressure and liquid composition. Versteeg et al. (1996) provide a fairly comprehensive review of kinetic data. The CO₂ uptake does not necessarily reflect a single rate of reaction and some analysis work is usually required to extract reaction kinetics data from the experimental results.

Calorimetric experiments can be used to obtain information on the enthalpy of CO₂ absorption. An example is the work by Oscarson et al. (1989). They report enthalpy data based on such calorimetric measurements for the CO₂-aqueous diethanolamine system. The same kind of measurements can also be used to determine heat capacities.

2 CO₂ Absorption

Physical properties such as density, boiling point and viscosity have also been measured for many pure amines and amine-water systems. The extent of such data is however more limited than for common organic molecules.

The types of experiment described so far do not give much direct insight into the composition of the liquid phase. In recent years some effort has however gone into experimental work that can provide such information about the nature and composition of the liquid. Most important is the use of NMR-measurements (Bishnoi 2000 and Poplsteinova 2004). NMR-data can provide information on the presence and concentration of various species. From such measurements more robust and quantitative conclusions can be drawn on the liquid composition. Such experiments do however also have their limitations. There can be difficulties in precisely measuring concentrations, protonation equilibria are difficult to study and measurement at higher temperatures is difficult.

A lot of the experimental work is done as part of the development of modelling tools. Models are constructed to predict the overall performance of the CO₂ absorption process. The work of Hoff (2004) is an example of such model development. Such models are based on fitting parameters to experimental data for a given system and their applicability for conditions beyond those at which they were fitted can be uncertain.

The main aspects of the absorption process are at present fairly well understood. The species formed are known and the reactions taking place are fairly well understood. Equilibrium and kinetic constants are however not that well established. The liquid consists of a significant number of components in equilibrium. Determining the relative concentrations of species in the liquid only from knowledge of amine concentration and CO₂ uptake is clearly not an easy task. The equilibria and thermodynamics of these systems are for this reason to some extent uncertain.

2 CO₂ Absorption

Most of the experimental work reported in the open literature has been carried out in the context of direct application to process-development and process-modelling. There is much less published work dedicated to studying the systems in terms of chemistry and physical chemistry. Data on liquid structure and molecular structure is for example very sparse. This means that there is little experimental data that can be used directly in the validation or parameterization of molecular level models such as the ones used in the present work.

3 Computational Chemistry

The underlying physical laws necessary for the mathematical theory of a large part of physics and the whole of chemistry are thus completely known, and the difficulty is only that exact application of these laws leads to equations much too complicated to be soluble.

Paul A. M. Dirac (1929)

3.1 Introduction

The present chapter will be devoted to introducing computational chemistry and its various branches. Computational chemistry can perhaps be loosely defined as chemistry modeling based on a molecular or atomic level description. The term covers a fairly broad range of theories and methods.

The various methods of computational chemistry can be thought of as offering a toolbox. For different problems studied choices must be made as to what methods are best suited. In the present work several different issues related to CO₂ absorption are studied. In studying these problems an eclectic approach has been chosen; namely to attempt to find the method best suited to each problem.

As a result a fairly large number of methods have been employed. And these methods again draw on different fields of theory. No attempt will be made to cover the underlying theory in any detail here. The present chapter will rather focus on introducing the various branches of computational chemistry in general terms. The introduction is intended to give general insight into the various methods, in particular their strengths, weaknesses and limitations. In addition the terminology to be used in the following chapters and papers will be introduced.

The chapter will be divided into two parts, first a brief presentation of the main elements of computational chemistry will be made. This presentation will follow the outline used by Grant and Richards (1995) in their textbook “Computational

Chemistry”. In the second part a discussion will be made on the general issue of the application of computational chemistry. The issue of modeling of chemistry in solution will be discussed in the next chapter. Where nothing else is indicated the material in this chapter is drawn from Grant and Richards (1995) and the textbook “Essentials of Computational Chemistry” by Cramer (2002).

3.2 Quantum Mechanics

3.2.1 Introduction

The claim made by Dirac regarding the laws of chemistry and physics (quoted in the beginning of this chapter) referred mainly to the postulation of the Schrödinger equation. In its barest, and most innocent, form it can be written as:

$$H\psi = E\psi \quad (3.1)$$

H is the shorthand form of the Hamilton operator which takes into account the contributions to the energy of the system. E is the energy of the system and ψ is the wave function. The energy has only certain allowed values, with a corresponding wave function for each allowed energy level.

The Hamiltonian consists of the potential and kinetic energy contributions. In the absence of external magnetic and electrical fields and ignoring relativistic effects it takes the following form:

$$H = -\sum_i \frac{\hbar^2}{2m_e} \nabla_i^2 - \sum_k \frac{\hbar^2}{2m_k} \nabla_k^2 - \sum_i \sum_k \frac{e^2 Z_k}{r_{ij}} + \sum_{i<j} \frac{e^2}{r_{ij}} + \sum_{k<l} \frac{e^2 Z_k Z_l}{r_{kl}} \quad (3.2)$$

where i and j run over electrons, k and l run over nuclei, \hbar is the Planck’s constant divided by 2π , m_e is the mass of the electron, m_k is the mass of the nucleus k . ∇^2 is the Laplacian operator, e is the charge on the electron, Z is an atomic number and r_{ab} is the distance between particles a and b . From the Hamiltonian it can be seen that the Schrödinger equation is a set of differential equations.

3 Computational Chemistry

For the wave function itself it is difficult to give a simple definition or direct physical interpretation. The product of the wave function with its complex conjugate $|\psi^* \psi|$ does however have a physical interpretation; it gives the probability density for the system. For an electron $|\psi^* \psi|$ multiplied with a volume element would give the probability of the electron being in that volume element. The normalized integral of $|\psi|^2$ over all space must be unity. The wave function can therefore be thought of as a kind of road-map to how the electrons are localized.

There is no way to directly derive the wave function itself, but there are some conditions it must meet. It must be “well-behaved”, displaying only smooth changes and going to zero at infinity. The variational principle states that the lower the ground state energy calculated by a wave function is, the higher is the quality of the wave function.

Assuming that each electron can be treated separately one can operate with one-electron wave functions also called orbitals. In a system with more than one atom, i. e. a molecule, we deal with molecular orbitals.

All electrons are characterized by a spin quantum number, with two possible eigenvalues. The Pauli principle states that two electrons can not have the same quantum numbers. One molecular orbital is therefore limited to two electrons with opposite spin.

The Schrödinger equation is a postulate, believed to be entirely accurate. The complexity of it is however such that the largest system for which it is analytically solvable is the hydrogen atom. It was this state of affairs that led Dirac to make his observation.

Since Dirac made his observation a lot of work has gone into making approximations that make it possible to make calculations on systems of practical interest. Some of the main approximations will be briefly outlined here.

3 Computational Chemistry

3.2.2 The Born-Oppenheimer Approximation

The atoms in a system are much heavier and move much more slowly than the electrons. It is therefore assumed that the movements can be decoupled. The energy of the electrons is calculated with the atoms in fixed positions. This approximation is in most cases entirely reasonable and universally applied.

3.2.3 Hartree-Fock Self-Consistent Field Method

Much of the difficulty of solving the Schrödinger equation stems from the need to simultaneously determine the energy of each electron in the presence all other electrons. In the Hartree-Fock (HF) method this is avoided by calculating the energy of each electron in the averaged static field of the others. Initially a guess is made of the electron energies. The energy of each electron is then calculated in the field of the initial electron configuration. This procedure is repeated in an iterative loop until convergence (Self-Consistent referring to this iterative calculation).

The Hartree-Fock method can therefore be thought of as a kind of mean-spherical approximation at the electron level. The difference between the Hartree-Fock energy and the energy for the full Schrödinger equation is called the correlation energy. Hartree-Fock calculations are sufficiently accurate to provide insight into many problems and they are widely used. As Hartree-Fock calculations have been applied to different problems it has however become increasingly clear that the correlation energy is of great significance in determining the properties of a system. Efforts have therefore been made to improve on the Hartree-Fock energy.

3.2.4 Post-HF Methods

There a number of different methods that go beyond Hartree-Fock calculations, one of the widely used approaches is perturbation theory. In perturbation theory the Hartree-Fock solution is treated as the first term in a Taylor series. The

3 Computational Chemistry

perturbation terms added involve the electron repulsion. One of the more common forms was developed by Møller and Plesset. The second order perturbation form is referred to as MP2. This form will be utilized in the present work.

It should be noted that the electron-electron repulsion energy is not necessarily a small perturbation. In cases in which this term is large the application of perturbation theory can become more difficult.

There are a number of other techniques to include electron correlation that can potentially provide very accurate results, such calculations can however become very time consuming and at present they tend to be used for small molecules with maybe 3-4 heavy (non-hydrogen) atoms. The molecules studied in the present work are somewhat larger and the decision has been made not to use such time-consuming methods.

3.2.5 Density Functional Theory

Density Functional Theory (DFT) is based on determining the electron density rather than the wave function. The electron density unlike the wave function is a physically observable quantity. It has been proven that given the electron density the Hamiltonian operator is also determined. A variational principle has also been established for DFT. Unlike HF theory DFT in itself contains no approximations. There is however no way to derive an energy contribution in DFT known as the exchange-correlation energy. The quality of the models is usually determined by some form of comparison with experimental data. DFT models are therefore in a sense semi-empirical models and once assumptions about the exchange-correlation energy are introduced (as they must be) there is no variational principle. This means that for DFT, unlike HF and post-HF methods, there is no a priori way to establish how good a given method is and no systematic way to improve upon it. This state of affairs led many researchers to look at DFT with skepticism. It has

3 Computational Chemistry

however become clear that DFT methods often produce results of comparable quality to much more expensive post-HF methods. It has also become fairly well established for what type of molecules and properties DFT methods are reliable. One of the most common DFT methods is the so-called B3LYP method, which is a form of hybrid between DFT and HF methods. It is considered to be fairly robust, perhaps because it balances some of the weaknesses of DFT and HF methods. B3LYP is the DFT method that will be used in the present work.

3.2.6 Basis Sets

HF and Perturbation Theory have taken us from the Schrödinger equation to a solvable set of equations (DFT offering an alternative route). In order to carry out calculations a representation of the wave function is also needed. Each molecular orbital is constructed from linear combinations of basis functions.

For computational reasons gaussian type orbitals (e^{-r^2}) are commonly used. Gaussian type orbitals do however not have the correct shape required to reproduce the form of a electron distribution. Orbitals are therefore usually constructed as combinations of a set of gaussians in order to reproduce the correct shape.

Basis-sets must be sufficiently flexible to allow the description of electron distribution in various forms of molecules and the quality of the results obtained do in general improve with increasing size and flexibility of the functions employed. On the other hand calculations will also become more time consuming with increasing basis set size. One of the common approaches is to add more basis sets for the valence electrons compared to inner orbitals.

In the present work the common 3-21G, 6-31G and 6-311G basis sets will be utilized. 3-21G indicates a single basis set consisting of 3 gaussian functions for inner electrons and two separate basisfunctions, one consisting of 2 gaussians functions and the other 1 gaussian function for valence electrons. In 6-31G the

3 Computational Chemistry

number of gaussian functions to represent the basis sets is increased and in 6-311G the number of separate basis functions for valence electrons is also increased.

It is common to add further sets of basis functions. One approach is to add higher level orbitals to electrons at a given level, one may for example add d-orbitals to electrons in a p-orbital and p-orbitals to electrons occupying s-orbitals. Such orbitals are called polarizable orbitals and the inclusion of such d-orbitals will in the present work be indicated with a (d) and p-orbitals with (p). It is common to indicate the use of polarizable orbitals with a (x,y) notation, where x is the number of polarizable orbitals on heavy (non-hydrogen) atoms and y indicates the polarizable functions on the hydrogen atoms. Another notation that is sometimes used is to indicate (d) polarization with a “*” and (d,p) polarization with “**”. This notation is utilized in one of the papers in the present work.

Finally there is in some cases a special need to allow electrons to localize far from the atom center. Standard basis-sets are in such cases augmented with so-called diffuse basis sets. In the present work such diffuse basis-sets on heavy (non-hydrogen) atoms are indicated with a “+”, if they are also included on hydrogen atoms it is indicated with “++”. One of the circumstances in which such diffuse basis sets are required is in the accurate modeling of hydrogen bonds.

Some basis-sets are regarded as being better than others in providing quality results for a given amount of computation time. Some basis sets have therefore become standard for calculations. In the present work all calculations will be done with such widely used basis-sets.

3.2.7 Basis Set Superposition Error

When atoms interact the basis sets allocated to each of them will overlap. This overlapping gives electrons greater freedom to localize and can result in a reduction of the energy. This reduction in energy would however not have occurred

3 Computational Chemistry

if the basis sets had been infinitely large. This energy reduction is therefore an artifact of working with limited basis sets. This is called the basis set superposition error (BSSE).

For atoms on different molecules there are schemes to correct for the BSSE. Most common is the so-called Counterpoise correction. For interactions within the same molecule application of such corrections is however more difficult (Reiling et al. 1996 and Lii et al. 1999). This is of importance in the present work because many alkanolamine molecules display intramolecular hydrogen bonding. The BSSE is expected to become smaller with increasing basis set and in calculating intramolecular hydrogen bonds it would therefore seem that larger basis sets are more reliable. In the present work the general approach will therefore be to use large basis-sets in order to obtain more accurate results.

3.2.8 Temperature

Standard quantum mechanical calculations are usually carried out on a single or small number of molecules at 0 K, and without accounting for the zero-point energy. The intramolecular effects of temperature are usually calculated by using the harmonic oscillator approximation. This relies on calculating the second derivative of the energy with respect to the displacement (r).

It should be noted that because quantum mechanical calculations are usually carried out on very small number of molecules in vacuum, pressure effects are not accounted for.

3.2.9 Performance

The quantum mechanics based methods are often referred to as *ab initio* methods, as none of the methods rely on parameterization to experimental data. This is an important point because it distinguishes quantum mechanical calculations from many other forms of modeling carried out in science. The development of such

3 Computational Chemistry

calculations has however not taken place without experimental input (this being particularly true for DFT methods). Comparison with experimental data is used to validate the calculations. Sometimes comparisons with experiment have shown methods to be less reliable than expected, while others have proven more reliable. This partly happens because there can occur various forms of fortuitous cancellation of errors.

It has already been noted that quantum mechanical calculations can be time-consuming. Some of the calculations in the present work took 2-4 days of CPU time.

Quantum mechanical calculations can today be carried out for systems of up to maybe a 100 atoms. The calculation time can increase quite steeply when increasing the size of the basis set or using more advanced methods.

In the present work quantum mechanical calculations will mainly be used to calculate geometries and energies of molecules.

For geometry optimization most quantum mechanical methods are fairly reliable. High level calculations are of quality comparable to experimental data, HF calculations with smaller basis sets also tend to be reasonably accurate.

Calculation of energy is in general more difficult. Results can vary quite significantly with the level of theory. Prediction of absolute energy values are difficult, but relative trends in energies can usually be calculated with reasonable accuracy.

3.3 *Molecular Mechanics*

3.3.1 Introduction

Quantum mechanical calculations are, as have already been mentioned, time-consuming. Molecular Mechanics (MM) offer a simplified form of molecular representation that makes it possible to perform significantly faster calculations.

3 Computational Chemistry

A molecular mechanics representation can best be summarized as soft spheres attached by springs to represent bonds. The potential energy between non-bonded atoms is usually expressed as the sum of Lennard-Jones and Coulomb potential functions:

$$U = \sum_{i<j} 4\varepsilon_{ij} \left[\left(\frac{\sigma_{ij}}{r_{ij}} \right)^{12} - \left(\frac{\sigma_{ij}}{r_{ij}} \right)^6 \right] + \sum_{i<j} \frac{q_i q_j}{r_{ij}} \quad (3.3)$$

where the sums are over all pairs of interaction sites and ε and σ are the Lennard-Jones potential parameters, q_i is the partial electric charge of interaction site i and r_{ij} is the separation between interaction sites. Interaction sites are usually, but not always, atomic centers. This form of representation only accounts for two-body interactions. In a real system many-body effects, such as three-body and four-body interactions, can also play a part. There is therefore an approximation involved in the form of such potential functions. To correct for this, parameters can be set to implicitly account for the many-body effects.

For bond-lengths simple harmonic stretching functions are often used where the energy increases as the bond-length deviates from some equilibrium bond-length. For bond angles harmonic functions of the following form are often utilized:

$$U(\theta) = k_\theta (\theta - \theta_0)^2 \quad (3.4)$$

where θ is the bond angle and the subscript 0 denotes the equilibrium value. k_θ is the spring constant. Dihedral angle energies around bonds are given by some form a fourier series. One of the common forms is the following:

$$U(\phi) = \sum_{i=1}^5 C_i \cos(\phi)^i \quad (3.5)$$

where ϕ is the dihedral angle and the C_i are constants.

3 Computational Chemistry

3.3.2 Force Field Parameterization

The quality of the results produced by MM calculations obviously depends on the parameters chosen for the various interactions and some form of parameterization must be undertaken. A set of parameters for a single molecule or groups of molecules are called force fields.

A fairly large number of schemes have been proposed to develop force fields, partly reflecting the fact that different researchers are looking at different applications. One of the main applications is biological systems, in which case the focus is often on reproducing the structural characteristics of molecules of biological importance. A second application is the modeling of liquids.

In the modeling of liquids, parameters are often chosen to reproduce the properties of liquids as determined from experimental work. There is however a number of different properties one can choose to reproduce. Among them are density, diffusion rates, dielectric constants and radial distribution functions. An example of such work is the “Optimized Parameters for Liquid Simulations” (OPLS) force field developed by Jorgensen and coworkers (Jorgensen et al. 1996 and Rizzo and Jorgensen 1999). In addition there is the choice of attempting to reproduce the properties for a given temperature, or to attempt the more ambitious task of reproducing properties over a range of temperatures as done by Walser et al. (2000). For some solvents such as water, a fairly large body of experimental data is available. In other cases, such as for the amines of interest in the present study, experimental data is however more sparse.

For a solvent such as water there exist a remarkably large number of force fields (Guillot 2002). This confronts the practitioner with some difficult choices when selecting force fields for a specific problem. It would seem that some work remains on determining which force fields are more reliably for specific tasks, and if any can be regarded as “better” in a general sense.

3 Computational Chemistry

Quantum mechanical calculations are often used for setting force field parameters. They can for example be used for determining molecular geometries and atomic charges.

3.3.3 Atomic Charges

One of the most important and difficult issues in the design of a force field is the selection of charges. In most common force fields fixed charges are used and they are often, but not always, located at the atom centers. These atomic charges are intended to reproduce the net effect of electrons and nuclei for a given atom. As electrons are not located at a single point operating with charges situated at the atomic centers does represent an approximation. Operating with fixed charges is also an approximation, as the location of electrons can be effected by the environment the molecule finds itself in.

Two main approaches to determining atomic charges can be identified in the literature. One approach is to fit the charges in simulations intended to reproduce various experimental properties. Such fitting is usually done for small organic molecules. For larger molecules experimental data is often more sparse and the number of charges to fit is much larger. In such cases one will often rely on atomic charges being transferable parameters. Having determined charges for alcohol-groups, amine-groups and alkane-groups in small molecules one assumes these to be the same in larger molecules. The OPLS force field is based on this approach (Jorgensen et al. 1996). The second approach is to determine the atomic charges from quantum mechanical calculations, an example of this is the work by Kollman and coworkers (Cornell et al. 1995). This second approach is very appealing because it reduces the need for experimental data and gives the modeling a stronger predictive character (provided it works).

3 Computational Chemistry

Even if a quantum mechanical calculation contains information about position of nucleus and electrons, the task of determining atomic charges is still a difficult one. Atomic charges are not uniquely defined and the task of assigning parts of the electron distribution to atoms in a molecule is ambiguous. The first such scheme was the Mullikan population, which is based on determining how much each atomic basis set contribute to the wave function. While Mullikan populations have been widely used, they have come to be regarded as unreliable (Franckl and Chirlian 2000). One of the newer schemes is to reproduce the electrostatic potential around the solute, even for this approach there are however a number of different implementations (Franckl and Chirlian 2000). Singh and Kollmann (1984) developed a procedure based on reproducing the electrostatic potential on gridpoints distributed spherically around each solute atom center, outside the van der Waals volume of the solute. This type of charges will be utilized in the present work, these will be referred to by their common acronym “MK”. It has become clear that the calculated charges are sensitive to the specific procedure chosen to fit the electrostatic potential (Franckl and Chirlian 2000). Other difficulties are that such procedures tend to work poorly for atoms buried inside a molecule and that charges can display a high degree of conformer dependency (Bayly et al. 1993).

There are also schemes that attempt to use the quantum mechanical representation while at the same time reproducing some experimentally measured property. One such hybrid scheme is CM2 charges (Li, Zhu, Cramer and Truhlar 1998) that reproduces experimental dipole moments. This type of charges will also be used in the present work.

While selection of atomic charges is a difficult issue, it should also be noted that in many contexts different force fields produce quite similar results. In such cases one does not have to worry too much about the selection of charges. In general different schemes to calculate atomic charges do also produce charges that are in reasonable qualitative agreement (da Silva, Yamazaki and Hirata 2005).

3 Computational Chemistry

3.3.4 Polarizable Force Fields

One of the most important approximations in standard simulations with molecular mechanics representation is the use of fixed charges. Introduction of polarizability is one way to improve the representation while avoiding the expense of quantum mechanical calculations. Such models were recently reviewed by Rick and Stuart (2002). There are some main approaches to adding polarization in simulations. Among them are shell models based on polarizable point dipoles, where fixed charges are attached to each other with harmonic springs. Another form of model is based on charges being allowed to fluctuate between sites in a molecule.

The charges in a molecule do depend on the surrounding environment. It is therefore to be expected that a model with fixed charges will have problems representing a molecule in different states such as solids, liquids and gases. Polarizable models should have the potential to represent a molecule in different states. Another difficulty with fixed charges is that they can not reflect changes in charge distribution that may take place as a molecule changes conformer. This is again something that a polarizable model has the potential to handle. On the other hand simulations with polarizable models do take longer time than simulation with fixed charges.

Rick and Stuart (2002) conclude that polarizable models in several respects do perform better than models with fixed charges. Compared to a model with fixed charges there is however a greater number of parameters to be set in a polarizable model and this does offer some added challenges.

While a polarizable model is in form more realistic than a model with fixed charges, it is not given that it will produce more realistic results. In using a ball-and-stick representation of molecules there is a number of assumptions involved, and in it is not given that overall performance will improve by improving on one of the approximations.

3 Computational Chemistry

In the present work simulations with polarizable molecular representations are not used. Mainly because I feel that such advanced and time-consuming modeling should only be utilized when simpler fixed charge models are shown to be inadequate. Such forms of models should however be considered if fixed charge models are found wanting in a given context.

3.4 Simulations

3.4.1 Introduction

There are two forms of simulations that are used in computational chemistry: Molecular Dynamics (MD) and Monte Carlo (MC). These are used for calculations of ensembles of molecules. Simulation techniques are described in detail in the textbooks “Computer Simulations of Liquids” (Allen and Tildesley 1987) and “Understanding molecular simulation” (Frenkel and Smit 2002).

Molecular Dynamics calculations are based on calculating the forces between molecules and atoms in a system and allowing them to move according to Newtons laws of motion. From the calculated forces the acceleration and velocity of the particles in the system are calculated. The particles are moved over a small time-step, forces and velocities are recalculated and the system is moved forward a new time-step. For each time-step the properties of the system such as energy and temperature are monitored. A simulation is carried out for whatever number of time-steps is deemed necessary to obtain reliable averages.

Monte Carlo simulations are on the other hand based on random alterations of the coordinates of the system. The energy change for each alteration is calculated, the probability of the alteration being accepted depending on the associated change in energy. For changes leading to lower energy the probability is higher. The standard approach is Metropolis sampling in which the sampling has a Boltzmann-weighted

3 Computational Chemistry

probability. As in MD the simulation is continued for whatever number of steps deemed necessary for sampling.

Often in simulations the purpose is to simulate the bulk behavior of liquids. Simply placing a number of molecules in a vacuum would produce a cluster that might have properties different from bulk liquid. It is therefore customary both in MD and MC to do calculations with periodic boundary conditions. The cell containing the ensemble is then surrounded by replicas of itself.

Simulations are usually carried out with a molecular mechanics level representation. Simulations with such a molecular representation can be carried out on ensembles of thousands of molecules. This is significantly more than in QM calculations, but is still an extremely small number compared to the number of molecules present in even the smallest droplet of water. In the present work most simulations are done on ensembles of 256 molecules. Such an ensemble is usually regarded as large enough for reliable calculations, at the same time as such calculations can be carried out in reasonable amounts of time.

The Lennard-Jones and Coulomb interactions are usually truncated at some value. This is mainly done to save time in the calculations. The Lennard-Jones potential decays steeply as a function of distance and its truncation is unproblematic. Coulomb interactions have a slower decay, but for neutral species the truncation can still be a reasonable simplification. For ionic species truncation is however usually not an acceptable option. Although there are schemes to handle long-range forces, simulations of ionic systems are challenging. The standard way of handling long-range electrostatics is the use of Ewald sums.

Simulations are often carried out in microcanonical (NVE), canonical (NVT) and constant number of particles-constant pressure-constant temperature (NPT) ensembles. The grand-canonical ensemble with constant free energy, volume and temperature (μVT) is also used in some types of simulation.

3 Computational Chemistry

When carrying out simulations the statistical sampling is always a concern. The question of whether the system has sampled sufficiently the full set of configurations it can take on (the phase space) must be addressed. Verifying this is difficult, and is not only an issue of doing a long enough simulation. If one can imagine the potential energy of phase space as a kind of landscape, one can think of the simulation as risking becoming trapped in a valley. As simulations are based on statistical averaging of properties, there is always some degree of statistical uncertainty in the results obtained.

While MD and MC can be used to calculate many of the same properties, they differ in some important respects. In MC simulations time is not a parameter and there is no easy way to obtain time-dependent properties such as diffusion-rates. MD has been developed further in handling of long-range electrostatic interactions. MC calculations can sometimes provide more efficient sampling of phase space.

3.4.2 Free Energy Perturbations

The free energy of solvation is the energy associated with a molecule going from the gas phase to solution and is a central concept in understanding chemistry in solution. Determination of free energies is also one of the main issues in this thesis. Kollman (1993) provided a review of the main simulation techniques for determining free energies. The main techniques are free energy perturbations (FEP), thermodynamic integration and slow growth. FEP sees the widest use and is also the technique I have adopted in my work. The fundamental equation that free energy perturbations are based on is the following (Kollman 1993):

$$G_B - G_A = \Delta G = -RT \ln \left\langle e^{-\Delta H / RT} \right\rangle_A \quad (3.6)$$

where $\Delta H = H_B - H_A$ and $\langle \rangle_A$ refers to an ensemble average over a system represented with the Hamiltonian H_A . If the systems differ in a significant way the

3 Computational Chemistry

equations will however not lead to a meaningful result. This problem can be overcome by performing multiple simulations over intermediate steps between A and B. A coupling parameter (λ) is introduced that allows the smooth conversion of system A to B. The mutation of any geometry or potential parameter of the system can then be represented in the following form (Jorgensen and Ravimohan 1985):

$$\xi(\lambda) = \xi_0 + \lambda(\xi_1 - \xi_0) \quad (3.7)$$

The total free-energy change is obtained by adding together the contributions from each single perturbation. In the present work calculations are performed with the double-wide sampling scheme (Jorgensen and Ravimohan 1985). In this scheme the free energy difference for $\lambda_i \rightarrow \lambda_{i+1}$ and $\lambda_i \rightarrow \lambda_{i-1}$ are evaluated in a single ensemble.

The mutation will usually be between two different solute molecules. The essence of the FEP is to mutate one molecule into another and compute the energy associated with the transformation. FEPs are in general more accurate for calculating differences between molecules with similar properties. More accurate results are for example obtained when perturbing between molecules of the same charge, as opposed to between species with different charges. Calculating the absolute free energy of solvation is more difficult than simply calculating relative free energies, the two systems one is calculating the energy between in this case being very different (differing by the number of molecules). In this work most calculations are done as relative free energy perturbations.

While the general concept of FEP calculations is easily understood, the technical issues involved are far from trivial. Kofke and Cummings (1997, 1998) have concluded that perturbations that involve growth are superior to those involving shrinking or deletion of molecules. They conclude that shrinking offers loss of accuracy due to biases in the sampling. More recently Kofke (2005) has however concluded that the error involved in insertion and deletion approaches may vary

3 Computational Chemistry

from system to system. The development of optimal FEP methods does therefore appear to be a work in progress.

The selection of methods in this work has been dictated mainly by available simulation codes, rather than any assessments of the merits of various methods to determine the free energy.

3.5 QM/MM

QM/MM is a general term for calculations combining quantum mechanical (QM) and molecular mechanics (MM) representations. Such calculations can be advantageous when one wishes to model parts of a system with greater accuracy. For studies of a reaction in solution one might for example represent the reacting molecules at a QM level, while solvent molecules are represented at MM level. In a more sophisticated calculation one might also represent the closest solvent molecules at QM level, while solvent molecules at a greater distance are represented at a MM level. While QM/MM calculations are less time consuming than pure QM calculations, they can still be prohibitively expensive.

Gao (1996) has reviewed the various types and levels of QM/MM coupling. In the present work QM geometries and atomic charges will be used in simulations. This can be regarded as a very weak form of QM/MM coupling.

3.6 Computational Chemistry and Experiment

Computational chemistry will never be a full replacement for doing experiments, but can often supplement experimental work. Very often neither experiment nor computational chemistry can by itself give us the full insight we could desire. In many cases one must therefore piece together whatever information can be drawn from either source, to draw whatever conclusions can be drawn. Sometimes computational chemistry can be used to calculate properties that are not at all available from experimental work, while some issues can be difficult both in the

3 Computational Chemistry

laboratory and on the computer. When working with results from modeling and the laboratory one should have a feeling for the quality of the data from different sources. Computational chemistry has grown as a field rather quickly, and many researchers are perhaps not fully aware of the potential of its methods. On the other hand I have the impression that researchers sometimes are more aware of the limitations of the tools they work with, than that of other methods, and may come to overestimate the quality of the work in a different field.

In the field of CO₂ absorption there is as noted in the last chapter considerable amount of experimental data. On the other hand it must also be noted that the systems in the process display considerable complexity. The systems consist of many components in an aqueous solution. Several of the components are ionic and many components can have large numbers of potential conformers. In addition the process runs at temperatures ranging from 50°C to 130°C. There are also degradation products, impurities and surface effects that may change the chemistry, or affect the process operation in some other way. Given the complexity of the system, the amount of experimental data available must actually be considered to be rather sparse. The multi-component nature of the liquid in the system also present challenges for computational chemistry work. The absence of experimental data at the molecular level also means that it can be difficult to validate models being used and conclusions drawn regarding the nature of the system.

The approach in this work has therefore been somewhat pragmatic. The most effort has been put into areas where computational chemistry was thought to give the most valuable new insight, where as some aspects have been approached tentatively.

3.7 Review of Computational Chemistry Work on CO₂ Absorption

There has been published some computational chemistry work on chemistry directly related to the CO₂ absorption process. Ohno and co-workers (Ohno et al. 1998 and Ohno et al. 1999) have done some very detailed work on 2-(N,N-Dimethylamino)ethanol and 2-(N-Methylamino)ethanol. These papers combine quantum mechanical calculations with infrared and Raman spectroscopy. These papers offers valuable results in terms of the adopted conformers of amines and CO₂ bound amine molecules.

Papers by Chakraborty et al. (1988) and Jamroz et al. (1997) deal with interactions between CO₂ and amine molecules. While interesting these papers provide no clear conclusions of direct relevance to CO₂ absorption. Suda et al. (1998) attempt to correlate the amount of CO₂ absorbed in a liquid with frontier orbital properties. While this is an interesting approach the correlations obtained were not very good. In summary may be concluded that very little computational chemistry work has been done for the specific purpose of understanding the CO₂-absorption process.

There has been done some computational chemistry work on the liquid structure of ethanolamine (Button et al. 1996, Alejandro et al. 2000 and Gubskaya and Kusilik 2004a) and ethanolamine in aqueous solution (Gubskaya and Kusilik 2004b). These papers do give some insight into the liquid structure of ethanolamine, but they do not deal with the more complex multi-component systems encountered in CO₂ absorption. For other amine solvents of interest in CO₂ capture I am not aware of any computational chemistry work having been done.

While there has been done very little computational chemistry work on CO₂ absorption, there has been done a lot of work on molecules similar to those utilized in this process. Molecules with amino- and hydroxyl-groups are important in all forms of living organism, and the modeling of them is subject of substantial work

3 Computational Chemistry

in biochemistry. Most of the models applied in this thesis originated in studies of systems of importance in biochemistry.

4 Modeling of Solvation Energy

Realistic relative gas-phase energies of ionization may soon be estimated by molecular quantum mechanics. If an accurate set of solution energies can be determined, we can expect that the next generation of calculations may include solvation energies, and thus complete quantum mechanical calculations for protonation reactions in solution might become possible.

Jones and Arnett (1974)

4.1 Introduction

This chapter is intended as a review of available approaches to modeling energies in solution. It will be mainly focused on issues directly relevant to CO₂ absorption, but will also touch upon some general issues. In addition to briefly describing different solvation models, results will also be presented comparing different models ability to predict relative base strength.

Liquids do in general probably represent the most difficult phase to model. In the gas phase intermolecular interactions are limited and it is often sufficient to look at the characteristics of a single molecule. In such a case quantum mechanical calculations can be applied successfully, examples of this will be shown later in this chapter. Solids are more complex, but the modeling of them is in some cases made easier by their periodic nature.

In a liquid a single molecule interacts with a large number of neighbor molecules that do not display any orderly structure. The interactions are also shifting continuously as molecules move around, and the observed properties of liquids represent averages of these interactions. Rigorous quantum mechanical calculations of all these interactions are simply not feasible at present or in the foreseeable future. This leaves scientists with the challenge of finding the best approximations in simplifying a complex problem.

4.2 The liquid state

While liquids do by nature not display any long term periodicity or regular structure, they do have some structural characteristics. One common way to describe such structural features is by use of radial distribution functions ($g(r)$). The radial distribution describes the probability of encountering two atoms at given distances (r_{12}). Usually it is given in a normalized form so that the probability density of 1 is the average density of the system. A radial distribution function will often look something like the one shown in Figure 4.1.

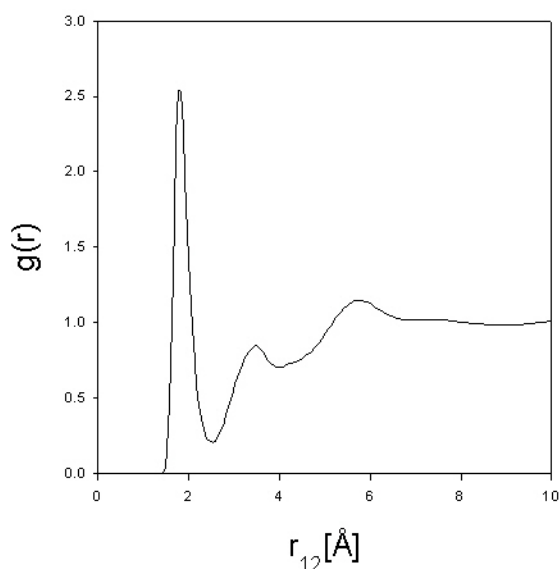


Figure 4.1 Radial distribution function.

Atoms do not overlap and at very short range the probability of finding a second atom will be zero. At slightly larger distances there is the ideal distance for direct interaction between the atoms and this usually results a peak in the function, atoms at this distance form what is called the first solvation shell. Because other atoms do not overlap with the ones in the first solvation shell the radial distribution function

4 Modeling of Solvation Energy

will usually show a marked drop after the first peak. At longer distances the radial distribution will average out to the average density of the system, which in other words means that positions of atoms at long range are not correlated. With radial distributions for all types of atomic sites in a liquid one can form a picture of the interactions. In addition to the radial distribution functions there are other properties that can be used to summarize the characteristics of liquids. An example of such a property is the angular pair correlation function, this carries information about how molecules in a liquid orientate relative to each other (Gray and Gubbins 1984). Another example is spatial distribution functions, these provide three dimensional pictures of interactions in a liquid, the work by Gubskaya and Kusilik (2004a) is an example of the use of such distribution functions.

4.3 Statistical Mechanics

Statistical mechanics offers tools for analytically describing interactions in liquids. Here a brief outline will be given based on a compendium by Kjellander (1992). One central parameter is the pair correlation function:

$$h(r_1, r_2) = g(r_1, r_2) - 1 \quad (4.1)$$

where g is the radial distribution function for atoms (or other form of site) located at r_1 and r_2 . At the heart of much of the statistical mechanics works on liquids is the Ornstein-Zernike equation. The Ornstein-Zernike equation states that the pair correlation function can be written in the following form:

$$h(r_1, r_2) = c(r_1, r_2) + \int c(r_1, r_3) n(r_3) h(r_3, r_2) dr_3 \quad (4.2)$$

Here $c(r_1, r_3)$ is the direct correlation function and $n(r_3)$ is the density at a given point. What this equation states is that the correlation between two particles in a liquid ($h(r_1, r_2)$) can be divided into two parts, one direct and one indirect. The direct part is called the direct correlation function. The indirect part comes from

4 Modeling of Solvation Energy

particle 2 again correlating with the other particles in the system, these particles again correlating directly with particle 1.

The $h(r_3, r_2)$ in the integral can be written in the same form as the Ornstein-Zernike equation:

$$h(r_3, r_2) = c(r_3, r_2) + \int c(r_3, r_4) n(r_4) h(r_4, r_2) dr_4 \quad (4.3)$$

Inserting this into the Ornstein-Zernike equation the following equation is obtained:

$$h(r_1, r_2) = c(r_1, r_2) + \int c(r_1, r_3) n(r_3) c(r_3, r_2) dr_3 + \int c(r_3, r_4) n(r_4) h(r_4, r_2) dr_4 dr_3 \quad (4.4)$$

This procedure can be repeated and the result is clearly an infinite sum of integral equations. The Ornstein-Zernike equation is by itself the definition of the direct correlation function and it should be noted that no approximations are required in formulating it. This function is expected to have a simpler form than the pair correlation function. If one combines the Ornstein-Zernike equation with a closure equation one can obtain a solvable set of equations. One of the simpler closure equations is the mean-spherical approximation:

$$h(r) = -1 \text{ for } r \leq \sigma \quad (4.5)$$

$$c(r) = -\frac{U}{kT} \text{ for } r > \sigma$$

where U is the interatomic potential energy and σ is the radius of the atom.

A widely used closure is the Percus-Yevick equation:

$$g(r) \approx e^{-u(r)/kT} (1 + h(r) - c(r)) \quad (4.6)$$

A second widely used closure equation is the so-called Hypernetted Chain(HNC) approximation:

$$g(r) \approx e^{-u(r)/kT + h(r) - c(r)} \quad (4.7)$$

4 Modeling of Solvation Energy

These closure equations represent approximations and the solutions obtained with these equations are therefore approximate. For simple idealized liquids such as hard spheres or soft spheres these equations can be solved and results can be compared with molecular simulations utilizing the same molecular representation. Such comparisons have revealed that most of the closure equations produce satisfactory results in some cases but fail in others. The Percus-Yevick closure is known to work well in describing interactions between hard spheres, but performs less well for systems with electrostatic interactions. The HNC closure performs well for a number of different types of systems, but can fail for some mixtures of different solvent molecules and can sometimes lead to diverging calculations (Hirata 2003). Efforts have been made to develop closure equations that produce results in better general agreement with those obtained from simulations. Hansen and McDonald (1990) provide a brief review of such efforts. A more recent example is the KH closure suggested by Hirata and co-workers (Hirata 2003).

The Ornstein-Zernike equation is for independent single-sites (atoms) and the extension to molecules consisting of several-sites is not trivial. One Ornstein-Zernike based model that is easily extended to molecules is the reference interaction site model (RISM). This model was first derived by Chandler and Anderson (1972). It can be written as:

$$\mathbf{h} = \boldsymbol{\omega} * \mathbf{c} * \boldsymbol{\omega} + \rho \boldsymbol{\omega} * \mathbf{c} * \mathbf{h} \quad (4.8)$$

Here “*” represents convolutions and \mathbf{c} and \mathbf{h} are in this case matrixes of the various correlation functions for the different sites in molecules. $\boldsymbol{\omega}$ is a matrix of intramolecular correlations. Hansen and McDonald (1990) refer to this theory as the “RISM approximation” and unlike the Ornstein-Zernike equation itself approximations have been made in deriving it. Hansen and McDonald (1990) summarize some of the failures of RISM and look at efforts to come up with more accurate models. They do observe that while there have appeared models that in a formal sense would appear more correct than RISM, they have not yielded better

4 Modeling of Solvation Energy

results. Work by Lue and Blankschtein (1995) provides an example of more recent efforts to develop integral equation theories. They present results for water for the site-site Ornstein-Zernike equation and the Chandler-Silbey-Ladanyi equations. It should also be noted that efforts have been made to improve or correct the RISM formulation (Hirata 2003 and Kvamme 2002). Development of such integral equation theories is clearly a difficult issue, the mathematics of formulating the equations is in itself demanding and so is the issue of solving these equations for a given system.

It should be emphasized that these integral equation models do not say anything about the nature of molecular interactions, rather they can be seen as an alternative to simulations that when coupled with a molecular representation offers a model of the liquid state. RISM as a model for solvation will be discussed in section 4.4 5.

4.4 Models to Calculate the Free Energy of Solution

4.4.1 Introduction

The free energy of the solvation (ΔG_s^0) is the free energy change associated with a molecule leaving the gas phase and entering a condensed phase. It is the liquid property that will be of greatest interest in the present work. It may for a given species A be determined from equilibrium data by the following equation (Cramer 2002):

$$\Delta G_s^0(A) = \lim_{[A]_{sol} \rightarrow 0} \left\{ -RT \ln \frac{[A]_{sol}}{[A]_{gas}|_{eq}} \right\} \quad (4.9)$$

This formulation draws on work by Ben-Naim (Ben-Naim and Marcus 1984 and Ben-Naim 1992). While the equation in the form it is stated here is for infinite dilution, it can also be formulated for other conditions. While the free energy of solvation is perhaps not a quantity that most people in chemical engineering are

4 Modeling of Solvation Energy

familiar with, it does contain information relevant to several aspects of liquids equilibrium that in chemical engineering is represented in other forms. If the energy for the reaction in the gas phase and the solvation energy for each component is known the reaction energy in solution can be calculated. The free energy of solution also conveys information about the vapor-pressure of a given species (Winget et al. 2000) and solvation energies can also be converted into activity coefficient data (da Silva 2004).

The present review is intended to cover all the main approaches to calculating solvation energies. The form of the present outline draws mainly on reviews by Bacskay and Reimers (1998) and Orozco and Luque (2000). While I have tried to make this review fairly broad the main focus will be on models that may be suitable for modeling CO₂ absorption. As noted in Chapter 2 the CO₂ capture processes is usually run with base molecules in water and most attention will also be given to the modeling of aqueous solution. Water is also, for obvious reasons, the solvent that has received the greatest attention in the literature.

4.4.2 Equation of State and Lattice Models

The interest of chemists in understanding, modeling and predicting the behavior of liquids predates computational chemistry and there are models not based on any form of computational chemistry. The present outline of such models is drawn from the textbook “Molecular Thermodynamics of Fluid-Phase Equilibria (Prausnitz, Lichtentaler and Gomes de Azevedo 1999). The authors distinguish between two main approaches. One is based on approaching a liquid with a gas model and the second on approaching it with a solid-like lattice model.

The first approach leads us to the equation of state models. From an equation of state the free energy (Helmholtz or Gibbs) can be determined and from an equation of state for mixtures the free energy of each component can be derived.

4 Modeling of Solvation Energy

The lattice models are based on thinking of molecules in liquids as occupying spaces in a grid. Mixing of two pure components can be envisioned as molecules exchanging places in the grid. If interaction parameters are introduced the energy and entropy change associated with mixing can be calculated.

Considering a liquid as a dense gas or a rigid lattice is a fairly drastic approximation and the first such models were not all that successful. More advanced models have however been developed that successfully capture the behavior of many types of solvents. Such models are however in general not able to predict properties for systems where no experimental data is available. The parameters in the equations are fitted to reproduce experimental data, and the parameters together with the equations can perhaps be thought of as a way to summarize experimental data for a given system. What such models can do is predict the behavior for a system over changing concentrations, temperature and pressure. Examples of such applications on CO₂ capture related issues can be found in the work of Solbraa (2002) and Hoff (2003).

There is however a family of models derived from equation of state and lattice models to do predictive calculations. These are group contribution models. The most famous of these is perhaps the UNIFAC model (Fredenslund, Gmehling and Rasmussen 1977). These are based on breaking up a molecule into units such as hydroxyl-, alkane- and amino-groups. The properties of the solvent are attributed to its various groups. Some form of database is constructed of groups and their parameters, when a new molecule is encountered the groups it is composed of is identified and from these the properties are predicted. While such models see fairly wide use they do have clear limitations.

In Figure 4.2 is shown two possible conformers of ethanolamine. In one of the conformers there is an intramolecular hydrogen bond, if such a bond is formed in solution then this will reduce the extent of bonding formed with other species. The interactions with other species will therefore depend on which conformer form is

4 Modeling of Solvation Energy

preferred. Yet present group contribution methods do not take account of such conformer effects and their reliability in cases where such issues arise would seem questionable, a conclusion also drawn by Wu and Sandler (1991).

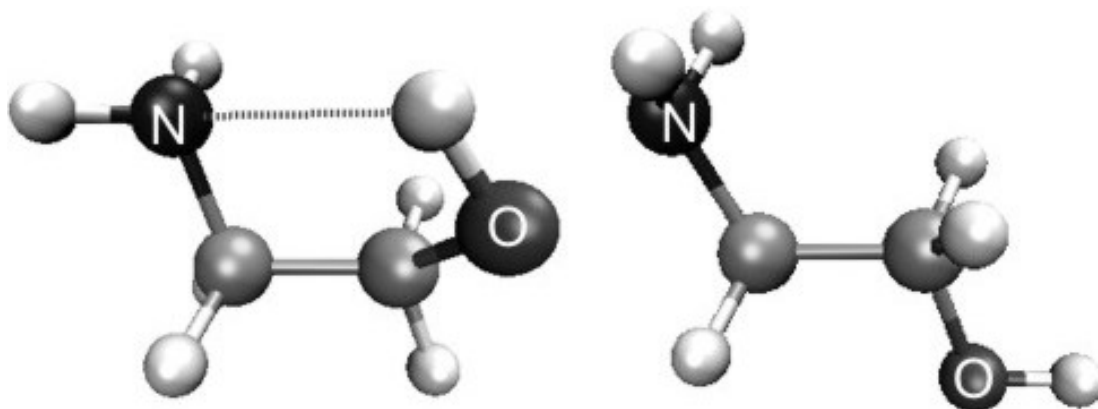


Figure 4.2 Conformers of ethanolamine.

Another, and perhaps more fundamental, issue is if the parameters in a model such as UNIFAC are sufficient to capture effects of all interactions in a liquid. UNIFAC is in form similar to traditional equations of state models such as UNIQUAC and NRTL. These are all sets of quite simple equations, energy interactions between different species are usually represented by a single parameter. It would seem questionable if such a small number of parameters can accurately capture the complex interactions in a liquid. In Figure 4.3 three pairs of water molecules are shown. The interaction energy is obviously different for the different pairs, the energy depending on distance and orientation of the molecules. A single parameter can perhaps express the average of all interactions in a given system, but if the composition of a system changes the average interaction for a given component might also change.

4 Modeling of Solvation Energy

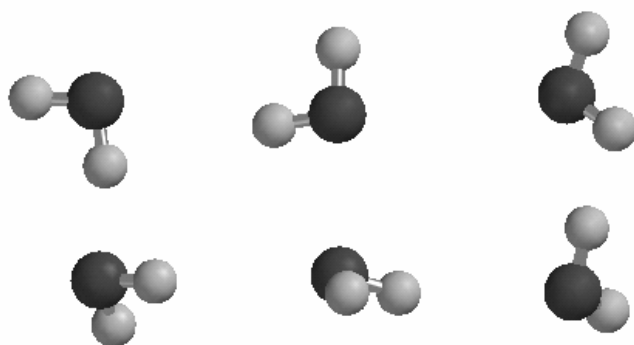


Figure 4.3 Interactions of water molecules.

More advanced models have been proposed in recent years, one notable model being the Statistical Associated-Fluid Theory (SAFT) (Chapman et al. 1989 and Chapman et al. 1990). This model has expressions to take account of contributions from short-range repulsion, long-range dispersion, chemical bonding and association or hydrogen bonding between different molecules. It is also noteworthy that the model was tested for consistency with molecular simulation during development.

While advanced models such as SAFT seem better formulated to capture the various effects that play a part in solution the number of parameters in the model is also inevitably greater than for the simpler models such as UNIQUAC. In the absence of more detailed experimental data the determination of parameters for a more advanced model can be a difficult task. While such advanced models do represent progress and may in general be considered to be better than simpler models, the underlying issues of parameter fitting must always be kept in mind.

4.4.3 Continuum Models

Continuum models are the group of solvation models in computational chemistry that have seen the greatest use. These models have a long history, some of the early work was carried out by the Norwegian Lars Onsager (Onsager 1936). Rather than explicitly representing solvent molecules, the solvent is represented by a

4 Modeling of Solvation Energy

continuous electric field that represents a statistical average over all solvent degrees of freedom. Such models are also known as implicit solvation models. The outline given here will be based on the textbook “Essentials of Computational Chemistry” (Cramer 2002). Continuum models have been the subject of numerous reviews in recent years (Tomasi and Persico 1994, Cramer and Truhlar 1999, Orozco and Luque 2000) and I will to some extent draw on these too in the present outline.

At the heart of the continuum models is the Poisson equation. This is valid when a surrounding dielectric responds linearly to embedding charges:

$$\nabla^2\phi(\mathbf{r}) = -\frac{4\pi\rho(\mathbf{r})}{\varepsilon} \quad (4.10)$$

where ρ is the charge density, ϕ is the electrostatic potential and ε is the dielectric constant. The Poisson equation is valid under conditions of zero ionic strength, for charged species the Poisson-Boltzmann equation applies:

$$\nabla\varepsilon(\mathbf{r})\cdot\nabla\phi(\mathbf{r}) - \varepsilon(\mathbf{r})\lambda(\mathbf{r})\kappa^2\frac{k_B T}{q}\sinh\left[\frac{q\phi(\mathbf{r})}{k_B T}\right] = -4\pi\rho(\mathbf{r}) \quad (4.11)$$

where λ is a function that switches from zero in areas not accessible to the electrolyte to one in areas that are accessible and q is the magnitude of the charge.

κ^2 is the Debye-Huckel parameter:

$$\kappa^2 = \frac{8\pi q^2 I}{\varepsilon k_B T} \quad (4.12)$$

where I is the ionic strength. The work needed to create a charge distribution can be determined from the following equation.

$$G = -\frac{1}{2}\int\rho(\mathbf{r})\phi(\mathbf{r})d\mathbf{r} \quad (4.13)$$

In continuum models the solute is placed in a cavity representing the space occupied by the solute in the solvent. Such a procedure is illustrated in Figure 4.4.

4 Modeling of Solvation Energy

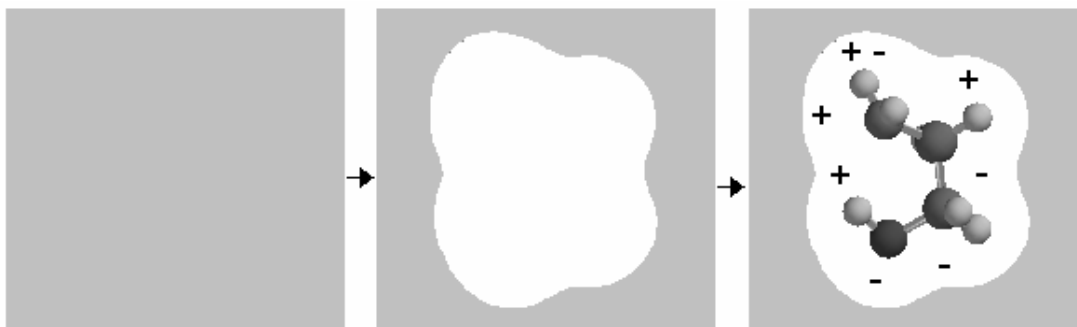


Figure 4.4 Creation of Cavity and Insertion of Solute in Solvent.

In the first continuum models cavities were simple spheres, while in most present models they are usually built as a set of spheres around each atomic centre. Continuum model calculations can be carried out with either a molecular mechanical or quantum mechanical representation of the solute, the latter does however represent a more rigorous model. In quantum mechanical continuum calculations an iterative cycle is often used. First the solute with its gas phase electron distribution is inserted into the cavity. The solvent electrostatic field that arises from the solute charges is calculated, this is usually called the reaction field. The reaction field is then introduced as an external potential in the quantum mechanical calculation. This is done by solving the following form of the Schrödinger equation:

$$\left(H - \frac{1}{2}V \right) \psi = E\psi \quad (4.14)$$

where V is the reaction field inside the cavity. The reaction field is then recalculated based on the new solute charge distribution. This is repeated in an iterative procedure until the energy of the system converges. The energy change obtained from such a calculation is usually called the electrostatic energy. There are however other contributions to the solvation energy.

The free energy of solvation can be thought of as consisting of three main contributions (Orozco and Luque 2000):

4 Modeling of Solvation Energy

$$\Delta G_s = \Delta G_{electrostatic} + \Delta G_{cavitation} + \Delta G_{van\ der\ Waals} \quad (4.15)$$

The electrostatic contribution is the term just described. The cavitation term represents the energy that is needed to create room for the solute in the solvent. Finally the van der Waals term is the energy that comes from dispersion and repulsion interactions between solute and solvent molecules. In addition it should be noted that if the solute causes rearrangement in the solvent structure that can also give a contribution to the solvation energy (Cramer and Truhlar 1999). The continuum models are in essence electrostatic models and estimates for the other contributions must be sought elsewhere. The cavitation and van der Waals terms are usually included as semi-empirical terms which size is made proportional to the size of the solute cavity.

It should be clear from this outline that determining the size and shape of cavities is a central issue in developing and applying continuum models. Cossi et al. (1996) describe the selection of cavities as “one of the most delicate steps in defining a continuum solvation model”. While cavities can be easily understood as the space occupied by a solute molecule in a solvent this is not an unambiguously defined property, nor is it experimentally observable. Many definitions have been proposed, one of the more common is the van der Waals surface, defined as the cavity formed by van der Waals spheres centered on the atoms (Cossi et al. 1996). There is also no requirement that the same definition of the cavity be used in the calculation of electrostatic and other terms, in the PCM model (to which I will return) different definitions are in fact utilized (Cossi et al. 1996).

As noted some of the energy contributions in continuum models are usually determined in some form of fitting to experimental data and there is also some arbitrariness in the selection of cavities. Continuum models are often directly fitted to free energies of solvation. This fitting process does mean that these models tend

4 Modeling of Solvation Energy

to be semi-empirical in nature. One consequence is that the models tend to be limited to the solvent and conditions for which they were parameterized. It also means that the validation of different models can be somewhat difficult. The empirical contributions may mask errors in the electrostatic model, this means that the underlying quality of the model is not that easily determined from comparisons with experimental data. This can perhaps create challenges in the further development of continuum models.

Continuum models are in general reasonably good at reproducing the free energies of neutral solutes, but less accurate for ions. The nature of the models does raise some questions about how reliable they can be. One of the issues often debated is to what extent they can capture effects of interactions in the first solvation shell such as hydrogen bonding (Cramer and Truhlar 1999 and Kawata et al. 1996).

In a continuum model a solvent is represented by a fairly small number of parameters, among them the dielectric constant. With such a form of solvent representation it is unclear if and how such models can be extended to mixtures of solvents. Many continuum models do also tend to be dedicated to calculations at infinite dilution.

A great number of variations of continuum models have been proposed, here I will briefly review some of the more common models.

PCM The Polar Continuum Models (Miertus, Scrocco and Tomasi 1981, Cossi, Barone, Cammi and Tomasi 1996 and Cancès, Mennucci and Tomasi 1997) are the continuum models that see the greatest use in the context of quantum mechanical calculations. One of the main reasons for this is that the models are implemented in the widely used Gaussian programs (Frisch et al. 1998). These models are also regarded as being fairly robust and flexible in the sense that they can be easily applied to different molecules and systems. In the PCM the cavity surface is divided into surface areas called tesserae.

4 Modeling of Solvation Energy

The reaction field of the solvent is represented by charges placed on the cavity surface. PCM calculations can be carried out in combination with most forms of quantum mechanical calculations.

SM The “Solvent Model” are a series of models developed by Cramer, Truhlar and co-workers (Chambers et al. 1996 Li et al. 1999). The philosophy behind these models is somewhat different from that behind the PCM models. In the development of SM models a number of different forms have been tested. The developers, rather than focusing on developing a single form of rigorous model, have implemented various models. They have studied how different models, when properly parameterized, are able to reproduce the experimental free energies. A particular feature is the use of atomic surface tensions (σ_k) (Li et al. 1999). The free energy in this model is the sum of electrostatic and surface tension contributions. These atomic surface tensions are purely empirical terms intended to capture cavitation, van der Waals contributions and any other contributions arising from the first solvation shell.

The SM models are in general based on simpler electrostatic calculations than the PCM models and offers results of comparable quality from calculations that are much less time consuming. They do however rely on more extensive use of empirical data.

COSMO-RS The COSMO model was originally only one type of implementation of a continuum model (Klamt 1995 and Andzelm, Kölmer and Klamt 1995). In the COSMO calculations the solvent was considered to be an electric conductor with an infinite dielectric constant, this having the virtue of facilitating the calculations. COSMO-RS (“Realistic Solvent”) represents the development by Klamt and co-workers (Eckart and Klamt 2002) of a model designed to study properties both for pure components and liquid mixtures. The model can therefore be used for a number of problems of interest in chemical engineering. While results published with the COSMO-RS model seem

4 Modeling of Solvation Energy

encouraging (Eckart and Klamt 2002) it must be noted that this is a proprietary model and that there might therefore perhaps be less transparency regarding its strength and weaknesses than is the case for other models. All the publications on this model have to my knowledge been by the developers themselves.

4.4.4 Molecular Simulation

In the last chapter MC and MD simulations were briefly introduced. In such calculations the solvent molecules are explicitly represented and such models are also called “explicit models” (while the continuum models are implicit). As noted in the last chapter simulations are time consuming, the simulation time increasing with the number of molecules being studied and the level of molecular representation. Today most simulations are done with molecular mechanics representation of solvent and solute. In both MD and MC there are techniques to obtain the free energy of the solvation, one of the most common methods being free energy perturbations.

As noted in the last chapter a key approximation made when using a molecular mechanics representation is that charges are fixed. Polarization is handled implicitly by using values for the charges intended to reflect the average polarization in the liquid. Compared to a continuum model the polarization effects are handled in a simpler manner in standard simulations.

Simulations are not packaged as models in the same way continuum models are. Most simulation codes give the user great freedom in selecting the force field parameters.

The parameters for many force fields are derived from fitting to empirical data. The parameterization is usually based on reproducing liquid properties, and is thus very different in nature from that used for the continuum models.

4 Modeling of Solvation Energy

As indicated in the last chapter there is also many ways in which quantum mechanical calculations can be used to determine force field parameters. The most important use is in determination of molecular geometry and atomic charges.

As noted in the last chapter there are a number of ways in which partial atomic charges can be derived from quantum mechanical calculations. What kind of schemes will lead to more accurate solvation energies is still an open question.

In the last chapter it was also observed that polarizable force fields are available. While such simulations are still too time-consuming to be done on a routine basis it is clearly an option to consider if a more realistic solvent representation is desired.

With simulations the study of liquids composed of two or more components is in principle no problem. As a system becomes less homogeneous it would however seem very likely that the sampling required for satisfactory average values will increase. Simulations can also quite readily be used to study systems with different temperature. Pressure conditions can also be controlled, although this is still perhaps somewhat more difficult than temperature control (Allen and Tildesley 1987).

4.4.5 RISM and RISM-SCF

In the statistical mechanics section of this chapter the RISM equations were introduced. RISM can be regarded as an alternative to simulations, that when combined with a molecular representation offers a solvent model from which the free energy of solution can be calculated. Calculations where the solute and solvent have a molecular mechanics representation is called a classical RISM calculation.

RISM-SCF (Hirata 2003 and references therein) combines a classical solvent representation with a quantum mechanical solute representation. The calculation procedure is analogue to the one described for the continuum models. From a quantum mechanical calculation in the gas phase partial atomic charges are

4 Modeling of Solvation Energy

calculated and a RISM calculation is carried out to determine the solvent structure around the solute. From the solvent structure the reaction field is calculated and a new quantum mechanical calculation is carried out to determine the atomic charges in the presence of the field. This is repeated until convergence.

An RISM-SCF calculation has the virtue of combining the explicit solvent representation of a classical simulation with the solute polarisation term found in the continuum models. As in a standard simulation polarization of solvent molecules is only included implicitly in present forms of RISM-SCF. As noted previously the RISM equations involve some approximations, and compared to simulations this adds a layer of uncertainty. The issues regarding force fields and atomic charges are the same in RISM calculations as in simulations. In present implementations of RISM-SCF (Kawata et al. 1996) the solute charges are determined by fitting the charges to the electrostatic potential.

The complexity of the underlying equations and problems that can appear in obtaining converged solutions have probably contributed to this type of model seeing less use than continuum models and simulations.

4.4.6 Supermolecule Approach

The supermolecule approach is a term used for calculating the entire system quantum mechanically. Traditionally this has been done by performing calculations with some few solvent molecules in vacuum. While such an approach can be useful in determining the direct effect of solvent molecules on the solute it is more difficult to use such an approach for systematic calculations of solvation energy. Solute molecules can vary in shape and size and the number of solvent molecules that is needed to represent the main interactions will vary. As noted in the first part of this chapter the observed properties of a liquid represent averages over large numbers of configurations, it is clear that a calculation based on a single geometry will often not reflect such averages.

4 Modeling of Solvation Energy

A more advanced form of supermolecule calculations are QM/MD (Quantum Mechanical Molecular Dynamics) and QM/MC (Quantum Mechanical Monte Carlo) calculations. In such calculations simulations are carried out on molecules represented at a quantum mechanical level. Such calculations are seeing increasing use. The most famous, but far from the only, such approach is the Car-Parrinello Molecular Dynamics scheme (Car and Parrinello 1985). Such calculations are obviously very time-consuming and I am not aware of any such model being used to calculate free energies of solution. Free energies from such simulations can perhaps be determined by a scheme similar to what has been suggested for QM/MM calculations (Cummins and Gready 1997).

4.4.7 Hybrids of Computational Chemistry approaches

Looking at a radial distribution function it is clear that the short-range and long-range interactions are different in nature. At short range the interactions take on the nature of weak bonding or repulsion, while at long range the solute molecule only “sees” the averaged effect of a large number of solvent molecules. This would suggest that one is perhaps best served by using a model that has a better solvent representation at short range than at long range.

One such approach is to combine the supermolecule approach with continuum models. A small number of explicit solvent molecules can be included inside the cavity. While such calculations see some use there is an issue of how many solvent molecules to include, and how to do it in a consistent way for molecules of different size and shape (Cramer and Truhlar 1999).

Another form of hybridization is QM/MM models introduced in the last chapter. In such models part of the system is described with a molecular mechanics representation and other parts have a quantum mechanical representation. The simplest form would involve representing the solute quantum mechanically and using a MM representation of the solvent. In more advanced calculations some of

4 Modeling of Solvation Energy

the solvent molecules closest to the solute can also be represented at a quantum mechanical level. Calculations are carried out using some kind of simulation. To obtain sufficient statistical sampling a simulation must usually be carried out for many thousand steps, if one needed a QM calculation for each step and each QM calculation took something like an hour, it is easy to see that such simulations can become very time-consuming. One approach taken to reduce the time consumption is to use very low level semi-empirical QM models (Kaminski and Jorgensen 1998 and Cummins and Gready 1997). Such an approach does on the other hand also reduce the quality of the results obtained. Another interesting proposal is to use MM simulations to calculate geometries and do set of QM calculations on energies only (Wood et al. 1999). This proposal does suggest that there is room for refinement of QM/MM methods by only using the QM calculations for the most vital part of the calculations.

4.4.8 Descriptor Models

One of the approaches often taken in science when confronted with predicting a certain property is to correlate it to another known property. While this approach has perhaps not been used that much to determine the free energy of solvation itself, it has often been used in estimating different equilibrium constants in solution. An example of this can be found in the work of Eimer (1994) that finds a correlation between an equilibrium constant and molecular weight, and uses this to estimate the value for molecules where the equilibrium constant is not known. Such applications involve a form of implicit estimation of solvation energies. Approaches based on correlations with experimentally observable properties have been in use for a long time and do not require any input from computational chemistry.

Computational chemistry methods can however be used to determine a large number of molecular characteristics that can otherwise not be obtained. This offers

4 Modeling of Solvation Energy

new sets of descriptors that can be applied in finding correlations with the solvation energy or equilibrium constants. A motivation for using such an approach is that computational chemistry methods may calculate some property with greater accuracy than the free energy itself can be calculated. One descriptor that can be determined from simulations and that is used in finding correlations with solvation energies is the solvent-accessible surface area (SASA) of a molecule, this can be thought of as a form of “efficient surface area”. Duffy and Jorgensen (2000) obtained encouraging results when looking at correlations between SASA, other descriptors related to extent of hydrogen bonding and solvation energies. Another model based on SASA has been developed by Kollman and coworkers (Wang et al. 2001). It can also be noted that some forms of the SM continuum models are similar in nature to descriptor models.

4.4.9 Other Models

The outline and classification of models so far covers the most widely applied approaches to determining solvation energies. There are however some methods that do not fall within any of these categories. The most notable is perhaps the Langevin-Dipole method (Warshel and Levitt 1976). The solvent is in this model represented as a grid of dipoles. This method lies somewhere between a continuum model and an explicit solvent model.

There are also a number of ways in which one can imagine combining different approaches to calculating solvation energies. New variations do appear from time to time in the literature, and combining aspects of different models is one way forward to obtaining models that produce more accurate results within a given timeframe.

4 Modeling of Solvation Energy

4.4.10 Hybridization of Gibbs Energy Models and Computational Chemistry Based Models

It is likely to take some time before computational chemistry methods can provide robust a priori quantitative predictions of solvation energy for multi-component systems. An option that might be worth exploring is to pursue a general semi-empirical approach, drawing on whatever information is available experimentally and using computational chemistry to fill in the gaps.

One way to do this would be to use methods in computational chemistry to determine parameters for a lattice or equation of state model while at the same time maintaining the model's reproduction of experimental observations.

Some early efforts along these lines are work by Jonsdottir et al. (1996) and Sum and Sandler (1999). Both these works are based on determining the parameters for the UNIQUAC model. The general problem with this work is that the UNIQUAC parameters do not have any clear definition. Fischer (1983) warns against assigning a physical meaning to these empirically determined parameters. Attempting to predict ill-defined parameters is obviously a most unpromising line of research. I comment in greater detail on the work by Sum and Sandler in a paper appearing as a part of this thesis (da Silva 2004).

While UNIQUAC and similar equations are not suitable for combinations with data from computational chemistry, more advanced models may be. The SAFT equations would seem to be a promising candidate.

It would seem that there is a potential to combine information from computational chemistry with some form of free energy model. This is however likely to be a time-consuming task, requiring careful work and patience.

4.5 Comparison of Methods to Calculate the Free Energy of Solution

4.5.1 Methods

In the last section a fairly broad review was made of models available to calculate the free energy of solvation. In the present section a direct comparison will be made between a series of models in the calculation of amine basicity. This comparison should give an idea of how far computational chemistry has come in meeting the expectations of Jones and Arnett (quoted in the beginning of this chapter).

In choosing models for this comparison an effort has been made to include as many as possible of what seems to be the most promising methods. Not all solvent models are however distributed as ready to use software. Some only exist as codes in the laboratories developing the model, and can only be obtained by cooperation with the researchers behind the model. Of such models the RISM-SCF model has been included in the present comparison. Two of the models chosen are among the widely used continuum models. The final models are MC simulations with free energy perturbation. As noted in the previous chapter, there are numerous ways to calculate the solute atomic charges from QM calculations. In the present work two somewhat different types of charges are tested.

The comparison is intended to assess the models on an equal basis. All models have been run with settings that were expected to be close to optimal, in general that has meant using types of calculations similar to the ones in the papers first describing the models. No effort has however been made to tune any of the models to be in better agreement with the experimental data in consideration. It should be emphasized that the present comparison does not attempt to address the overall potential or quality of different models.

4 Modeling of Solvation Energy

The RISM-SCF and simulation results appear in a paper in this thesis (da Silva, Yamazaki and Hirata 2005). A detailed discussion of methods and results for these calculations can be found in that paper.

PCM. In the present work the IEFPCM (Cances, Mennucci and Tomasi 1997) model was used with its default settings in Gaussian 98 (Frisch et al. 1998) with 60 tesserae per atomic sphere. Calculations were carried out on HF/6-31G(d) gas phase geometries (IEFPCM/HF 6-31G(d)//HF 6-31G(d)).

SM. The SM 5.42R model implemented in Gamesol (Xidos et al. 1993) has been utilized. This model uses gas phase geometries and is parameterized for a series of basis-sets. Calculations are carried out with HF/6-31G(d) gas phase geometries and energies (SM 5.42R/HF 6-31G(d)//HF 6-31G(d)). Data in the Gamesol distribution manual (Xidos et al. 1993) suggests that this level of calculation should be close to optimal for the SM solvation model.

RISM-SCF. RISM-SCF calculations were carried out at the HF/6-31G(d,p) level. The solute Lennard-Jones parameters are from the all-atom OPLS force field (Jorgensen et al. 1996 and Rizzo and Jorgensen 1999) while the solvent was represented with the TIP3P (Jorgensen et al. 1983) water model. Solute atomic charges were determined by fitting to the electrostatic potential.

FEP-MK. A set of free energy perturbations were carried out with MK type charges (described in the last chapter). The solute Lennard-Jones parameters are from the all-atom OPLS force field (Jorgensen et al. 1996 and Rizzo and Jorgensen 1999) while the solvent in this case was represented with the TIP4P (Jorgensen et al. 1983) water model. Both the solute and solvent representation in these free energy perturbations were similar to what is utilized in the RISM-SCF calculation.

FEP-CM2. A second set of free energy perturbations were carried out with CM2 type charges (also described in the last chapter). The solute and solvent representation was otherwise the same as for the FEP-MK simulations.

4 Modeling of Solvation Energy

4.5.2 The Basicity

The property that has been chosen for the present comparison is the relative basicity of amines. Amines are the family of molecules that are of main interest in the present work. The basicity is in itself one of the amine properties of greater interest. The calculation of basicity requires the calculation of solvation energy of a neutral molecule and its protonated (and ionic) form and the gas phase basicity. This can therefore provide a fairly rigorous test of how good a solvation model is, provided accurate gas phase basicities are available. In addition there is accurate experimental data available with which to compare the model results. For base reaction the following equilibrium can be set up:

$$K_a = \frac{a_B a_{H^+}}{a_{BH^+}} \quad (4.16)$$

The free energy of protonation in aqueous solution (ΔG_{ps}) is related to K_a by the following equation:

$$\Delta G_{ps} = -2.303RT \log K_a \quad (4.17)$$

The calculations are based on the following thermodynamic cycle.

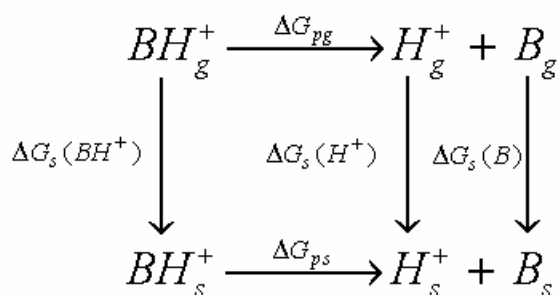


Figure 4.5. Thermodynamic cycle.

4 Modeling of Solvation Energy

Quantum mechanical calculations are used to determine gas phase basicities, while solvation models are used to determine solvation energies (ΔG_s). These results can be added together to give the free energy in aqueous solution. In the present comparison only the relative basicities will be studied. The quality of a model is given by how close calculated relative basicities are to the relative experimental values.

4.5.3 Amines

The amines included in the present study are shown in Figure 4.6. To reduce the complexity of the comparison amines with uncertain conformer forms are not included. This study does however include amine molecules that display significant variations in geometry.

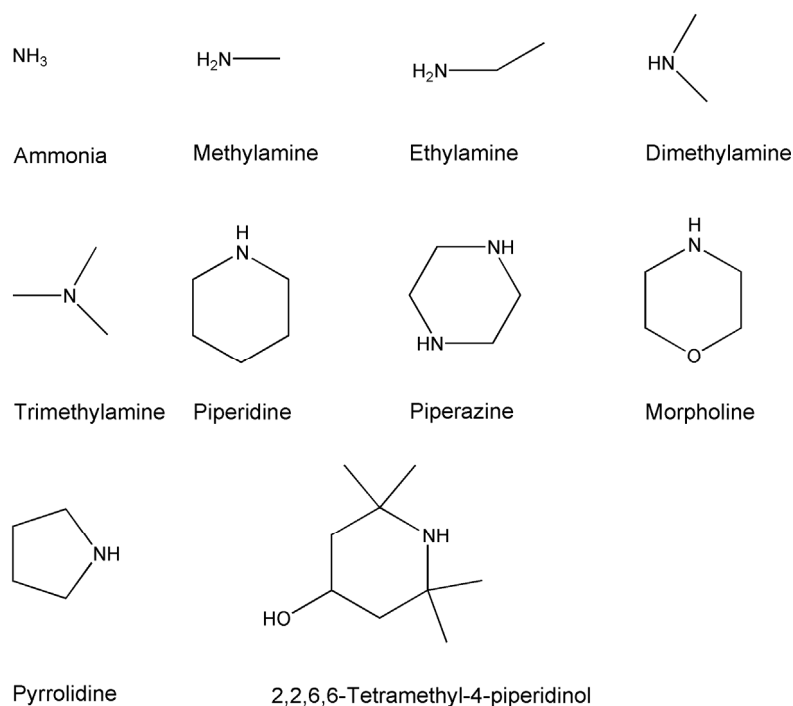


Figure 4.6 Amines in present study.

4 Modeling of Solvation Energy

4.5.4 Results

In Table 4.1 the calculated gas phase basicity data are shown. These can be seen to be in good agreement with experimental data.

Table 4.1 Relative Gas Phase Protonation Energies. Data in [kcal/mol].

Molecule	Theoretical ^a	Experimental ^b
Ammonia	0.0	0.0
Methylamine	10.2	10.9
Ethylamine	14.3	14.1
Dimethylamine	17.9	18.5
Trimethylamine	22.2	23.7
Piperidine	24.2	24.4
Piperazine	23.3	22.9
Morpholine	17.0	17.3
Pyrrolidine	23.6	23.0
2,2,6,6-Tetramethyl-4-piperidinol (TMP)	29.7	

^a B3LYP/6-311++G(d,p) energy with thermal correction and ZPE calculated at HF/6-31G(d) level. ^b Data from Hunter and Lias(2003).

In Table 4.2 and 4.3 the solvation energies determined with the different models are shown. The simulations have only been used to calculate relative solvation energies between the amines. To facilitate the comparison with the other data in the tables the absolute energy from the SM continuum model has been added. The RISM-SCF calculations have a systematic error that leads to an overestimation of the size effect on the solvation energy (da Silva, Yamazaki and Hirata 2005). In determining the basicity it is the difference of solvation energies between two

4 Modeling of Solvation Energy

species of approximately the same size that is important and this error is therefore expected to cancel out.

Table 4.2 Free Energy of Solvation for Neutral Amines. Data in [kcal/mol].

Molecule	RISM-SCF	FEP-MK	FEP-CM2	PCM	SM	Exp. ^a
Ammonia	-0.3	-4.87 ^b	-4.87 ^b	-4.30	-4.87	-2.41
Methylamine	5.1	-4.26	-6.72	-4.75	-5.14	-2.68
Ethylamine	10.1	-5.13	-6.36	-4.48	-4.90	-2.61
Dimethylamine	13.6	-1.40	-4.24	-4.30	-3.78	-2.41
Trimethylamine	23.3	1.44	-3.67	-2.76	-2.98	-1.34
Piperidine	24.1	-2.26	-4.65	-4.91	-4.33	-0.83
Piperazine	16.7	-7.41	-5.8	-10.65	-9.08	
Morpholine	15.8	-5.34	-7.14	-9.01	-7.24	
Pyrrolidine	21.5	-2.08	-9.50	-5.56	-6.03	
TMP	47.9	-25.36	-6.98	-8.34	-5.62	

^aData from Jones and Arnett (1974).^b SM model values.

4 Modeling of Solvation Energy

Table 4.3 Free Energy of Solvation for Protonated Amines. Data in [kcal/mol].

Molecule	RISM-SCF	FEP-MK	FEP-CM2	PCM	SM
Ammonia	-57.6	-87.19 ^a	-87.19 ^a	-79.9	-87.19
Methylamine	-43.5	-76.23	-80.90	-70.25	-76.39
Ethylamine	-37.8	-75.48	-79.63	-67.79	-72.70
Dimethylamine	-29.7	-69.14	-71.78	-65.45	-67.07
Trimethylamine	-16.6	-62.60	-63.57	-59.12	-59.38
Piperidine	-9.5	-61.60	-69.09	-62.35	-61.70
Piperazine	-21.3	-61.60	-70.92	-69.22	-66.20
Morpholine	-22.1	-72.43	-75.08	-71.78	-67.73
Pyrrolidine	-17.2	-66.06	-70.89	-63.79	-63.91
TMP	23.9	-86.64	-65.29	-57.61	-56.23

^a SM model values.

In Table 4.4 the relative free energy of protonation determined from experimental data and the various solvation models are shown. All data are given relative to ammonia.

4 Modeling of Solvation Energy

Table 4.4 Basicity in solution. Data in [kcal/mol].

Molecule	exptl pK_a	G_{ps}^a					
		exptl	RISM-SCF	FEP-MK	FEP-CM2	PCM	SM
Ammonia	9.24 ^b	0.00	0.0	0.0	0.0	0.0	0.0
Methylamine	10.65 ^b	1.92	1.5	-0.2	2.1	0.1	-0.9
Ethylamine	10.78 ^b	2.10	5.0	2.3	5.3	2.0	-0.2
Dimethylamine	10.8 ^b	2.13	3.9	3.3	3.1	3.5	-1.1
Trimethylamine	9.80 ^b	0.90	4.8	3.9	-0.2	3.0	-3.7
Piperidine	11.12 ^c	2.56	0.5	1.2	6.3	6.0	-0.8
Piperazine	9.83 ^c	0.80	4.0	6.0	10.2	6.3	-1.9
Morpholine	8.49 ^c	-1.02	-2.3	1.7	2.6	4.2	-4.8
Pyrrolidine	11.30 ^c	2.81	5.1	5.2	2.7	6.2	-0.9
TMP	10.05 ^c	1.10	-3.5	8.6	5.7	3.4	-2.0

^a Energies relative to ammonia. ^b Data from Jones and Arnett (1974). ^c Data from Perrin (1965).

In Figure 4.7 the gas phase basicity is plotted against the experimental pK_a . This figure illustrates the importance of solvation energies in determining relative basicities in solution. Figure 4.8 shows the results for the RISM-SCF, FEP-MK and FEP-CM2 models. Finally in Figure 4.9 the PCM and SM results are shown.

4 Modeling of Solvation Energy

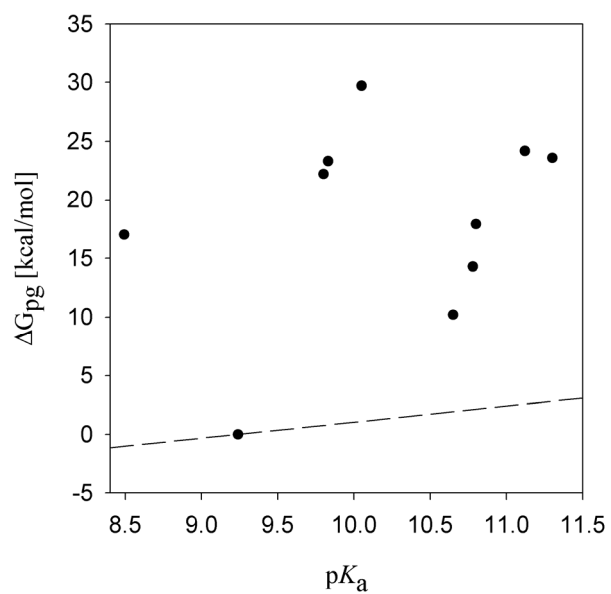


Figure 4.7 Calculated gas phase basicity versus experimental pK_a . The stippled line indicates the theoretical trend (in solution) relative to ammonia.

4 Modeling of Solvation Energy

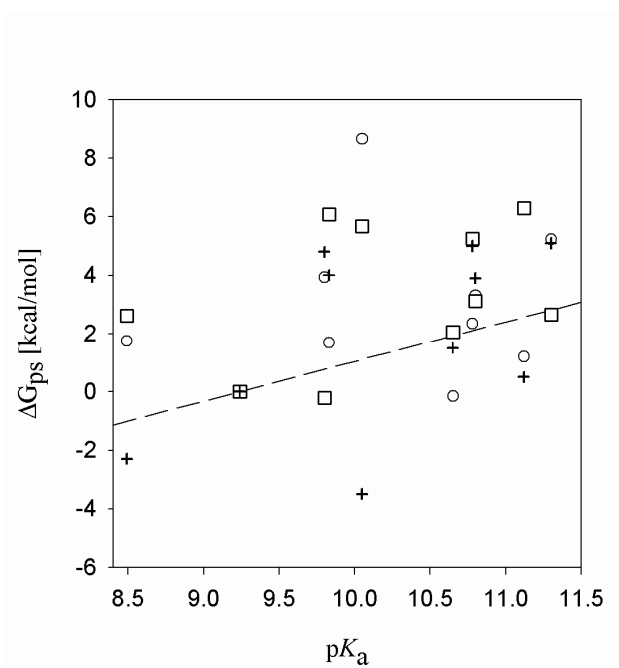


Figure 4.8 Calculated solution phase basicity versus experimental pK_a . Crosshairs are RISM-SCF, open circles are FEP-MK and squares are FEP-CM2. The stippled line indicates the theoretical trend relative to ammonia.

4 Modeling of Solvation Energy

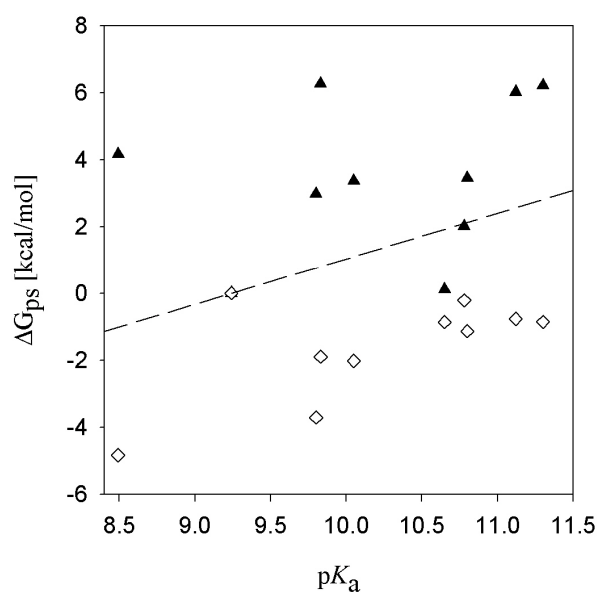


Figure 4.9 Calculated solution phase basicity versus experimental pK_a . Triangles are PCM results while diamonds are SM model. The stippled line indicates the theoretical trend relative to ammonia.

4.5.5 Conclusion

Looking at Figure 4.8 and 4.9 it is clear that none of the models produce results in full agreement with experimental data. All the models do however successfully close the large differences between relative basicities in gas phase and solution (Figure 4.7). It must however be concluded that the expectation expressed by Jones and Arnett (quotation in beginning of this chapter) over 30 years ago have only partly been met.

Cramer and Truhlar (1999) did in their review note that accurately predicting the relative basicity in solution between ammonia, methylamine, dimethylamine and trimethylamine has proven to be difficult. Amines distinguish themselves from most other functional groups in having varying number of hydrogen atoms, thereby

4 Modeling of Solvation Energy

also having a varying potential to form intermolecular hydrogen bonds. None of the present models are accurate enough to capture differences caused by such changes at a quantitative level.

The agreement with experimental data is comparable for the different models. The SM model does produce the best trend, the main error being in the solvation energy of ammonia. A rather odd feature of Figure 5.8 is that the two continuum models appear to have errors of same dimension and opposite sign for the different molecules. Agreement with experimental data for the SM model is consistent with its reported uncertainty for ionic species (Li et al. 1999). The level of agreement with experimental data for the other models is also generally in line with what is reported in the literature. It should be emphasized that all models are reasonably robust in a qualitative sense, capturing larger trends in solvation energies.

5 Reaction Mechanisms and Equilibrium

Kinetics is nature's way of preventing everything from happening all at once.

S. E. LeBlanc

5.1 Introduction

This chapter is intended to give an overview of the reaction mechanisms of CO₂ absorption in aqueous amine systems. On several key points it draws on my own work. Most of it published (da Silva and Svendsen 2004a and da Silva and Svendsen 2004b), but some not previously presented. This chapter also serves as a review of observations in the literature. In addition to providing an overview of the important aspects of CO₂ capture, this chapter is also intended to show to what extent central equilibrium constants can be modeled. This part is mainly based on my own modeling work.

5.2 Reaction Mechanisms

5.2.1 Introduction

CO₂ reacts in aqueous amine systems to form either bicarbonate or carbamate. These species are shown in the figure below. The R groups in NR₂ can be a proton or any form of substituent group.

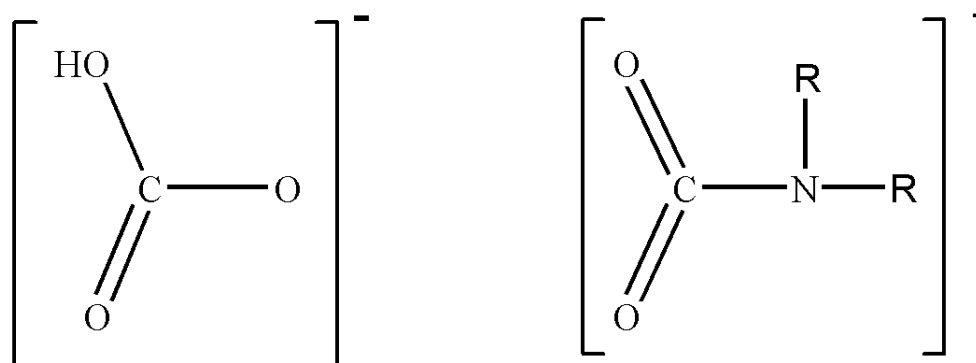


Figure 5.1 Bicarbonate and carbamate.

5 Reaction Mechanisms and Equilibrium

Bicarbonate is produced by the reaction of a CO₂ molecule with a water molecule, while carbamate is formed by the reaction of a CO₂ molecule with an amine molecule. CO₂ in the liquid is bound almost entirely in one of these two forms, and only a small fraction is found as free CO₂.

5.2.2 Bicarbonate Formation

The formation of bicarbonate from CO₂ and water is a well known reaction in chemistry. There are three (related) mechanisms for this reaction.



Bicarbonate can again be deprotonated by a base molecule (B).



The base molecule is usually an amine molecule or a hydroxyl ion (OH⁻). By itself bicarbonate formation is however a rather slow reaction. It has been observed that this reaction proceeds more quickly in the presence of amine molecules, an effect beside the direct effect of the amines acting as bases (Donaldsen and Nguyen 1980). It is also known that Brønsted bases can act to catalyze the formation of bicarbonate (Sharma and Danckwerts 1963).

Calculations have been performed to identify a mechanism that might account for this increased reaction-rate. These calculations were performed with PC Spartan (1999) at the HF/6-31G(d,p) level. Calculations were performed with one water molecule and one CO₂ molecule in the presence of an ethanolamine molecule. In

5 Reaction Mechanisms and Equilibrium

this case the reaction coordinate chosen was $O(H_2O)-C(CO_2)$. The determined transition-state geometry is shown in Figure 5.2.

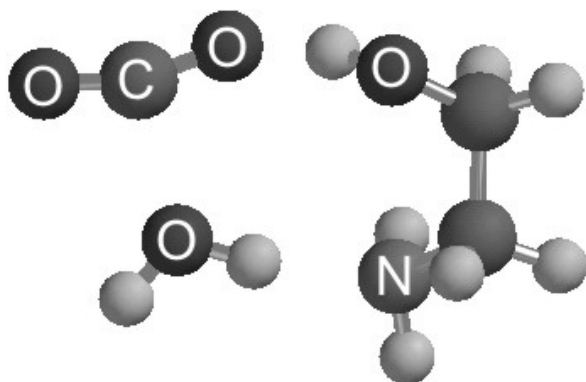


Figure 5.2 Transition state of bicarbonate formation.

The transition state identified in these calculations is consistent with the mechanism proposed by Donaldsen and Nguyen (1980):

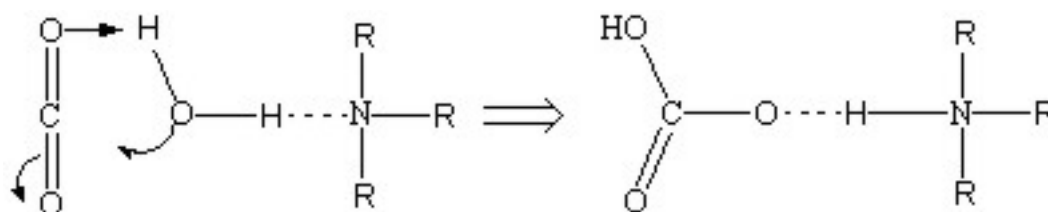


Figure 5.3

At the HF/6-31G(d,p) level this mechanism was found to have a barrier of 29.5 kcal/mol. For the bicarbonate formation in water a reaction-barrier of 42.5 kcal/mol has been reported with the same type of calculation at the same level of theory (Nguyen et al. 1997). The presence of base-molecules can therefore be seen to give a significantly lower barrier to bicarbonate formation.

5 Reaction Mechanisms and Equilibrium

While this mechanism is usually mentioned in the context of tertiary amines I do not believe it is unique to them. As observed above, it is known that base catalysis can take place for a number of Brønstad bases. The calculations suggest that this reaction will take place with any base molecule of appropriate strength. For primary and secondary amines the kinetics will however often be dominated by carbamate formation and base catalysis will play a lesser role and perhaps be more difficult to detect experimentally. Base catalysis may however be significant for primary and secondary amines in systems where bicarbonate formation dominates.

5.2.3 Carbamate formation

The carbamate formation is one of the main reactions of CO₂ absorption. Two mechanisms have been proposed for this in the literature. One is the zwitterion mechanism originally proposed by Caplow (1968):

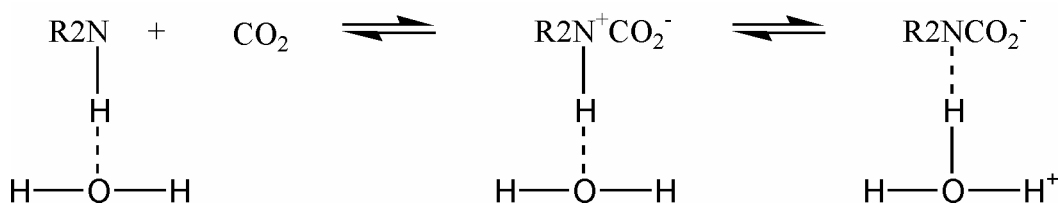


Figure 5.4

In this mechanism CO₂ forms a bond to the amine functionality in a first step. In a second step an amine-proton is transferred to a second molecule. In Caplows article the second molecule was water, but this can be any base-molecule.

The intermediate species in the reaction is a zwitterion. Caplow assumed (as shown in Figure 5.4) that a hydrogen bond is formed between the amine and a water (base) molecule before the amine reacts with the CO₂ molecule. This feature has however been omitted in the recent literature, as can be seen in the work by Danckwerts (1979), Versteeg et al. (1996) and Kumar et al. (2003).

5 Reaction Mechanisms and Equilibrium

Crooks and Donnellan (1989) proposed the following single-step mechanism:

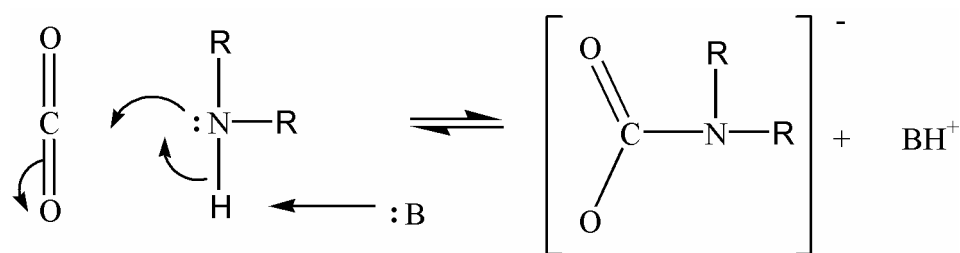


Figure 5.5

Here B is a base molecule. In this mechanism the bonding between amine and CO₂ and the proton transfer take place simultaneously.

It has been argued that the rate-expression of the zwitterion mechanism can be better used to account for experimental observations such as broken order kinetics in some solvents (Versteeg et al. 1996). In a paper appearing in this thesis (da Silva and Svendsen 2004a) the experimental evidence was reviewed and quantum mechanical calculations were carried out to determine the most likely mechanism.

A central finding from these calculations was that a CO₂ molecule does not react with an ethanolamine molecule in gas phase. The calculations strongly suggest that base molecules must be present for CO₂ to bond with amine molecules. This would again suggest that if any reaction intermediate exists it can not be very stable and is likely to be short-lived. Calculations also suggest that if a strong base (such as another amine molecule) is interacting with the amine functionality there is no barrier to the proton-transfer. This is consistent with a single-step mechanism. What could not be resolved by the calculations is what would happen if the CO₂-amine complex was solvated entirely by water molecules. In this case it is possible that the water molecules could transfer a proton to a base molecule located further away. Alternatively the CO₂-amine complex can remain stable, awaiting the approach of a base molecule. The calculations, while not entirely conclusive, suggest a single-step mechanism, or a short-lived reaction intermediate.

5 Reaction Mechanisms and Equilibrium

The two reaction mechanisms give rise to similar expressions for reaction kinetics. It was found in the review (da Silva and Svendsen 2004a) that most experimental data can be accounted for with both mechanisms. The zwitterion mechanism based rate-expression is somewhat more flexible than expressions based on the single-step mechanism, i. e. it can be fitted to a greater variety of data. There is however no experimental data that I am aware of suggesting this flexibility to be required. An argument against the zwitterion mechanism is that some parameters at times take on values that do not seem plausible (Crooks and Donnellan 1989 and Aboudheir et al. 2003). If the overall order of reaction is three it follows from the zwitterion mechanism that a proton transfer is rate-determining, a conclusion that would seem somewhat implausible.

The difficulty in drawing any definite conclusion as to what mechanism is correct stems in part from the fact that they are very similar. The zwitterion mechanism becomes equivalent to the single-step mechanism when the lifetime of the zwitterion-intermediate approaches zero. This has been somewhat obscured in the literature where the zwitterion mechanism has been written without hydrogen bonds to base molecules. The calculations would suggest that while the zwitterion mechanism is not necessarily wrong the single-step mechanism is more suited to conveying the nature of the reaction taking place.

From the quantum mechanical calculations potential reaction-barriers were also identified. The mechanism was found to have no intrinsic barrier. The kinetics is therefore likely to be dominated by the need for molecular encounters for the reaction to take place. One barrier may arise from the CO₂ molecule having to displace the solvation-shell around the amine functionality. A second barrier may be caused by the need for the CO₂, amine and a base-molecule to be aligned for reaction to take place. A study on the liquid structure of ethanolamine-water mixtures (da Silva, Kuznetsova and Kvamme 2005, also part of the present thesis) suggest that the latter of these barriers is the most significant.

5 Reaction Mechanisms and Equilibrium

As can be seen from the mechanism in Figure 5.5, the carbamate-formation involves the transfer of a proton from the amine functionality. It is well-known that amines without such protons, such as tertiary amines, do not form carbamate (Versteeg et al. 1996 and da Silva and Svendsen 2005).

5.2.4 Bases

A base molecule can by definition undergo the following reaction:



Amine molecules are all bases and they are usually the strongest bases present in the system. Water itself is a weak base, the hydroxyl-ion (OH^-) is a strong base, but usually present in small quantities. Bicarbonate is a very weak base. The carbamate species might act as a base, bonding a proton to one of the CO_2 oxygen atoms. There is however nothing in the experimental data to suggest that such protonation takes place.

5.2.5 Alcohol-Group Bonding to CO_2

It has been suggested that at very high pH values, CO_2 can bond to alcohol-groups (Jørgensen and Faurholt 1954). To investigate the possibility of such a reaction taking place calculations were carried out at HF/3-21G(d) level with PC Spartan (1999). The calculations were carried out for two ethanolamine molecules and a CO_2 molecule in vacuum. Calculations were carried out with C(CO_2)-O(ethanolamine) as a restrained reaction coordinate. The results suggest a mechanism analog to carbamate formation:

5 Reaction Mechanisms and Equilibrium

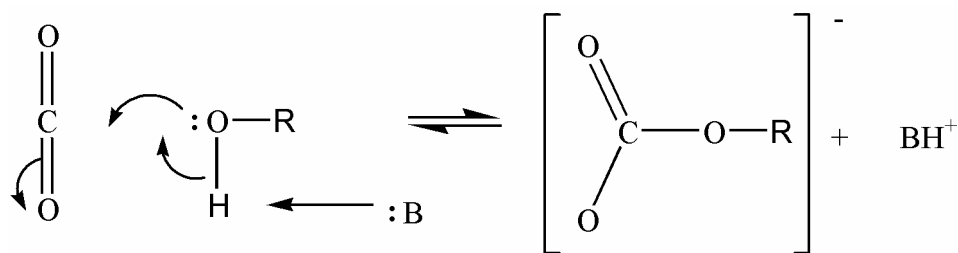


Figure 5.6

This reaction is however in general not expected to play a significant role in industrial CO₂ absorption processes as the pH of the system is usually not high enough (Versteeg et al. 1996).

5.2.6 Carbamate as Reaction Intermediate

It has been suggested that carbamate undergoes a direct hydrolysis reaction (Smith and Quinn 1979), meaning a direct reaction with water to form bicarbonate and amine. The figure below shows a HF/3-21G(d) geometry of a water molecule placed next to MEA carbamate.

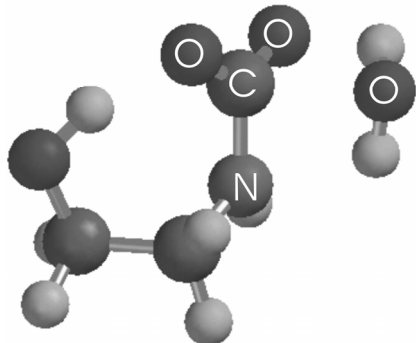


Figure 5.7 Ethanolamine carbamate interacting with a water molecule.

From such calculations no reaction path or transition-state was found. It is apparently not possible for a water molecule to bond to the CO₂-group as long as it remains bonded to the amine functionality. The water oxygen molecule must

5 Reaction Mechanisms and Equilibrium

interact with the CO₂ group in the same site as it interacts with the amine-group. I am also not aware of any experimental data that suggest that direct carbamate hydrolysis takes place. Shifts in concentration between carbamate and bicarbonate are not particularly fast and can be readily explained as the shift of equilibrium through a set of reversible reactions. If equilibrium conditions change some carbamate will revert back to amine and CO₂. This CO₂ can then go on to form bicarbonate.

In general it would seem that the bonding of carbamate species is such that it is unlikely to act as any form of reaction intermediate.

5.2.7 Molecules with Multiple Amine Functionalities

Molecules can have more than one amine functionality. Among the solvents being considered for CO₂ capture piperazine, and piperazine-derivatives have multiple amine functionalities. So does N-(2-hydroxyethyl)ethylenediamine (AEEA) which has received some attention recently (Ma'mun, Svendsen, Hoff and Juliussen 2004 and Bonenfant et al. 2005). The nature of the functional groups is the same in such molecules as in simpler amines. The form of interactions with CO₂ is therefore also likely to be the same. In the case of multiple amine functionalities there is however a greater number of species that can be formed. In Figure 5.8 the species that can be formed by piperazine are shown.

5 Reaction Mechanisms and Equilibrium

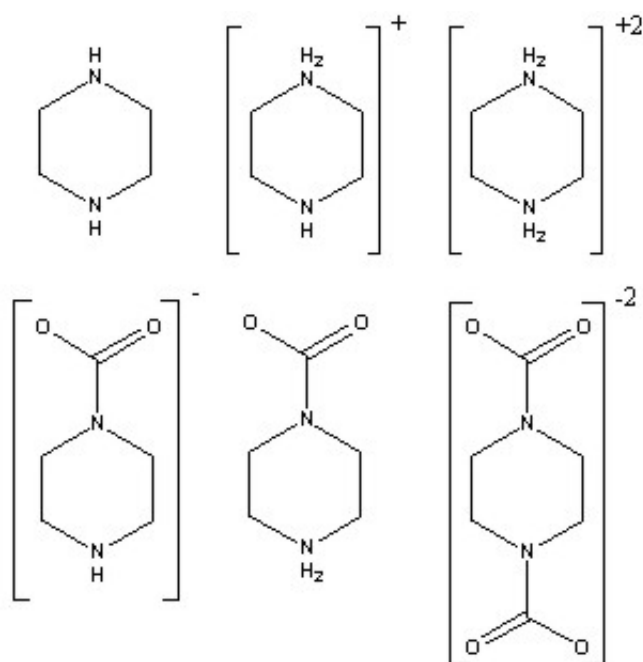


Figure 5.8 Piperazine species.

In addition to the carbamate and protonated amine there is a diprotonated species, a dicarbamate, and a form with combined protonation and carbamate formation. Experimental work and analyses by Bishnoi (2000) suggest that these species can exist in significant concentration. In piperazine the two amine functionalities are equivalent, for AEEA and other molecules with non-equivalent amine sites the number of potential species would be even greater. Systems with such amines are more difficult to study experimentally, as the number of experimentally observable properties often remains the same while the number of equilibrium constants to be determined increases significantly.

5 Reaction Mechanisms and Equilibrium

5.2.8 Shuttle Mechanism

In the absorption process CO_2 must be transferred from the gas-liquid interphase to the bulk of the liquid. The CO_2 can diffuse as a free molecule or in one of the bound forms. The diffusion process takes a significant amount of time, and may under some conditions determine the overall absorption rate.

It has been observed that mixtures of amines can absorb CO_2 more quickly than would be expected from considering the kinetics of the different species involved (Versteeg et al. 1996). This has been explained as resulting from carbamate forming species transporting CO_2 from the interface to the bulk of the liquid, where it goes on to undergo bicarbonate formation. This process has been demonstrated in absorption models and it is referred to as the shuttle mechanism (Versteeg et al. 1990). This is not a chemical reaction, but rather a phenomenon arising from the differing diffusion-rates of different species. The carbamate forming amine in this process is usually referred to as a “promoter” or “activator”.

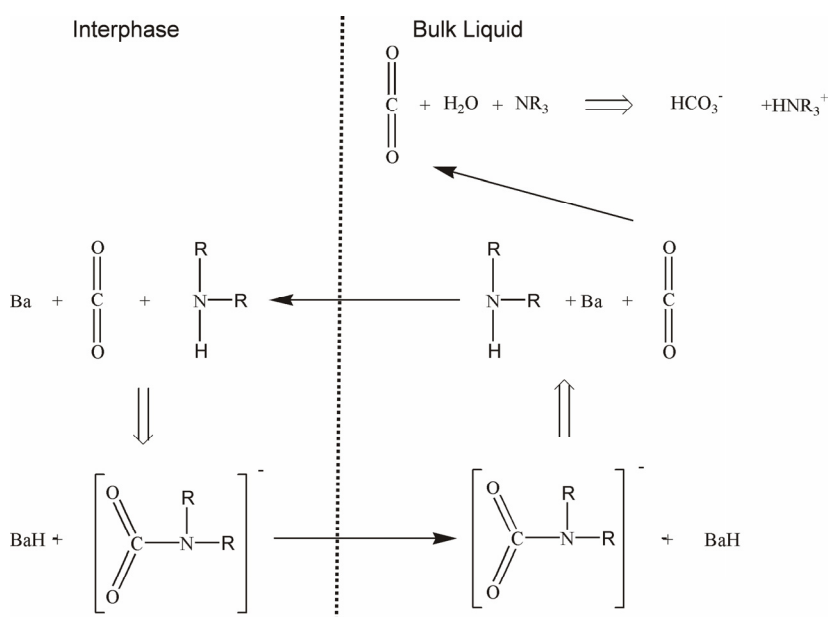


Figure 5.9 The shuttle mechanism.

5.2.9 Summary and Conclusion

As is shown in this chapter the number of reactions involved in the CO₂ absorption process is quite small. It can not be ruled out that other reactions take place, but the present set of reactions can to my knowledge account for all the observed behavior of CO₂ absorption in amine systems. Thus, all the reactions involving CO₂ can be generalized in the following simple form:

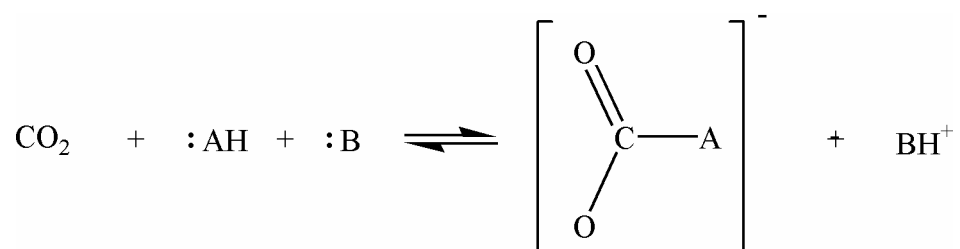


Figure 5.10

B is again a base molecule and AH is any molecule with a free-electron pair and a hydrogen atom on the same site. If AH is an amine molecule and B is a water molecule or a second amine molecule this is the carbamate formation mechanism. If AH is a water molecule and B an amine molecule the reaction is base catalysed bicarbonate formation. Finally with both AH and B as water the reaction becomes standard bicarbonate formation.

Below is given a summary of the main reaction mechanisms. Alcohol-group bonding to CO₂ is in most conditions expected not to be significant, and is omitted from this list.

5 Reaction Mechanisms and Equilibrium



B is again used to indicate a base molecule, usually an amine molecule or hydroxyl ion. This set of reactions is in itself quite small, and there are only four reactions (*I*, *II*, *III* and *VI*) that are amine specific. Three of the four amine reactions depend on the base strength of the amine, the final reactions depend on the stability of the carbamate molecule formed by a given amine. The base strength is usually given as the pK_a , and the equilibrium constant for carbamate formation will be written as K_c . The CO_2 absorption process is usually based on temperature (T) variation, and the temperature dependency of the equilibrium constants is clearly required to predict the performance of a given solvent. The equilibrium constants in the system do also change as a function of the composition (c) of the liquid, and the concentration dependency of the equilibrium constants is clearly also of importance. This means that if $pK_a(T, c)$ and $K_c(T, c)$ can be determined the absorption process for different solvents can be predicted. In other (and more correct) words it means determining the equilibrium constants, their temperature dependencies and the activity coefficients of the various components present in the liquid. This is the main goal of the present thesis. Tertiary amines do not form carbamate and for such molecules the base strength is the only equilibrium constant governing the reactivity towards CO_2 .

5.3 *Determining Equilibrium*

5.3.1 Equilibrium and Kinetics

Comparison of calculated and experimental base strengths of a series of amines (results in Chapter 4 and da Silva and Svendsen 2003) showed the models to be reasonably accurate. Determination and prediction of base strength can however be an easier task than implied by the results of these papers. Determination of base strength is fairly routine experimental work and fairly accurate data is available for a large number of molecules (Perrin 1965). Very often the pK_a of a molecule being considered as a solvent has been reported in the literature. In most of the cases where the pK_a for the molecule itself has not been reported, it has been reported for some closely related substance. The modeling task can then be reduced to determining the difference in base strength for two closely related compounds; this can usually be done with a fairly high degree of confidence.

The modeling results for carbamate stability (da Silva and Svendsen 2005) appear to be of the same quality as the results for base strength. The experimental determination of carbamate stability is much more difficult than the determination of base strength, and it is in this case much more difficult to draw on experimental data to refine estimation of equilibrium constants for new molecules.

The set of modeling results for base strength and carbamate stability together provide what can perhaps be summarized as a semi-quantitative model for new solvents.

In modeling work (da Silva and Svendsen 2005) a linear correlation was found between carbamate stability and rate of reaction. For tertiary amines a similar correlation has been found between the base strength and rate of reaction (Versteeg et al. 1996). This is not entirely surprising since all the molecules undergo analog reactions. This simple relationship between equilibrium constants and reaction

5 Reaction Mechanisms and Equilibrium

rates, suggest that predictions of equilibrium constants can also serve to predict reaction rates.

CO₂ in aqueous amine solutions reacts, as already noted, to form either carbamate or bicarbonate. Carbamate formation is in general a far more exothermic reaction than bicarbonate formation. It is in general faster than bicarbonate formation, but more energy is also required to reverse the reaction in the stripper. Two amine molecules are required to form a carbamate molecule. The loading (mol CO₂/mol amine solvent) will therefore not be much higher than 0.5 in a system dominated by carbamate formation.

An issue I have not addressed so far is what the ideal values are for base strength and carbamate stability, or to which extent carbamate formation or bicarbonate formation is preferable. At present this remains unknown. This is not a question that can be addressed with the tools of computational chemistry. A complete model of the CO₂ absorption process is required. While such models exist they have so far not been applied to this question. In Chapter 7 I will look at what the ideal characteristics might be.

5.3.2 Temperature Dependency of Equilibrium Constants

In the work on basicity (da Silva and Svendsen 2003) it was found that entropies calculated from quantum mechanical calculations could be used to predict the change in basicity over temperature. The quality of the correlation obtained was very good. The results suggest that the change in basicity over temperature depends on the nature of the intramolecular hydrogen bonding of a given molecule. Only eight molecules were however included in the study of temperature effects. A difficulty in expanding the comparison with experimental data is that experimental data for basicity is not always consistent at higher temperatures (Kamps and Maurer 1996). The prediction of changes in basicity over temperature can be a

5 Reaction Mechanisms and Equilibrium

valuable tool, particularly for higher temperatures where very little, if any, experimental data is available.

Predicting the change in the carbamate stability over temperature is more difficult. Almost no experimental data of quantitative quality is available for carbamate stability at any temperature, and this is required to obtain the change over temperature (da Silva and Svendsen 2005). Computational chemistry could be used to determine both the absolute equilibrium constant and absolute entropy values, but without any experimental data with which to compare the results, the quality of predictions made would be uncertain.

5.3.3 Activity Coefficients

The equilibrium constant models results are for infinite dilution, far from the composition that is utilized in industrial CO₂ absorption. There is therefore a need to predict how the equilibrium constants change as function of system composition. Such concentration dependency is usually given as activity coefficients for the various components

I have made some effort to model the activity coefficients for the ethanolamine-water mixture (da Silva 2004). The quality of the results was however not particularly good, no effort had been made to find an optimal force field for ethanolamine and the accuracy of the simulations could have been better. In later work I have looked at force field parameterization for ethanolamine (da Silva, Kuznetsova and Kvamme 2005), this force field has however yet not been applied in determination of activity coefficients. While I am not entirely confident that the force field presented in that paper will produce activity coefficients in full agreement with values derived from experiment, I am confident that a force field can be developed that reproduces both the properties of ethanolamine-water mixtures and pure ethanolamine.

5 Reaction Mechanisms and Equilibrium

The CO₂ absorption system consists of many components, not only water and ethanolamine. I am not aware of any work having been done to determine activity coefficients in such multi-component systems. Long simulations would probably be required to produce results with a reasonable degree of confidence; this is something that can be carried out with sufficient patience and computer-resources. Another issue is how accurate activity coefficients from simulations will be.

Vorholz et al. (2004) were able to demonstrate the salting-out effect in molecular simulation. This is an interesting result, suggesting that simulations are able to capture different effects of changing concentrations at a qualitative, if not a quantitative level.

Activity coefficients are not likely to be one of the most important factors in determining the overall performance of a solvent. A first approximation for a new solvent could be to assume that the system has the same activity coefficients as some structurally similar solvent for which experimental data is available.

5.3.4 Process Energy Consumption

I have not dealt specifically with modeling of the reaction energies and energy consumption of the system, but it can be readily determined from the modeling results for equilibrium constants. Once the constants are determined, reaction energies can be derived with thermodynamic calculations.

Reaction energies determined from computational chemistry work in the present thesis are not likely to be close to experimental values. As with the equilibrium constants I believe the best results will be obtained by using computational chemistry results to obtain relative values, these can then be anchored to results for a solvent where experimental data are available.

5 Reaction Mechanisms and Equilibrium

5.3.5 Summary

The models presented in this thesis can be used to predict the main equilibrium constants for CO₂ absorption in aqueous amine systems with a fair degree of confidence. From such predictions the solvents effectiveness as an absorber for CO₂ capture can be estimated. Results also suggest that quantum mechanical calculations can be used to predict changes in equilibrium constants over temperature. Less work has been done on determining the activity coefficients of the systems in question. Confident prediction of activity coefficients is likely to require considerable simulation work. While knowledge of activity coefficients is clearly desirable, they are not likely to be that important in predictions of the relative differences between solvents.

6 Other Solvent Properties

Why, a four-year-old child could understand this. Someone get me a four-year-old.

Grocho Marx

6.1 Introduction

In the last chapter the reaction mechanisms and equilibrium of amine-CO₂-water systems were discussed. While the equilibrium is central to the applicability of an amine solvent to CO₂ absorption there are other issues that are also of importance. The present chapter will deal with these other properties.

Properties is here used in a loose sense, issues ranging from solvability to cost will be covered. The outline will follow a prioritized order, with the properties I believe to be of greatest importance presented first. This chapter is essentially a review; the current state of knowledge for each property will be briefly discussed and the issue of modeling and prediction of behavior of new solvents will be considered.

6.2 Solubility in Water

Loss of solvent by evaporation in the stripper and absorber can be a problem. If a solvent has low solubility in water that will also limit the amine concentration under which the process can be operated. The calculation of solvation energy has been one of the main topics of my work, for the solvent itself (which is a neutral molecule) any of the solvation models utilized in the present work can produce results with a fairly high degree of confidence. The continuum models are particularly well suited for this task.

6.3 Solvent Degradation

There is in a aqueous amine system the possibility that the amine will undergo undesirable side reactions. Such reactions can result in the amine molecules degrading irreversibly. The degradation rate of the solvent can greatly influence the overall cost of operating a CO₂ absorption plant.

The solvent can be subject to three types of degradation: thermal, carbamate polymerization and oxidative (Goff and Rochelle 2004). Exhaust gases usually have a high content of oxygen, oxidative degradation can in such systems be expected to be the main cause of degradation. Thermal degradation can however be an issue for some solvent molecules (Nagao et al. 1998). Degradation is a problem for several reasons (Goff and Rochelle 2004); because the solvent is degraded new solvent must be added at regular intervals. Degradation products might also have unfavorable characteristics that the solvent itself does not have; degradation products may be toxic and corrosive. There is therefore an interest in understanding degradation mechanisms.

Degradation reactions are inherently difficult to study. Experimental work can be time-consuming as the reactions may be relatively slow, degradation may also be catalyzed by impurities in the system. Experimental monitoring of degradation is also made difficult by the lack of a priori knowledge of what degradation products are formed in a given system.

It is today believed that the oxidation process proceeds by radical reactions (Chi and Rochelle 2002 and Goff and Rochelle 2004). Radical chemistry is often complex and a large number of different products can be formed. Goff and Rochelle (2004) present a series of possible steps in degradation mechanisms for ethanolamine, but the mechanism remains uncertain.

Blanc et al. (1982) did experimental work on the degradation of diethanolamine and N-methyldiethanolamine. They separated the degradation products into basic and acid products. The basic products were amine molecules of complex structure,

6 Other Solvent Properties

while the acid products were small carboxyl acid molecules such as formic acid. Ammonia is also known to be formed in amine degradation (Goff and Rochelle 2004).

There is little reliable data on the relative degradation of different amines in the open literature. The work by Blanc et al. (1982) suggests that ethanolamine (a primary amine) degrades more quickly than secondary and tertiary amines. Kohl and Nielsen (1997) accepted this conclusion in their textbook. Substituent groups on the amine functionality itself, or on neighboring atoms, appear to protect the solvent from oxidative reactions. This insight can be used to make rough predictions of the degradation rates of different amines. Another issue is if it is the solvent molecule itself, the carbamate form or the protonated form that is most vulnerable to oxidation. There is to my knowledge no work in the literature that has brought any clear insight on this issue.

I do believe that computational chemistry calculations could be used to elucidate the reaction mechanisms and gain some insight into how the degradation rate will vary between different solvents.

For environmental reasons solvents that are biodegradable are preferable. It is however possible that a solvent resistant to oxygen and water at high temperatures is not going to degrade easily in nature. There is therefore a potential conflict between the properties desirable in a solvent in the process and after disposal.

6.4 Corrosion

Kohl and Nielsen (1997) describe corrosion as the most serious problem affecting amine gas absorption plants. They also observe that the corrosion rates vary with amine solvent. Why this is so, is however not well-understood. It is known that primary amines such as ethanolamine do have a high corrosion rate. Secondary amines such as diethanolamine have a lower corrosion rate and even lower

6 Other Solvent Properties

corrosion rates are observed for tertiary amines. It would seem, and is suggested by Kohl and Nielsen (1997), that the corrosion rate depends on the concentration of carbamate species (carbamate species often dominate in ethanolamine systems while they are not formed by tertiary amines). Predictions of carbamate formation can be obtained from the work in this thesis and this might serve to give a rough estimate of the corrosion rate associated with different solvents.

The corrosion rate is probably not only a function of the solvent and operating conditions, it can also depend on impurities in the system. Degradation products formed may also contribute to corrosion in different ways than the solvent itself. The extent of corrosion obviously depends not only on the solvent, but also on the structure of the absorption equipment and the choice of materials.

6.5 Foaming

Kohl and Nielsen (1997) describe foaming as the most common problem in amine treating plants. Foaming may result in higher loss of amine and reduced liquid-gas interphase area, thereby reducing the efficiency of the separation.

Kohl and Nielsen (1997) attribute foaming to impurities in the system. Their textbook, and much of the earlier literature on the amine absorption technology, look at plants separating CO₂ from natural gas. The amount and nature of impurities is clearly different in exhaust gases, which is the application of interest in the present work. It has been observed (Ma'mun, Svendsen, Hoff and Juliussen 2004) that 2-methylaminoethanol produces significant foam, while ethanolamine foams much less.

Foaming is a fairly complex and an, at present, not entirely predictable phenomenon (Morrison and Ross 2002). Foaming is caused by some components acting as surfactants. In an aqueous solution, amines with hydrophobic functionalities are therefore perhaps the most likely to act as surfactants and cause foaming. Methods in computational chemistry can be used to determine the extent

6 Other Solvent Properties

of hydrophobic and hydrophilic groups in a molecule. From data on hydrophobic and hydrophilic groups some estimates can perhaps be made of the likelihood of an amine contributing to foaming.

6.6 Toxicology

CO₂ absorption is a large scale industrial process and it is clearly preferable that solvents used are not highly toxic. The European Chemical Substances Information System (ESIS, European Chemicals Bureau 2005) provide data on many amine compounds. The ESIS data would suggest that most amines utilized in CO₂ absorption are to some extent toxic. This is a consequence of the amines being fairly strong organic bases. Some amines may however pose additional problems. Piperazine is for example reported by ESIS to be harmful to aquatic organisms.

Some solvents are in wide use in the industry and for these it would seem likely that issues regarding toxicology are well known. For amines that are not widely used the effects of long term exposure might be unknown. I am not aware of any correlation between amine structure and toxicology. Prediction of toxicology is likely to be extremely difficult. This is however an important issue that must be kept in mind during screening for new solvents.

6.7 Cost

The overall cost of a solvent depends on the cost of producing it and the degradation rate. If a solvent is to be applied in an industrial scale process it is of great importance that the solvent cost is not too high. The cost of producing an amine depends on the synthesis process. Determining the optimal synthesis process is a science in itself. For the solvents that are presently utilized on an industrial scale it would seem likely that the production method has been carefully selected and that costs will not change too much in the future.

6 Other Solvent Properties

For solvents that are not presently produced on a large scale it would seem likely that less work has gone into finding optimal synthesis routes. If demand for any solvent was to rise, the cost might therefore go down. It is probably at present not possible to predict the cost of producing a molecule on bulk scale. The cost of a solvent is however likely to rise with molecular size and complexity.

6.8 Precipitations

It has been observed that in some absorption systems precipitations can be formed. Some precipitations are probably the result of the amine itself precipitating as a result of lowered solvability, there might also be circumstances where some form of salt can be formed. Kumar et al. (2003) reported precipitations for CO₂ absorption with amino acid salts. This is however an issue that has received little attention in the open literature. For most solvents and under most operating conditions this is probably not an issue.

7 Present and Potential Solvents

“Tracking something,” said Winnie-the-Pooh very mysteriously.

“Tracking what?” said Piglet, coming closer

“That’s just what I ask myself. I ask myself, What?”

A. A. Milne (From Winnie-the-Pooh)

7.1 Introduction

In the last two chapters the solvent properties of importance for the performance of a CO₂ capture process were reviewed. The extent to which to different properties can be modelled and predicted was also discussed. The present chapter deals with the likelihood of finding solvents better than the ones currently in use. The first part of the chapter is a brief review of the most important solvents in use. In the second part a discussion is made of what the ideal solvent properties are. Finally the likelihood of finding a molecule with a set of properties that are ideal or at least better than ethanolamine (which represents the benchmark to beat) is discussed.

7.2 Solvents in Use

7.2.1 Ethanolamine

Ethanolamine (MEA) is currently being provided commercially as a solvent for exhaust gas CO₂ capture. It is sold under the name Econamine by Fluor enterprises (Reddy et al. 2003). The main problem with the ethanolamine processes is that the energy consumption is fairly high. MEA is known to form a stable carbamate form (da Silva and Svendsen 2005). The energy needed to free CO₂ from the carbamate form in the stripper is the cause of the high energy consumption. Ethanolamine is highly solvable in water, not very toxic and does not cause significant foaming.

7 Present and Potential Solvents

The molecule is noteworthy for being the second smallest of all alkanolamine molecules.

Ethanolamine does have a high degradation rate and can cause corrosion. In Econamine inhibitors are added to reduce degradation rates and limit corrosion.

7.2.2 Tertiary Amines

Tertiary amines do not form carbamate. They only act as bases, contributing to the formation of bicarbonate. The advantage of tertiary amines is that the equilibrium is more easily reversed in the stripper. Because the amine-CO₂ stoichiometry of bicarbonate formation is 1 to 1 tertiary amines do also have the potential to absorb large amounts of CO₂. As observed in the last chapter tertiary amines do also tend to have low degradation rates. For natural gas treatment the tertiary amine N-methyldiethanolamine (MDEA) is widely used (de Koeijer and Solbraa 2004). In exhaust gases the fraction of CO₂ in the gas phase is however lower and MDEA is thought to have too low reactivity to work efficiently in such a case. Tertiary amines are often combined with promoters in order to take advantage of the shuttle-effect (Bishnoi and Rochelle 2002 and Zhang et al. 2003).

7.2.3 Sterically Hindered Amines

Amines with one or more substituent-group on the carbon-atoms bonded to the nitrogen atom are called sterically hindered amines (Sartori and Savage 1983). Such molecules tend not to form stable carbamate forms. They will therefore mainly work as bases and contribute to bicarbonate formation. Their reactivity towards CO₂ is very similar to that of the tertiary amines. The sterically hindered amine that has seen the greatest use is probably 2-amino-2-methylpropanol (AMP).

In addition to tertiary amines and sterically hindered amines there is likely to be other amines that form less stable carbamate forms.

7 Present and Potential Solvents

7.2.4 Multiple Amine Functionalities

Some research has gone into molecules with multiple amine functionalities. Of such molecules piperazine has probably seen the greatest use. Piperazine is usually used as a promoter (Bishnoi and Rochelle 2002, Zhang et al. 2003 and Jenab et al. 2005). A problem with piperazine is that it has fairly low solvability in water. Recent work (Ma'mun et al. 2004 and Bonenfant et al. 2005) has suggested that N-(2-hydroxyethyl)ethylenediamine (AEEA) is a promising diamine solvent.

Multiple amine functionalities would suggest a potential to bind more CO₂ with a single solvent molecule. Further research is probably required to determine if there is a particular benefit in using such solvents.

7.2.5 Ionic solvents

Some research has been done on the use of solvents where the active component is an ionic amine species. Examples of this are potassium salts of taurine and glycine (Kumar et al. 2003). One advantage of such ionic amines is that there is very little loss of solvent through evaporation. The solution formed is in this case highly ionic. There is to my knowledge no data in the open literature to support any general conclusions on the merits of such solvents.

7.2.6 Patented Solvents

There are some amine systems for which data has been presented in some context (publications in journals, patents or advertisement brochures) but where the composition has been kept secret. Most notable among these are the solvents KS 1-3 (Mimura et al. 1999) developed by Mitsubishi Heavy Industries. I believe KS 1 to be a mixture of AMP with a promoter. Less is known about KS 2 and 3. The researchers at Mitsubishi have however done work on amino-amide molecules (Nagao et al. 1998) and these could be possible ingredients.

7 Present and Potential Solvents

The Canadian company Cansolv has recently filed a patent application for absorbents for CO₂ capture (Hakka and Ouimet 2004). This again appears to be a promotor based system. In this patent tertiary amines are utilized. The promoter is piperazine or a derivative of piperazine. The novel feature of this patent appears to be the use of oxidation inhibitors and molecules with two tertiary amine functionalities, such as N, N, N',N'-tetrakis(hydroxyethyl) 1,6-hexanediamine.

7.3 Ideal Solvent Properties

7.3.1 Equilibrium Constants

The chemistry of CO₂ absorption is governed by the basicity and carbamate stability of the solvent. Too high equilibrium constants will result in a too high energy consumption, while too low equilibrium values will result in CO₂ not being absorbed to any significant degree. It is therefore not an issue of simply finding the solvent with strongest or weakest bonding to CO₂, there is rather some intermediate values that will provide an optimum trade-off between uptake of CO₂ and energy consumption. I am however not aware of any work that provides insight into what these optimal values are. This is not an issue that can be addressed by computational chemistry. To answer the question of what the optimal equilibrium values are a model of the entire absorption process is required. While such models are available their application is not trivial and most are developed for a specific solvent, rather than as general models. It does however seem likely that these models, with some further development, can be utilized to answer this question.

While modelling work is required to determine optimal equilibrium constants some suggestions can be made based on the performance of solvents presently in use. The optimal process may utilize a single solvent or a mixture of different solvent components. Use of solvents with multiple amine functionalities is a further option. I will consider each option separately.

7 Present and Potential Solvents

Use of a single amine solvent is the simplest option. Two solvents for which the performance is fairly well understood are MEA and MDEA. MEA forms a fairly stable carbamate form and is regarded as having too high energy consumption. MDEA only acts as a base and only bicarbonate is formed. This solvent is also a relatively weak base having a pK_a of only 8.5 (Perrin 1965) where as MEA has a pK_a of 9.5 (Perrin 1965). While use of MDEA results in a lower energy consumption than is the case for MEA, it is regarded as having a too low capacity to bind CO_2 for the exhaust gas application. The ideal amine solvent should then have base strength and carbamate stability somewhere between these two solvents. It is not clear if a non-carbamate forming amine is suitable as a single solvent for exhaust gas applications, if it were to work it would have to have a high base strength. A carbamate forming molecule should probably have carbamate stability somewhat lower than ethanolamine.

Mixtures of solvents are usually used to draw advantage of the shuttle-effect described in Chapter 5. In such cases one amine works as a carbamate forming promoter, while another amine mainly works to form bicarbonate. For the bicarbonate forming molecule a stronger base than MDEA is probably preferable (for the same reason as given for a single solvent system). The shuttle-mechanism probably works optimally for some given level of carbamate strength. While it is difficult to determine what that ideal carbamate stability is for this mechanism, some tentative conclusions can perhaps be drawn from the promoters currently in use. Both piperazine and MEA are used as promoters (Bishnoi and Rochelle 2002 and Aroonwilas and Veawab 2004). Both these molecules form relatively stable carbamate forms (da Silva and Svendsen 2005). This would suggest that ideal promoters are relatively strong carbamate formers. If KS1 (Mimura et al. 1999) is indeed promoted AMP, its properties fall within the present recommendations, AMP having a pK_a of 9.7 (Perrin 1995).

7 Present and Potential Solvents

In addition to taking advantage of the shuttle-effect, solvent mixtures can also be used to control the degree of CO₂ capture or energy consumption. If a single solvent does not have ideal performance, a mixture of solvents can be utilized. By varying concentration ratios the overall performance can be controlled. In such a case both solvents should have properties that would have made them viable in a single component system.

Finally there is the use of solvents with multiple amine functionalities. These can be utilized as a single solvent, or as promoter or bicarbonate former in a mixture of solvents. The chemistry is in this case more complex than for a solvent with a single amine functionality. The conditions given for a single amine functionality solvent in terms of base strength and carbamate stability should also be met by a solvent with multiple amine functionalities. I have however no basis to suggest what the ideal equilibrium values for secondary protonation or carbamate formation is. Some degree of chemical reactivity on all sites is probably preferable; otherwise part of the molecule will be “dead weight”.

For the temperature dependence the issue is more straightforward; the greater the fall in carbamate stability and base strength over temperature the better. Greater temperature dependency increases the net amount of CO₂ that can be transported from the absorber to the stripper (the cyclical capacity). It could also be taken advantage of to operate the stripper at lower temperature, thereby reducing the energy consumption.

7.3.2 Other Properties

For the other properties discussed in the last chapter the ideal characteristics are obvious. The solvent should have as high solvability in water as at all possible. It should not foam, have low degradation rate, be inexpensive and not toxic.

7.4 Comparison with Ethanolamine

From these conclusions we can then turn to the crucial issue: What is the likelihood of finding solvent molecules that are better than MEA. Since the ideal equilibrium constants are not known, it is difficult to draw any conclusions as to how far ethanolamine is from being an optimal solvent and how much room there is for improvement. I suspect that a less stable carbamate form is optimal, but how much the energy consumption can be lowered is hard to estimate.

MEA is probably the smallest and simplest solvent molecule that can be applied in the CO₂ capture process. It is for that reason likely to remain one of the cheapest solvents to manufacture. It is also not particularly toxic. MEA does however have a high degradation rate (Blanc et al. 1982) and many other solvents are likely to offer improvements over ethanolamine in this respect.

Overall this analysis would suggest that it is likely that solvents better than ethanolamine can be found. The KS1 solvent (Mimura et al. 1999) has perhaps already achieved this, and there is no reason to believe that this can not be improved further upon. How great improvements that can be expected in terms of energy consumption and operating cost is however difficult to estimate.

7.5 Conclusion

I have in this work not presented a specific list of candidate molecules for the absorption process. To the question of what the ideal solvent molecule(s) is, the present work provides a fairly detailed blueprint of how to answer the question, but not the answer itself.

The screening process required to come up with a range of candidate molecules would in itself be time-consuming. At the same time there have not been resources available at our laboratory to test new candidate molecules resulting from such a screening process.

7 Present and Potential Solvents

Some general rules for design of solvent molecules can however be proposed. The ratio of hydrophilic to hydrophobic groups must be kept high, that usually means high number of hydroxyl-groups and low number carbon-based groups. For a reasonable basicity to be obtained there should be at least two carbon-groups between hydroxyl- and amine-functionalities.

In general it appears that high basicity is desirable. High carbamate stability may be desirable for promoters, but is probably not so for the main solvent component.

8 Future Work

“Begin at the beginning,” the King said gravely, “and go on till you come to the end; then stop.”

Lewis Carroll (from Alice in Wonderland)

8.1 Continuation of the Present Research

There are several ways in which the present work can be expanded and improved upon. Degradation mechanisms are one particular area where I believe computational chemistry could be applied to obtain greater insight. Computational chemistry methods can also be utilized together with experimental spectroscopy work to obtain a more detailed understanding of the various species present in a CO₂ absorption process.

On the issue of liquid structure and activity coefficients the present work is quite limited. It should with simulations be possible to form a quite detailed understanding of the liquid structure of amine-water systems. Such work can also contribute to the determination of activity coefficients of various species.

Computers and the methods of computational chemistry are in continuous development, and it is almost certain that the calculations of reaction energies presented in this work can be improved upon.

The purpose of this work has been to contribute to the development of new solvents. The next step should be to apply this model work in the selection of new solvents for experimental work. New experimental data can also be used to validate the modeling work, and offer guidance for further modeling.

8.2 Other Applications of Present Work

Determining free energies of solution and reactivity of organic molecules in aqueous solution is a major topic in computational chemistry. My own work has to

8 Future Work

a large extent consisted of applying models in this area to the particular issue of CO₂ capture technology. The present work should therefore also be of interest as an exercise in applying and validating models to calculate free energies in solution.

The present work has shown that computational chemistry tools can be successfully applied to further the understanding of the CO₂ absorption process. While the work has been focused on the treatment of exhaust gases the work could also be used to find optimal solvents for CO₂ removal from natural gas. It is also likely that the same methods as applied in the present work can be applied to study other issues in gas processing.

8.3 Beyond Amines

My work has focused solely on absorbing CO₂ with amine solvents. There are however other chemical reactions resulting in CO₂ being bonded, and some of these reactions might perhaps be used to capture CO₂. CO₂ is captured in large amounts in the natural photosynthesis process (Lawlor 2000). Another noteworthy process is the catalyzed formation of CO₂ from bicarbonate in the human body (Palmer and van Eldik 1983). There are also other reactions where CO₂ binds to metal-complexes or organic compounds (Halmann 1993).

Many reagents or catalysts might turn out to be too expensive to be used in the large scale capture of CO₂. It would however seem worthwhile to carry out a more general study of the various ways CO₂ can interact with other molecules to see if any mechanism can be taken advantage of in capture technology.

References

Aboudheir, A., Tontiwachwuthikul, P., Chakma, A. and Idem, R. (2003) Kinetics of the reactive absorption of carbon dioxide in high CO₂-loaded, concentrated aqueous monoethanolamine solutions *Chem. Eng. Sci.* 58, 5195-5210.

ACIA (2004) Impacts of a Warming Arctic: Arctic Climate Impact Assessment. Cambridge University Press.

Alejandro, J.; Rivera, J. L.; Mora, M. A.; de la Garza, V. J. (2000) Force Field of Monoethanolamine *Phys. Chem. B* 104, 1332-1337.

Allen, M. P. and Tildesley, D. J. (1987) Computer Simulations of Liquids, Oxford Science Publications, UK.

Andzelm, J. Kölmer, C. and Klamt, A. (1995) Incorporation of solvent effects into density functional calculations of molecular energies and geometries *J. Chem. Phys.* 103, 9312-9320.

Aroonwilas, A. and Veawab, A. (2004) Characterization and comparison of the CO₂ absorption performance into single and blended alkanolamines in a packed column *Ind. Eng. Chem. Res.* 443, 2228-2237.

Bacskay, G. B. and Reimers, J. D. (1998) In *Encyclopaedia of Computational Chemistry*, Schleyer, P. von R., Ed., Wiley.

Bayly, C. I., Cieplak, P., Cornell, W. D. and Kollman, P. A. (1993) A Well-Behaved Electrostatic Potential Based Method Using Charge Restraints for Deriving Atomic Charges: The RESP Model *J. Phys. Chem.* 1993, 97, 10269-10280.

Ben-Naim, A. (1992) *Statistical Thermodynamics for Chemists and Biochemists*, Plenum.

Ben-Naim, A. and Marcus, Y. (1984) Solvation thermodynamics of nonionic solutes *J. Chem. Phys.* 81, 2016-2027.

References

Bishnoi, S. (2000) Carbon Dioxide Absorption and Solution Equilibrium in Piperazine Activated Methyldiethanolamine, Dissertation, University of Texas at Austin, USA.

Bishnoi, S. and Rochelle, G. T. (2002) Absorption of Carbon Dioxide in Aqueous Piperazine/Methyldiethanolamine *AIChE J.* 48, 2788-2799.

Blanc, C., Grall, M. and Demarais G. (1982) The part played by degradation products in the corrosion of gas sweetening plants using DEA and MDEA, Laurence Reid Gas Conditioning Conference Proceedings, Univ. of Oklahoma, Norman, USA.

Bolland, O. (2004) CO₂ Capture Technologies-an Overview. The Second Trondheim Conference on CO₂ Capture, Transport and Storage.

Bonenfant, D., Mimeault, M. and Hausler, R. (2005) Comparative analysis of the carbon dioxide absorption and recuperation capacities in aqueous 2-(2-aminoethylamino)ethanol (AEE) and blends of aqueous AEE and N-methyldiethanolamine solutions *Ind. Eng. Chem. Res.* 44, 3720-3725.

Button, J. K., Gubbins, K. E., Tanaka, H. and Nakanishi, K. (1996) Molecular Dynamics Simulation of Hydrogen Bonding in Monoethanolamine *Fluid Phase Eq.* 116, 320-325.

Cances, M. T., Mennucci, V. and Tomasi, J. (1997) A new integral equation formalism for the polarizable continuum model: Theoretical background and applications to isotropic and anisotropic dielectrics *Chem. Phys.* 107, 3032-3041.

Caplow, M. (1968) Kinetics of Carbamate Formation and Breakdown *J. Am. Chem. Soc.* 90, 6795-6803.

Car, R. and Parrinello, M. (1985) Unified Approach for Molecular Dynamics and Density-Functional Theory *Phys. Rev. Lett.* 55, 2471-2474.

Chakraborty, A. B., Bischoff, K. B., Astarita, G. and Damewood, J. R. (1988) Molecular Orbital Approach to Substituent Effects in Amine-CO₂ Interactions *J. Am. Chem. Soc.* 110, 6947-6954.

Chambers, C. C., Hawkins, G. D., Cramer, C.J. and Truhlar, D. G. (1996) Model for aqueous solvation based on class IV atomic charges and first solvation shell effects *J. Phys. Chem.* 100, 16385-16398.

References

Chandler, D. and Andersen, H. C. (1972) Optimized Cluster Expansions for Classical Fluids. II Theory of Molecular Liquids *J. Chem. Phys.* 57, 1930-1937.

Chapman, W. G., Gubbins, K. E., Jackson, G and Radosz, M (1989) SAFT: Equation-of-State Solution Model for Associating Fluids *Fluid Phase Eq.* 52, 31-38.

Chapman, W. G., Gubbins, K. E., Jackson, G and Radosz, M (1990) New Reference Equation of State for Associating Liquids *Ind. Eng. Chem. Res.* 29, 1709-1721.

Chi, S. and Rochelle, G. T. (2002) Oxidative Degradation of Monoethanolamine *Ind. Eng. Chem. Res.* 41, 4178-4186.

Cornell, W. L., Cieplak, P., Bayly, C. I., Gould, I. R., Merz, K. M., Ferguson, D. M., Spellmeyer, D. C., Fox, T., Caldwell, J. W. and Kollman, P. A. (1995) A Second Generation Force Field for the Simulation of Proteins, Nucleic Acids, and Organic Molecules *J. Am. Chem. Soc.* 117, 5179-5197.

Cossi, M. Barone, V. Cammi, R. and Tomasi, J. (1996) Ab initio study of solvated molecules; a new implementation of the polarizable continuum model *Chem. Phys. Lett.* 255, 327-335.

Cramer, C. C. (2002) *Essentials of Computational Chemistry*. John Wiley & Sons, UK.

Cramer, C. J. and Truhlar, D. G. (1999) Implicit Solvation Models: Equilibria, Structure, and Dynamics *Chem. Rev.* 99, 2161-2200.

Crooks, J.E. and Donnellan, J.P. (1989) Kinetics and Mechanism of the Reaction between Carbon Dioxide and Amines in Aqueous Solution *J. Chem. Soc. Perkins Trans., II*, 331-333.

Cummins, P. L. and Gready, J. E. (1997) Coupled Semiempirical Molecular Orbital and Molecular Mechanics Model (QM/MM) for Organic Molecules in Aqueous Solution *J. Comp. Chem.* 18, 1496-1512.

Danckwerts, P. V. (1979) The Reaction of CO₂ with Ethanolamine *Chem. Eng. Sci.* 34, 443-446.

da Silva, E. F. (2004) Use of Free Energy Simulations to predict Infinite Dilution Activity Coefficients *Fluid Phase Eq.* 221, 15-24.

References

- da Silva, E. F., Kuznetsova, T. and Kvamme, B. (2005) Molecular Dynamics Study of Ethanolamine as a Pure Liquid and in Aqueous Solution.
- da Silva, E. F. and Svendsen, H. , F. (2003) Prediction of the pKa Values of Amines Using ab Initio Methods and Free Energy Perturbations *Ind. Eng. Chem. Res.* 42 , 4414-4421.
- da Silva, E. F. and Svendsen, H. , F. (2004a) Ab Initio study of the reaction of carbamate formation from CO₂ and alkanolamines *Ind. Eng. Chem. Res.* 43, 3413-3418.
- da Silva, E. F. and Svendsen, H. , F. (2004b) The Chemistry of CO₂ Absorption in Amine Solutions studied by Computational Chemistry. 7th International Conference on Greenhouse Gas Control Technologies, Vancouver, Canada.
- da Silva, E. F. and Svendsen, H. , F. (2005) Study of the Carbamate Stability of Amines Using ab Initio Methods and Free-Energy Perturbations.
- da Silva, E. F., Yamazaki, T. and Hirata, F. (2005) Comparison of Solvation Models in the Calculation of Amine Basicity.
- de Koeijer, G. (2004) CCP Technologies-The Norwegian Scenario. International Test Network for CO₂ capture: Report on 6th Workshop.
- de Koeijer, G. and Solbraa, E. (2004) High Pressure Gas Sweetening with Amines for Reducing CO₂ Emissions. 7th International Conference on Greenhouse Gas Control Technologies, Vancouver, Canada.
- Donaldson, T. L. and Nguyen, Y. N. (1980) Carbon Dioxide Reaction Kinetics and Transport in Aqueous Amine Membranes *Ind. Eng. Chem. Fundam.* 19, 260-266.
- Duffy, E. M. and Jorgensen, W. L. (2000) Prediction of Properties from Simulations: Free Energies of Solvation in Hexadecane, Octanol and Water *J. Am. Chem. Soc.* 122, 2878-2888.
- Eckart, F. and Klamt, F. (2002) Fast Solvent Screening via Quantum Chemistry: COSMO-RS Approach *AIChE J.* 48, 369-385.
- Eimer, D. (1994) Simultaneous Removal of waater and hydrogen sulphide from natural gas, Dissertation, Norwegian University of Science and Technology, Norway.

References

Erga, O. Juliussen, O. and Lidal, H. (1995) Carbon Dioxide Recovery by Means of Aqueous Amines *Energy Convers. Mgmt.* 36, 387-392.

European Chemicals Bureau, European Chemical Substances Information System (accessed 2005) <http://ecb.jrc.it/>

Fischer, J. (1983) Remarks on molecular approaches to liquid mixtures *Fluid Phase Eq.* 10, 1-7.

Franckl, M. M., Chirlian, L. (2000) In Reviews in Computational Chemistry Lipkowitz, K. B., Boyd, D. B., Ed., Volume 14, Wiley-VCH, 1-31.

Fredenslund, A., Gmehling, J. and Rasmussen, P. (1977) Vapour-liquid equilibrium using UNIFAC, Elsevier, Amsterdam, the Netherlands.

Frenkel, D. and Smit, B. (2002) Understanding molecular simulation, Academic Press, USA.

Frisch, M. J., Trucks, G. W., Schlegel, H. B., Scuseria, G. E., Robb, M. A., Cheeseman, J. R. Zakrzewski, V. G. Montgomery, Jr. J. A., Stratmann, R. E. Burant, J. C. Dapprich, S. Millam, J. M. Daniels, A. D. Kudin, K. N. Strain, M. C. Farkas, O. Tomasi, J. Barone, V. Cossi, M. Cammi, R. Mennucci, B. Pomelli, C. Adamo, C. Clifford, S. Ochterski, J. Petersson, G. A. Ayala, P. Y. Cui, Q. Morokuma, K. Malick, D. K. Rabuck, A. D. Raghavachari, K. Foresman, J. B. Cioslowski, J. Ortiz, J. V. Baboul, A. G. Stefanov, B. B. Liu, G. Liashenko, A. Piskorz, P. Komaromi, I. Gomperts, R. Martin, R. L. Fox, D. J. Keith, T. Al-Laham, M. A. Peng, C. Y. Nanayakkara, A. Challacombe, M. Gill, P. M. W. Johnson, B. Chen, W. Wong, M. W. Andres, J. L. Gonzalez, C. Head-Gordon, M. Replogle, E. S. and Pople, J. A. (1998) Gaussian 98, Revision A.9, Gaussian, Inc., Pittsburgh PA.

Gao, J., (1996) In Reviews in Computational Chemistry Lipkowitz, K. B., Boyd, D. B., Ed., Volume 7, Wiley-VCH, 119-185.

Goff, G. S. and Rochelle, G. T. (2004) Monoethanolamine Degredation: O₂ Mass Transfer Effects under CO₂ Capture Conditions *Ind. Eng. Chem. Res.* 43, 6400-6408.

Grant, G. H. and Richards, W. G. (1995) Computational Chemistry. Oxford University Press, UK.

References

Gray, C. G. and Gubbins, K. E. (1984) *Theory of Molecular Fluids*, Clarendon Press, Oxford, UK.

Gubskaya, A. V. and Kusilik, P. G. (2004a) Molecular Dynamics Simulation Study of Ethylene Glycol, Ethylenediamine, and 2-amionethanol. 1. The Local Structure in Pure Liquids *J. Phys. Chem. A* 108, 7151-7164.

Gubskaya, A. V. and Kusilik, P. G. (2004b) Molecular Dynamics Simulation Study of Ethylene Glycol, Ethylenediamine, and 2-amionethanol. 2. Structure in Aqueous Soutlions *J. Phys. Chem. A* 108, 7165-7178.

Hakka, L. and Ouimet, M. A. (2004) Method for recovery of CO₂ from gas streams, US patent application 2004/0253159.

Halmann, M. M. (1993) *Chemical Fixation of Carbon Dioxide*. CRC Press, USA.

Hansen, J. P. and McDonald, I. R. (1990) *Theory of Simple Liquids*, 2nd ed., Academic Press, London, UK.

Haug, M. (2004) IEA World Energy Investment Outlook and the Prospects for Carbon Capture and Storage. 7th International Conference on Greenhouse Gas Control Technologies, Vancouver, Canada.

Hepple, R. P. and Benson, S. M. (2005) Geologic storage of carbon dioxide as a climate change mitigation strategy: performance requirements and the implications of surface seepage *Environ. Geol.* 47, 576-585.

Herzog H., Eliasson, B. and Kaarstad, O. (2000) Capturing greenhouse gases *Scientific American* 282, 72-79.

Hirata, F. Ed. (2003) *Molecular Theory of Solution*, Kluwer Academic Publishers.

Hoff, K. A. (2003) *Modeling and Experimental Study of Carbon Dioxide Absorption in a Membrane Contactor*, Dissertation, Norwegian University of Science and Technology, Norway.

Hunter, E. P. and Lias, S. G. (2003) Proton Affinity Evaluation, National Institute of Standards and Technology, Gaithersburg, MD, <http://webbook.nist.gov>.

International Panel on Climate Change (2001a) *Climate Change 2001: The Scientific Basis*.

References

International Panel on Climate Change (2001b) Climate Change 2001: Impacts, Adaptation and Vulnerability.

International Panel on Climate Change (2001c) Climate Change 2001: Mitigation.

Jamroz, M. H., Dobrowolski, J. and Borowiak, M. (1997) Ab initio study on the 1:2 reaction of CO₂ with dimethylamine *J. Mol. Struct.* 404, 105-111.

Jenab, M. H., Abdi, M. A., Najibi, S. H., Vahidi, M. and Matin, N. S. (2005) Solubility of Carbon Dioxide in Aqueous Mixtures of *N*-Methyldiethanolamine + Piperazine + Sulfolane *J. Chem. Eng. Data* 50, 583-586.

Jones, F. M. and Arnett, E. M. (1974) Thermodynamics of Ionization and Solution of Aliphatic Amines in Water *Prog. Phys. Org. Chem.* 11, 263-322.

Jónsdóttir, S. O., Klein, R. A. and Rasmussen, K. (1996) UNIQUAC interaction parameters for alkane/amine systems determined by Molecular Mechanics *Fluid Phase Eq.* 115, 59-72.

Jorgensen, W. L., Maxwell, D. S. and Tirado-Rives, J. (1996) Development and Testing of the OPLS All-Atom Force Field on Conformational Energetics and Properties of Organic Liquids *J. Am. Chem. Soc.* 118, 11225-11236.

Jorgensen, W. L. and Ravimohan, C. (1985) Monte Carlo simulation of differences in free energies of hydration *J. Chem. Phys.* 83, 3050-3054.

Jørgensen, E. and Faurholt, C. (1954) Reactions between Carbon Dioxide and Amino Alcohols *Acta Chem. Scand.* 8, 1141-1144.

Kaminski, G. A. and Jorgensen, W. L. (1998) A Quantum Mechanical and Molecular Mechanical Method Based on CM1A Charges. Applications to Solvent Effects on Organic Equilibria and Reactions *J. Phys. Chem. B* 102, 1787-1796.

Kamps, A. P.-S. and Maurer, G. (1996) Dissociation Constant of *N*-Methyldiethanolamine in Aqueous Solution at Temperatures from 278 K to 368 K *J. Chem. Eng. Data* 41, 1505-1513.

Kawata, M., Ten-no, S., Kato, S. and Hirata, F. (1996) Theoretical study of the basicities of methylamines in aqueous solution: A RISM-SCF calculation of solvation Thermodynamics *Chem. Phys.* 203, 53-67.

References

- Kjellander, R. (1992) The basis of statistical thermodynamics, University of Göteborg, Sweden.
- Klamt, A. (1995) Conductor-Like Screening Model for Real Solvents: A New Approach to the Quantitative Calculation of Solvation Phenomena *J. Phys. Chem.* 99, 2224-2235.
- Klamt, A., Jonas, V., Bürger, T. and Lohrenz, J. C. W. (1998) Refinement and Parameterization of COSMO-RS *J. Phys. Chem. A* 102, 5074-5085.
- Kofke, D. (2005) Free energy methods in molecular simulation *Fluids Fluid Phase Eq.* 228-229, 41-48.
- Kofke, D. A. and Cummings, P. T. (1997) Quantitative comparison and optimization of methods for evaluating the chemical potential by molecular simulation *Mol. Phys.* 92, 973-996.
- Kofke, D. A. and Cummings, P. T. (1998) Precision and accuracy of staged free-energy perturbation methods for computing the chemical potential by molecular simulation *Fluid Phase Eq.* 150-151, 41-49.
- Kohl, A. and Nielsen, R. (1997) Gas Purification, Gulf Publishing Company, Houston, USA.
- Kollman, P. (1993) Free Energy Calculations: Applications to Chemical and Biochemical Phenomena *Chem. Rev.* 93, 2395-2417.
- Kumar, P. S., Hogendoorn, J. A., Versteeg, G. F. and Feron, P. H. (2003) Kinetics of the reaction of CO₂ with aqueous potassium salt of taurine and glycine *AIChE J.* 49, 203-213.
- Kuuskra, V., DiPietro, P., Klara, S. and Forbes, S. (2004) Future U.S. Greenhouse Gas Emission Reduction Scenarios Consistent with Atmospheric Stabilization of Concentrations. 7th International Conference on Greenhouse Gas Control Technologies, Vancouver, Canada.
- Kvamme, B. (2002) Thermodynamic properties and dielectric constants in water/methanol mixtures by integral equation theory and molecular dynamics simulations *Phys. Chem. Chem. Phys.* 4, 942-948.

References

- Kvamsdal, H. M., Maurstad, O., Jordal, K. and Bolland, O. (2004) Benchmark of gas-turbine cycles with CO₂ capture. 7th International Conference on Greenhouse Gas Control Technologies, Vancouver, Canada.
- Lawlor, D. W. (2000) Photosynthesis, 3rd edition, BIOS Scientific Publishers Ltd, Oxford, UK.
- Li, J., Zhu, T., Cramer, C. J. and Truhlar, D. G. (1998) New Class IV Charge Model for Extracting Accurate Partial Charges from Wave Functions *J. Phys. Chem. A* 102, 1820-1831.
- Li, J., Zhu, T., Hawkins, G. D., Winget, P., Daniel A. Liotard, D. A., Cramer, C. J., and Truhlar, D. G. (1999) Extension of the platform of applicability of the SM5.42R universal solvation model *Theor. Chem. Acc.* 103, 9-63.
- Lue, L. and Blankshtein, D. (1995) Application of integral equation theories to predict the structure, thermodynamics and phase behavior of water *J. Chem. Phys.* 102, 5427-5437.
- Ma'mun, S. Nilsen, R. and Svendsen, H. F (2005) Solubility of Carbon Dioxide in 30 mass% Monoethanolamine and 50 mass% Methyl-diethanolamine Solutions *J. Chem. Eng. Data.* 50, 630-634.
- Ma'mun, S., Svendsen, H. F., Hoff, K. A. and Juliussen, O. (2004) Selection of new absorbents for carbon dioxide capture. 7th International Conference on Greenhouse Gas Control Technologies, Vancouver, Canada.
- Miertus, S., Scrocco, E, and Tomasi, J (1981) Electrostatic Interaction of a Solute with a Continuum. A direct Utilization of Ab Initio Molecular Potentials for the Prevision of Solvent Effects *Chem. Phys.* 55, 117-129.
- Mimura, T., Satsumi, S., Iijima, M. and Mitsuoka, S. (1999) Development on Energy Saving Technology for Flue Gas CO₂ Recovery by the Chemical Absorption Method in Power Plant. *Greenhouse Gas Control Technol., Proc Int Conf., 4th* 71.
- Morrison, I. D. and Ross, S. (2002) Colloidal Dispersions. John Wiley & Sons, New York, USA.
- Nagao, Y., Hayakawa, A., Suzuki, H., Iwaki, T., Mimura, T. and Suda, T. (1998) Comparative study of various amines for the reversible absorption capacity of carbon dioxide *Studies in Surf. Sci. and Catalysis* 114, 669-672.

References

- Nguyen, M. T., Raspoet, G., Vanquickenborn, L. G. and Van Duijnen, P. T. (1997) How Many Water Molecules Are Actively Involved in the Neutral Hydration of Carbon Dioxide *J. Phys. Chem.* 101, 7379-7388.
- Ohno, K., Inoue, Y., Yoshida, H. and Matsuura, E. (1999) Reaction of aqueous 2-(N-methylamino)ethanol solutions with carbon dioxide. Chemical species and their conformations studied by vibrational spectroscopy and ab initio theories *J. Phys. Chem. A* 103, 4283-4292.
- Ohno, K., Matsumoto, H., Yoshida, H., Matsuura, H., Iwaki, T. and Suda, T. (1998) Vibrational spectroscopic and ab initio studies on conformations of the chemical species in a reaction of aqueous 2-(N,N-dimethylamino)ethanol solutions with carbon dioxide. Importance of strong NH+center dot center dot center dot O hydrogen bonding *J. Phys. Chem. A* 102, 8056-8062.
- Onsager, L. (1936) Electric Moments of Molecules in Liquids *J. Am. Chem. Soc.* 58, 1486-1493.
- Orozco, M. and Javier Luque, F. (2000) Theoretical Methods for the Description of the Solvent Effect in Biomolecular Systems *Chem. Rev.* 100, 4187-4225.
- Oscarson, J. L., Vandam R. H., Christensen, J. J. and Izatt, R. M. (1989) Enthalpies Of Absorption Of Carbon-Dioxide In Aqueous Diethanolamine Solutions *Thermochimica Acta* 146, 107-114.
- Palmer, D. A. and van Eldik, R. (1983) The Chemistry of Metal Carbonato and Carbon Dioxide Complexes *Chem. Rev.* 83, 651-731.
- PC Spartan (1999) Version 1.0.7, Wavefunction, Inc., 18401 Von Karmen Ave. #370 Irvine, CA 92715, USA.
- Perrin, D. D. (1965, Supplement 1972) Dissociation Constants of Organic Bases in Aqueous Solution. Butterworths, London.
- Poplsteinova, J. (2004) Absorption of Carbon Dioxide-Modeling and Experimental Characterization, Dissertation, Norwegian University of Science and Technology, Norway.
- Prausnitz, J., Lichtentaler, R. and Gomes de Azevedo, E. (1999) Molecular Thermodynamics of Fluid-Phase Equilibria, 3rd ed., Prentice Hall.

References

- Rao, A. B. and Rubin, E. S. (2002) A Technical, Economic, and Environmental Assessment of Amine-Based CO₂ Capture Technology for Power Plant Greenhouse Gas Control *Environ. Sci. Technol.* 36, 4467-4475.
- Reddy, S., Scherffius, J., Freguia, S. and Roberts, C. (2003) Fluor's Econamine FG PlusSM Technology. Second International Conference on Carbon Sequestration.
- Rick, S. W. and Stuart, S. J. (2002) In Reviews in Computational Chemistry, Lipkowitz, K. B.; Boyd, D. B.; Ed.; Volume 18, Wiley-VCH, 89-146.
- Rizzo, R. C. and Jorgensen, W. L. (1999) OPLS All-Atom Model for Amines: Resolution of the Amine Hydration Problem *J. Am. Chem. Soc.* 121, 4827-4836.
- Sartori, G. and Savage, D. W. (1983) Sterically Hindered Amines for CO₂ Removal from Gases *Ind. Eng. Chem. Fundam.* 22, 239-249.
- Sharma, M. M. and Danckwerts, P. V. (1963) Catalysis by Brønsted bases of the reaction between CO₂ and water *Trans. Faraday Soc.*, 59, 386-395.
- Singh, U. C. and Kollman, P. A. (1984) An Approach to Computing Electrostatic Charges for Molecules *J. Comp. Chem.* 5, 129-145.
- Smith, D. R. and Quinn, J. A. (1979) The Prediction of Facilitation Factors for Reaction Augmented Membrane Transport *AIChE J.* 25, 197-200.
- Solbraa, E. (2002) Equilibrium and Non-Equilibrium Thermodynamics of Natural Gas Processing, Dissertation, Norwegian University of Science and Technology, Norway.
- Suda, T., Zhang, Y., Iwaki, T. and Nomura, M. (1998) Correlation of the Frontier Orbital Properties of Alkanolamines with the Experimental CO₂ loading *Chem. Lett.* 2, 189-190.
- Sum, A. K. and Sandler, S. I. (1999) Use of ab initio methods to make phase equilibria predictions activity coefficient models *Fluid Phase Eq.* 158-160, 375-380.
- Thambimuthu, K. and Davidson, J. (2004) Overview of CO₂ Capture. 7th International Conference on Greenhouse Gas Control Technologies, Vancouver, Canada.

References

- Tobiesen, F. A., Svendsen, H. F. and Hoff, K. A. (2005) Desorber Energy Consumption in Amine Based Absorption Plants *Int. J. Green Energy*, in press.
- Tomasi, J. and Persico, M. (1994) Molecular Interactions in Solution: An Overview of Methods Based on Continuous Distributions of the Solvent *Chem. Rev.* 94, 2027-2094.
- Versteeg, G.F., van Dijck, L.A.J. and van Swaaij, W.P.M. (1996) On the Kinetics Between CO₂ and Alkanolamines both in Aqueous and Non-Aqueous Solution. An Overview *Chem. Eng. Comm.* 144, 113-158.
- Versteeg, G.F., Kuipers, J. A. M., Van Beckum, F. P. H. and van Swaaij, W. P. M. (1990) Mass Transfer with Complex Reversible Chemical Reactions-II. Parallel Reversible Chemical Reactions *Chem. Engng. Sci.* 45, 183-197.
- Vorholz, J., Harismiadis, V. I., Panagiotopoulos, A. Z., Rumpf, B. and Maurer, G. (2004) Molecular Simulation of the Solubility of carbon dioxide in aqueous solutions of sodium chloride *Fluid Phase Eq.* 226, 237-250.
- Wang, J., Wang, W., Huo, S., Lee, M. and Kollman, P. A. (2001) Solvation Model Based on Weighted Solvent Accessible Surface Area *J. Phys. Chem. B* 105, 5055-5067.
- Warshel, A. and Levitt, M. (1976) Theoretical studies of enzymic reactions: Dielectric, electrostatic and steric stabilization of the carbonium ion in the reaction of lysozyme *J. Mol. Biol.* 103, 227-249.
- Winget, P., Hawkins, G. D., Cramer, C. J. and Truhlar, D. G. (2000) Prediction of Vapor Pressures from Self-Solvation Free Energies Calculated by the SM5 Series of Universal Solvation Models *J. Phys. Chem. B* 104, 4726-4734.
- Wood, R. H., Yezzdimer, E. M., Sakane, S., Barriocanal, J. A. and Doren, D. J. (1999) Free Energies of solvation with quantum mechanical interaction energies from classical mechanical simulations *J. Chem. Phys.* 1110, 1329-1337.
- Wu, H. S. and Sandler, S. I. (1991) Use of ab Initio Quantum Mechanics Calculations in Group Contribution Methods. 1. Theory and the Basis for Group Identifications. *Ind. Eng. Chem. Res.* 30, 881-889.

References

Yagi, Y., Mimura, T., Iijima, M., Ishida, K., Yoshiyama, R., Kamijo, T. and Yonekawa, T. (2004) Improvements of Carbon Dioxide Capture Technology. 7th International Conference on Greenhouse Gas Control Technologies, Vancouver, Canada.

Xidos, J.D., Li, J., Zhu, T., Hawkins, G. D., Thompson, J. D., Chuang, Y.-Y., Fast, P. L., Liotard, D. A., Rinaldi, D., Cramer, C. J. and Truhlar, D. G. Gamesol-version 3.1, University of Minnesota, Minneapolis (2002), based on the General Atomic and Molecular Electronic Structure System (GAMESS) as described in Schmidt, M. W., Baldridge, K. K., Boatz, J. A., Elbert, S. T., Gordon, M. S., Jensen, J. H., Koseki, S., Matsunaga, N., Nguyen, K. A., Su, S. J., Windus, T. L., Dupuis, M. and Montgomery, J. A. (1993) *J. Comp. Chem.* 14, 1347.

Zhang, X., Wang, J., Zhang, C. F., Yang, Y. H. and Xu, J. J. (2003) Absorption rate into a MDEA aqueous solution blended with piperazine under a high CO₂ partial pressure *Ind. Eng. Chem. Res.* 42, 118-122.

Paper I and II are not included due to copyright restrictions.

Paper III

Use of Free Energy Simulations to predict Infinite Dilution Activity

Coefficients

Eirik Falck da Silva

2004

Fluid Phase Equilibria, 221, 15-24 and
Erratum *Fluid Phase Equilibria* 231, 252-253.

Use of Free Energy Simulations to Predict Infinite Dilution Activity Coefficients
Fluid Phase Equilibria, 221, 15-24 and Erratum *Fluid Phase Equilibria* 231, 252-253.

Eirik F. da Silva*

Department of Chemical Engineering, Norwegian University of Science and Technology,

N-7491 Trondheim, Norway

Abstract

An important challenge in applied thermodynamics is the prediction of mixture phase behavior without the use of experimental data. Current group contribution methods are sometimes, but not always successful in this regard. In the present work Monte Carlo free energy perturbations are used in calculating the free energies of solvation for pure component and infinite dilution using the OPLS force field. Infinite dilution activity coefficients are calculated by pure simulation and simulations used in combination with experimental vapour-pressures. The activity coefficients are then used to fit the parameters in Wilson's equation thereby giving overall predictions of activity. Results are compared with free energies and activity coefficients based on experimental values. The systems studied are methanol + water, ethanol + water, acetonitrile + water, formic acid + water and ethanolamine (MEA) + water.

Keywords: Vapour-liquid equilibria; Activity coefficient; Molecular Simulation; Ethanolamine

Introduction

Knowledge of chemical activity is an important component in understanding various chemical processes, chemical gas-absorption being one example of this [1]. Infinite dilution activity coefficients can for example be used to make overall predictions of activity and approximate vapour-liquid equilibrium curve.

Traditionally Gibbs excess free energy models have been used to model activity coefficients. The only predictive models have been group contribution models such as UNIFAC [2]. These models are to some extent limited by access to experimental data. In systems with a large number of chemical species and limited experimental data such as in gas-absorption the use of such models becomes difficult.

The value of models that can predict activity coefficients is therefore clear. And it should be emphasized that even models that are only qualitative can in some cases be a useful tool, particularly in understanding complex systems.

The ideal would be some form of ab initio (quantum mechanical) model without any need of parameterization to experimental data. It is however clear that treating the condensed phase at a quantum mechanical level is computationally very expensive. Guillot [3] reports a vaporization enthalpy for water of 7.38 kcal/mol calculated using ab initio molecular dynamics (Car-Parrinello), while the experimental vaporization enthalpy for water is around 11 kcal/mol [3]. While this result is encouraging it is clear that many issues remains before ab initio molecular dynamics methods can be used for quantitative predictions of solvation.

In a recent work Sum and Sandler [4] use ab initio calculations on clusters of eight molecules to calculate parameters for an excess Gibbs energy model (UNIQUAC). The results presented in the article show very good agreement with experimental data. The procedure does however involve a number of approximations and uncertainties that are not fully acknowledged in the article. The ab initio method used is Hartree-Fock, involving approximations that usually makes it unsuited for obtaining absolute bonding energies [5]. It is also assumed that the interactions of a cluster of eight molecules is representative of the interactions in a liquid. The size of the cluster at the same time also results in a very small number of data for the statistical averaging that is done. Finally there is the approximation in the use of the UNIQUAC equation itself which is known not to be generally accurate [6,7]. It is therefore difficult to reconcile the large uncertainties and

numerous approximations in the method with the apparent high quality in the results. This work does not in any case represent any true ab initio modeling of the condensed phase.

Classical simulations have been central in developing the understanding of the condensed phase. Despite their fairly long history it has been observed [8] that their use for the practical prediction of chemical activity is at an early stage. There are two main issues regarding use of simulations:

One is the representation of the molecule used. Some models such as OPLS (Optimized Parameters for Liquid Simulation) [9] include polarization only implicitly, while some other force fields are polarizable. There are also differences in the flexibility of molecules and the number of sites used. Force fields such as OPLS can be thought of as offering a molecular level group contribution method [10].

There are numerous choices in how to optimize a force field model. There are also many ways ab initio calculations can be used to parameterize force fields. Examples are determination of torsional potential parameters [11] and atomic charges [12].

The second issue is how accurate data for the free energy can be achieved for a given molecular representation. There are a number of calculation schemes based on forms of thermodynamic integration and free energy perturbation [10,13]. For each scheme there is usually also a number of simulation parameters to set. There would not seem to be any general agreement on which methods are superior. Particularly if one considers the tradeoffs between accuracy and simulation time it is difficult to know what methods to choose.

In this work Monte Carlo free energy perturbations are used with OPLS force field representation of the molecules. The simulation method is one of the most widely used, its main appeal being that it is relatively inexpensive in terms of computation time.

The focus of this work is on binary systems with water. Methanol, ethanol, acetonitrile and formic acid are chosen because parameters for them are available in the OPLS force field and because experimental data is available for binary systems with water.

Ethanolamine, also known as MEA, is an important molecule in gas-purification [1,14]. For ethanolamine itself considerable experimental data is available, for other alkanolamines the data is however often very limited. If a molecular force field (such as OPLS) was found to offer parameters that could be transferred to alkanolamines it could be used in modeling of a number of systems of importance in gas-purification.

Theory

The difference between the chemical potential in a mixture and the ideal gas-phase is called the residual chemical potential and at infinite dilution is directly related to the activity coefficient [10] by the following equation:

$$kT \ln \gamma_1^\infty = (\mu_{12} - \mu_{12})^{res} = (\mu_{12} - \mu_{22})^{res} + (\mu_{22} - \mu_{11})^{res} \quad (1)$$

Where μ_{12} is the chemical potential of a molecule of type 1 in a pure solvent of type 2. The equation is valid for constant temperature (T) and pressure, k is the Boltzmanns constant.

There are several ways in which data can be obtained to solve Eq. (1). One can directly calculate the free energy of a single particle by insertion or removal. This can for example be done stepwise:

$$\mu_{21}^{res} = (\mu_{21} - \mu_{11})^{res} - (\mu_{11} - \mu_{01})^{res} \quad (2)$$

The subscript 0 is used to indicate that a particle does not exist in the system, it has either been removed or will be inserted. The experimental vapour-pressures can also be used to calculate the difference in the residual free energy of the pure components by use of the following equation [10]:

$$(\mu_{22} - \mu_{11})^{res} = kT \ln \left(\frac{f_1^0}{f_2^0} \right) \approx kT \ln \left(\frac{P_1^{sat}(T)}{P_2^{sat}(T)} \right) \quad (3)$$

where f is the fugacity and P^{sat} is the saturation pressure. Lazaridis and Paulaitis [15] used Eq. (3) in combination with equation 1 to obtain activity coefficients at infinite dilution.

In the present work the free energy of solvation will be calculated. While differences in the residual chemical potential and the free energy of solvation are the same at infinite dilution their relative values for pure components is different. The free energy of solvation ($\Delta\mu_s$) has the following relationship to the saturation pressure[16]:

$$\Delta\mu_s = kT \ln(P^{sat} M_s / RTd_s) \quad (4)$$

where M_s is molar mass and d_s is density. To obtain the difference in residual free energies for the pure components from solvation energies the M_s/d_s ratio for each component must be subtracted.

For the pure component there are also other techniques available for the calculation of the free energy. Hermans et al. [17] and Mezei [18] have presented results based on thermodynamic integration of the entire ensemble.

Once both infinite dilution activity coefficients in a binary system are estimated the data can be fit to any two-parameter Gibbs excess model such as Wilson's or UNIQUAC to get an estimate of activity coefficients for all compositions, a possibility mentioned by Haile [19]. In this work the Wilson equation has been chosen [6]:

$$\ln(\gamma_1) = -\ln(x_1 + \Lambda_{12}x_2) + x_2 \left(\frac{\Lambda_{12}}{x_1 + \Lambda_{12}x_2} + \frac{\Lambda_{21}}{x_2 + \Lambda_{21}x_1} \right) \quad (5)$$

Methods

The free energy perturbation (FEP) approach centers on the relationship [20]:

$$A_1 - A_0 = -kT \ln \langle \exp[-\beta(E_1 - E_0)] \rangle_0 \quad (6)$$

The equation expresses the free energy difference between systems 0 and 1 by an average of a function of their energy difference that is evaluated by sampling based on E_0 . This calculation works if the two systems are similar to each other. A coupling parameter λ is introduced to allow gradual interconversion of the potential functions and geometries. This interconversion can be represented by the following equation [20]:

$$\xi(\lambda) = \xi_0 + \lambda(\xi_1 - \xi_0) \quad (7)$$

Where ξ is any feature of the system. In the present work the “double-wide” sampling technique described by Jorgensen and Ravimohan [20] will be used. This is a so-called single-topology method.

The calculation of absolute free-energy is somewhat more difficult than calculating relative free-energies. In obtaining absolute free energies insertion schemes are considered superior to deletion schemes[21]. Standard double-wide calculations involve both deletion and insertion steps and their use in this context is therefore questionable. In this work staged insertion of argonlike particles will therefore be used to obtain the absolute free-energy of solvation. A very similar approach has been used previously by Jorgensen et al. [22] in obtaining the absolute free energy of solvation of TIP4P water, the method was in that work called single solvent perturbation.

As an alternative approach the free-energies of the pure components can be determined from experimental vapour-pressure (Eq. 3). The simulations are then only used to obtain relative free-energies of solvation.

In BOSS [23] the potential energy is expressed as the sum of Lennard-Jones and Coulomb potential functions:

$$U = \sum_{i<j} \frac{A_i A_j}{r_{ij}^{12}} - \sum_{i<j} \frac{C_i C_j}{r_{ij}^6} + \sum_{i<j} \frac{q_i q_j}{r_{ij}} \quad (8)$$

where the sums are over all pairs of interaction sites, $A_i=(4\epsilon_i\sigma_i^{12})^{1/2}$, $C_i=(4\epsilon_i\sigma_i^6)^{1/2}$, q_i is the partial electric charge of interaction site i and r_{ij} is the separation between interaction sites.

The interaction sites are usually atoms; however, non-polar hydrogens bonded to carbon atoms can be combined with the carbon atom to form a single «united» atom (UA).

For the water molecule two representations were used: the TIP3P model [24] for water as solute and the TIP4P for water as solvent. The TIP4P model has a total of four interaction sites: the oxygen atom, the two hydrogen atoms, and a center for the negative charge located along the dipole vector. The TIP3P model was chosen as solute because the three-center model can more easily be used in perturbations. Calculations have also been done on TIP4P as solute to offer comparison with data reported in the literature.

Internal rotations were included for ethanol, formic acid and ethanolamine. The rotational potential is represented by the Fourier series in Eq. (9):

$$V(\phi) = \frac{1}{2}V_1(1 + \cos(\phi)) + \frac{1}{2}V_2(1 - \cos(2\phi)) + \frac{1}{2}V_3(1 + \cos(3\phi)) \quad (9)$$

where V is a coefficient and ϕ is the torsional angle. Following Jorgensen et al. [11] the intramolecular energy interactions between molecules separated by 3 bonds (1-4 interactions) were scaled down by a factor of 2. Coefficients for internal rotations are given in Table 1.

Table 1 Fourier Coefficients (in kcal/mol)

Molecule	Dihedral Angle	V_1	V_2	V_3
ethanol	H-O-CH ₂ -CH ₂	0.834	-0.116	0.747
formic acid	H-O(H)-C-O	0.000	0.000	0.000
ethanolamine	H-O-CH ₂ -CH ₂	0.834	-0.116	0.747
	N-CH ₂ -CH ₂ -O	9.900	0.000	0.000
	H(N)-N-CH ₂ -CH ₂	-0.190	-0.417	0.418

OPLS geometries published by Jorgensen et al. were used for TIP4P [24], TIP3P [24], UA methanol [25], UA ethanol [25] and UA acetonitrile [26]. For formic acid unpublished geometry included in the BOSS program distribution [23] was used. Bond lengths for formic acid were 1.2258 Å (C=O), 1.356851 (C-O(H)), 1.09 (C-H) and 0.943611 (O(H)-

H). Angles are 119.277520 (O(H)-C-O), 108.159159 (H(O)-O(H)-C) and 124.451989 (H(C)-C-O). It should be noted the formic acid parameters in BOSS were for a fully flexible molecule, in the present work the parameters are used with rigid bond-lengths and angles.

For ethanolamine no OPLS parameterization has been published. The amine parameters are taken from Rizzo and Jorgensen [9] and for the alcohol functionality the UA ethanol parameters are used. The CH₂ group neighboring the amine group is given the same Lennard-Jones parameters as the ethanol functionality CH₂ group, finally the charge of this group is chosen to give the molecule a total charge of zero. Geometry parameters are based on mixture of HF/6-31G* ab initio geometry and AM1 semiempirical geometry. Bond-lengths are set to 1.012 Å (N-H), 1.45 Å (N-CH₂), 1.53 Å (CH₂-CH₂), 1.43 Å (CH₂-O) and 0.945 Å (O-H). Angles are 108.5 (H-CH₂-O), 112 (CH₂-CH₂-O) 108.46 (N-CH₂-CH₂) and 109.69 (H-N-CH₂). Ethanolamine has four dihedral angles. The relative positions of the amine-group hydrogens are fixed by setting the dihedral angle H1(N)-N-CH₂-H2(N) to 121.68. The three other dihedral angles are chosen to be flexible. Using HF/6-31G* ab initio calculations on a single ethanolamine molecule the most stable *gauche* conformer was found to be 2.81 kcal/mol more stable than the most stable *trans* conformer. Following Jorgensen et al. [11] the coefficients for the rotations are set to reproduce this conformer energy difference. For the alcohol-group the same coefficients as used for ethanol are chosen. The coefficients are given in Table 1. All Lennard-Jones and charge parameters for the molecules studied are listed in Table 2.

Table 2 Force Field Parameters

Molecule	United Atom	(Å)	(kcal/mol)	Q (Electron units)
argon		3.401	0.2339	0.000
water (TIP4P)	O	3.15365	0.155	0.000
	H	0.000	0.000	0.520
	M	0.000	0.000	-1.040
water (TIP3P)	O	3.15061	0.1521	-0.834
	H	0.000	0.000	0.417
methanol	O	3.070	0.170	-0.700
	CH ₃	3.775	0.207	0.265
	H	0.000	0.000	0.435
ethanol	CH ₃	3.905	0.175	0.000
	CH ₂	3.905	0.118	0.265
	O	3.070	0.170	-0.700
	H	0.000	0.000	0.435
acetonitrile	C	3.650	0.150	0.280
	CH ₃	3.775	0.207	0.150
	N	3.200	0.170	-0.430
formic acid	C	3.750	0.105	0.520
	O	2.960	0.210	-0.440
	H(C)	2.420	0.015	0.000
	O(H)	3.000	0.170	-0.530
	H(O)	0.000	0.000	0.450
ethanolamine	N	3.300	0.170	-0.900
	H(N)	0.000	0.000	0.360
	CH ₂ (N)	3.905	0.118	0.180
	CH ₂ (O)	3.905	0.118	0.265
	O	3.070	0.170	-0.700
	H(O)	0.000	0.000	0.435

Formic acid and ethanolamine have an intramolecular contribution to the free energy. To obtain the free energy of solution the intramolecular free energy in the gas-phase must be subtracted from the value in solution. Results in this work will be presented with the gas-phase contribution subtracted.

The OPLS force field is intended to offer transferable parameters for molecules both as solute and solvent, they are usually fitted to density and vaporization enthalpy. The representations for water (TIP4P), UA methanol, UA ethanol and UA acetonitrile are all reported to reproduce fairly accurately densities and heats of vaporization for pure components (see Table 3).

The particle insertion simulations were done by growing a uncharged (UC) TIP4P molecule in the ensemble. The particle was not grown from zero but from a small particle with negligible free-energy. This particle had a Lennard-Jones $\sigma=0.01$ Å and a $\epsilon=0.015$ kcal/mol. Most of the other simulations were done directly between the solutes and a water molecule. The size difference between the ethanolamine molecule and water is however

very large, in this case ethanolamine was first perturbed to an argonlike uncharged (UC) ethanolamine molecule. This uncharged molecule was then perturbed to UC TIP4P.

Boxes with 267 solvent molecules were used. All solvent boxes were equilibrated for at least 10 million configurations before use. Double-wide perturbations were done with $\Delta\lambda = +/-0.05$, with $\lambda = 0.05, 0.15, 0.25, 0.35, 0.45, 0.55, 0.65, 0.75, 0.85$ and 0.95 . Each step had 500 000 configurations of equilibration and 500 000 configurations of averaging. The particle insertions were done with $\Delta\lambda = +0.05$ and same amount of sampling and equilibration for each step as for the double-wide perturbations.

Periodical boundary conditions were used. Preferential sampling of the solvent near the solute [20] was used for the double-wide sampling calculations based on the following weighting:

$$\frac{1}{(r^2 + wkc)} \quad (10)$$

Following recommendations in the BOSS documentation [23] wkc values between 200 and 300 were used. This procedure was however not used for the particle insertion calculations. All simulations were done in a NPT ensemble at a pressure of 1 atmosphere, the ethanolamine simulations were done at 60°C , while the other simulations were done at 25°C . Attempts to change the volume of the system were done every 700-1625 configurations. Lowest frequency of volume changes was for ethanolamine while the highest was for TIP4P. Each volume change was 130 \AA^3 . New configurations are generated by selecting a molecule, translating it randomly in all three Cartesian directions, rotating it randomly about a randomly selected axis and performing any internal rotations. Ranges for translations are set at 0.15 \AA while ranges for angular rotations and dihedral rotations are set at 15 degrees.

Interactions were cut off with a quadratic “switching” function. The same cutoffs as previously used by Jorgensen et al. were used: 8.5 \AA for water (TIP4P) [22], 9.5 \AA for methanol [25], 11.0 for ethanol [25], 10 \AA for acetonitrile [26] and 12 \AA for formic acid (value used for acetic acid [27]). Ethanolamine is a larger molecule and in this case a cutoff of 14 \AA was chosen. The same cutoffs were chosen for solvent-solvent interactions and solute-solvent interactions, except in water where a 10 \AA solute-solvent interaction was chosen. The statistical uncertainty was estimated by the batch means procedure [9] and standard deviations from the total energy of separate runs using different starting configurations. For each free energy difference three separate simulations from different

starting configurations were used. Each free energy calculation took between 2 and 12 hours on a single processor PC.

The heat of vaporization to the ideal gas has been calculated to make comparison with experimental data and with previous work by Jorgensen et al. (Table 3). It is calculated according to the following equation [27]:

$$\Delta H_{\text{vap}} = E_{\text{intra}}(g) - (E_i(l) + E_{\text{intra}}(l)) + RT \quad (11)$$

where $E_{\text{intra}}(g)$ and $E_{\text{intra}}(l)$ are the intramolecular rotation energies for the gas and the liquid, $E_i(l)$ is the intermolecular energy for the liquid. There has apparently not been published any estimates for the enthalpy of vaporization of ethanolamine except at the boiling temperature. Antoine equations have however been published and in the present work this will be used to estimate the experimental vaporization enthalpy using the Clapeyron equation:

$$\frac{dP}{dT} = \frac{\Delta H_{\text{vap}}}{T \Delta V_{\text{vap}}} \quad (12)$$

where P is the pressure and ΔV_{vap} is the molar volume change upon vaporization. The calculation will be done assuming ideal gas and neglecting the molar volume in the liquid phase.

Results and Discussion

In Table 3 densities and vaporization enthalpies for the solvents studied are shown. While some of the experimental vaporization enthalpies are not for ideal gas, the energy differences between ideal gas and real gas are in these cases small.

Table 3 Densities and Energy Results

Solvent	T [°C]	d [g/cm ³]			ΔH_{vap} [kcal/mol]		
		Calcd	Calcd	Exptl	Calcd	Calcd	Exptl
water (TIP4P)	25	1.012	0.999 [24]	0.997 [28]	10.60 ^a	10.66 [24] ^a	10.51 [24]
methanol	25	0.720	0.759 [25]	0.786 [28]	8.97 ^a	9.05 [25] ^a	8.94 [25]
ethanol	25	0.741	0.748 [25]	0.785 [28]	9.90 ^a	9.99 [25] ^a	10.11 [25]
acetonitrile	25	0.750	0.765 [26]	0.776 [28]	7.57 ^a	8.03 [26] ^a	8.01 [31] ^a
formic acid	25	1.236		1.214 [28]	12.39 ^a		11.03 [31] ^a
ethanolamine	25	1.056		1.012 [29]	14.59 ^a		
ethanolamine	60	1.029		0.984 [30]	13.59 ^a		13.79 ^b

^a: Heat of vaporization to ideal gas. ^b: Obtained by using the Clapeyron equation (Eq. 12) with Antoine equation data given in [32].

For TIP4P, methanol, ethanol and acetonitrile the simulation results are in good agreement with the experimental values, reflecting the fact that the OPLS force field has been parameterized to reproduce these properties. The results are slightly different from those obtained for the same systems by Jorgensen et al. The number of molecules in the simulation boxes is in the present study different (in all cases larger) than used in the original studies and this probably explains part of the discrepancy. It should also be noted that the present simulations with use of preferential sampling are not optimal for estimating overall solvent properties.

The agreement for formic acid is slightly worse reflecting that this model has not been parameterized in the same way.

For ethanolamine the parameters are taken from other molecules, it is therefore very encouraging to see the good agreement with the experimental data. The densities are overestimated by around 4.5% at both temperatures. The agreement with the vaporization enthalpy is even better. These results suggest that the OPLS force field has reasonable transferability to alkanolamines.

In Table 4 the results for the separate free energy calculations based on double-wide sampling are shown. For most calculations free energy differences have been calculated using three simulations based on different starting configurations, the result shown is the average of all simulations. The uncertainty given with the result is the standard deviation over subsets in the calculations, again the average for all runs is shown

(the standard deviation not varying that much from run to run). The standard deviation of the total free energy from repeated runs is shown in a separate column.

Table 4 Free Energy Differences (Results in kcal/mol)

	Solvent	T [°C]	ΔG_{calc}^a	S.D. ^b
methanol \rightarrow water ^c	water ^d	25	-1.97 +/-0.21	0.26
water ^d \rightarrow UC water	water ^d	25	8.25 +/-0.15	0.54
water ^c \rightarrow UC water	water ^d	25	8.93 +/-0.18	0.30
methanol \rightarrow water ^c	methanol	25	-0.53 +/-0.16	0.31
water ^c \rightarrow UC water	methanol	25	6.43 +/-0.19	0.15
ethanol \rightarrow water ^c	water ^d	25	-1.97 +/-0.37	0.38
ethanol \rightarrow water ^c	ethanol	25	0.36 +/-0.25	0.44
water ^c \rightarrow UC water	ethanol	25	5.64 +/-0.17	0.76
acetonitrile \rightarrow water ^c	water ^d	25	-3.49 +/-0.46	0.49
acetonitrile \rightarrow water ^c	acetonitrile	25	1.07 +/-0.15	0.12
water ^c \rightarrow UC water	acetonitrile	25	4.57 +/-0.06	0.12
formic acid \rightarrow water ^c	water ^d	25	-0.22 +/- 0.51	0.23
formic acid \rightarrow water ^c	formic acid	25	0.59 +/-0.33	1.52
water ^c \rightarrow UC water	formic acid	25	10.26 +/-0.13	1.11
MEA ^e \rightarrow UC MEA ^e	water ^d	60	11.40 +/-0.20	0.40
MEA ^e \rightarrow UC water	water ^d	60	0.39 +/-0.16 ^f	
water ^c \rightarrow UC water	water ^d	60	8.82 +/-0.14	0.47
MEA ^e \rightarrow UC MEA ^e	MEA ^e	60	7.90 +/-0.20	0.61
UC MEA ^e \rightarrow UC water	MEA ^e	60	0.57 +/-0.33 ^f	
water ^c \rightarrow UC water	MEA ^e	60	7.07 +/-0.17	0.76

^a Standard deviation from batch means procedure. ^b Standard deviation of total free energy for three separate simulations. ^c TIP3P. ^d TIP4P. ^e ethanolamine. ^f Single simulation.

For the methanol to water (TIP3P) in water Lazaridis and Paulaitis [15] obtained a value of -1.77 kcal/mol using almost identical method. While the difference in the results is significant it is in fact within the uncertainties observed both in the work by Lazaridis and Paulaitis and in the present one. The present result is based on greater sampling and is probably the more accurate value. Using slightly different molecular representation Slusher [33] obtained a value of -1.58 kcal/mol for the same energy difference.

For the methanol to water free energy difference in methanol Slusher [33] obtained a value of -1.65 kcal/mol using somewhat different molecular representation. The present result is -0.53 kcal/mol and the difference is clearly greater than can be accounted for by the uncertainties in the calculations.

The standard deviations based on calculations from repeated runs are in general somewhat higher than those based on the subsets of a single run.

In Table 5 the results of the particle insertion calculations are shown. In the appendix underlying simulation results are shown for the insertion calculations together

with results based on deletion. Results from the present work do not give grounds to draw general conclusions regarding insertion and deletion. As noted in the Methods section double-wide sampling involves both deletion and insertion steps and should only be used when deletion and insertion are equivalent. Further work might therefore be required to clarify under which conditions double-wide sampling and insertion are equivalent.

Table 5 Free Energy of Insertion (Results in kcal/mol)

	Solvent	T [°C]	$\Delta G_{\text{calc}}^{\text{a}}$	S.D. ^b
0 → argon	water ^c	25	2.44 +/-0.19	0.13
0 → UC water	water ^c	25	2.51 +/-0.18	0.30
0 → UC water	methanol	25	1.1 +/-0.10	0.09
0 → UC water	ethanol	25	0.95 +/-0.10	0.27
0 → UC water	acetonitrile	25	1.29 +/-0.12	0.15
0 → UC water	formic acid	25	2.93 +/-0.19	0.77
0 → UC water	water ^c	60	2.98 +/-0.17	0.36
0 → UC water	ethanolamine	60	2.83 +/-0.18	0.49

^a Standard deviation from batch means procedure. ^b Standard deviation of total free energy for three separate simulations. ^c TIP4P.

Adding together the free energy differences from Table 4 and Table 5 the total free energy of solvation at infinite dilution, or for pure component can be calculated. In Table 6 total simulation free energies are compared with values estimated from experimental data. The present result for water (TIP4P) is in good agreement with a Helmholtz free energy of TIP4P obtained by Thermodynamic Integration reported by Hermans et al. [17]. They reported a Helmholtz free energy of -5.3 kcal/mol that translates to a Gibbs free energy of -5.9 kcal/mol, while the present result is -5.74 ± 0.24 . Using a method very similar to the one used in the present work Jorgensen [22] obtained a value of -6.06 kcal/mol for the free energy of solvation of TIP4P.

Table 6 Free Energy of Solvation (Results in kcal/mol)

Solute	Solvent	T [°C]	$\Delta G_{s,calc}^a$	$\Delta G_{s,exp}^b$	$\gamma_{calc}^\infty^c$	$\gamma_{calc}^\infty^d$	γ_{exp}^∞
argon	water ^e	25	2.44 +/- 0.19	2.002			
water ^e	water ^e	25	-5.74 +/- 0.24	-6.324			
water ^f	water ^e	25	-6.42 +/- 0.26				
methanol	water ^e	25	-4.45 +/- 0.33	-5.1	4.0	5.2	1.74 ^g
water ^f	methanol	25	-5.33 +/- 0.21		2.8	2.2	1.57 ^h
methanol	methanol	25	-4.80 +/- 0.26	-4.859			
ethanol	water ^b	25	-4.45 +/- 0.46	-5.05	9.1	11.3	3.91 ^g
water ^f	ethanol	25	-4.69 +/- 0.19		5.7	4.6	
ethanol	ethanol	25	-5.06 +/- 0.32	-5.079			
acetonitrile	water ^e	25	-3.78 +/- 0.52		7.8	1758	11.1 ^g
water ^f	acetonitrile	25	-3.28 +/- 0.16		68.3	29	
acetonitrile	acetonitrile	25	-4.35 +/- 0.31				
formic acid	water ^e	25	-7.02 +/- 0.42		9.6	0.1	0.64 ^g
water ^f	formic acid	25	-7.33 +/- 0.23		0.1	10.1	
formic acid	formic acid	25	-7.92 +/- 0.41	-5.538			
water ^f	water ^e	60	-5.85 +/- 0.22				
ethanolamine	water ^e	60	-8.81 +/- 0.31		0.02	0.0002	0.27 ⁱ
water ^f	ethanolamine	60	-4.24 +/- 0.25		4.4	333.6	0.51 ⁱ
ethanolamine	ethanolamine	60	-5.65 +/- 0.43				

^a Standard deviation from batch means procedure. ^b Ref. [16]. ^c Pure simulation activity coefficients (*sim*). ^d Activity coefficients based on simulations and experimental vapour pressures (*sim-P*). ^e TIP4P. ^f TIP3P. ^g Data from Kojima et al. [34]. ^h Data from Slusher [33]. ⁱ Data from fitting of vapour-liquid equilibria to UNIQUAC [35].

The overall agreement between FEP results and experimental free energies is quite good. Only in the case of formic acid does the energy deviate by more than 1 kcal/mol. This overestimation of the free energy of formic acid is probably due to the use of a molecular representation that gives too high vaporization enthalpy (Table 3).

Comparing infinite dilution activity coefficients calculated from the simulations with experimental values good overall agreement is found in most cases. In the case of ethanolamine the agreement is however poor. The results suggest that the simulated solvation energies in pure ethanolamine are too low both for water and ethanolamine itself, leading to the activity coefficient of water being too high in ethanolamine and at the same time giving too low activity coefficient for ethanolamine in water.

Figures 1-4 show activity coefficients based on simulations together with experimental activity coefficients. Two different estimates of the activity coefficients are shown.

Using the data in Table 4 and Table 5 with Eq. (1) and the molar mass-density correction from Eq. (4) the infinite dilution activity coefficients are obtained. Density data

are from references given in Table 3. Using these values one can determine the parameters for Wilson's Eq. (4) and thereby obtain a general prediction for the activity coefficients. Results based on this calculation are referred to as simulation (*sim*) in Figures 1 to 4.

The other approach is to use Eq. (3) with experimental data for the saturation vapour pressure [35] to obtain the free energies for the pure components and only use the simulations for the free energy differences in the same solvent $(\mu_{21} - \mu_{11})^{res}$. This gives the activity coefficients at infinite dilution, which again can be used to fit the parameters in Wilson's equation. Results based on this are shown as *sim-P* in Figures 1-4. The infinite dilution activity coefficients obtained using this method are shown in Table 6.

With experimental liquid composition-vapour pressure data and liquid composition-vapour composition data a set of equations is obtained that can be solved to obtain the activity coefficients. The experimental results shown in figures 1-4 are based on this approach. Data from Gmehling et al. [35] has been used. Experimental methanol + water and ethanol + water systems were at 25 C, while acetonitrile + water and formic acid + water systems were at 30 C. To obtain the activity coefficients the data for formic acid + water were corrected for vapour phase association of formic acid following Gmehling et al. [35].

For ethanolamine isothermal vapour-composition data are not available. In this case only the vapour pressure is shown. Here the activity coefficients from the simulations have been used together with experimental vapour pressures for pure components to obtain a vapour-liquid equilibrium curve on the same form as the experimental data. Experimental vapour pressures are from Nath and Bender [29] (same data given in Gmehling et al. [35]), while vapour pressures for pure components are from Antoine equations given in Gmehling et al. [35]. Plots are shown in figure 5.

Experimental activity coefficients are obtained from liquid composition-vapour pressure data and vapour composition data.

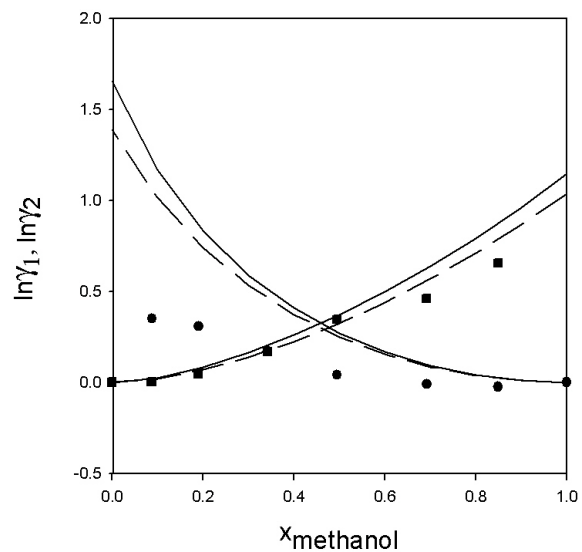


Figure 1. Activity coefficients for methanol + water at 25 C. Points are experimental data. Dashed lines are activity coefficients based purely on simulations (*sim*). Solid lines are based on simulations and experimental vapour pressures (*sim-P*).

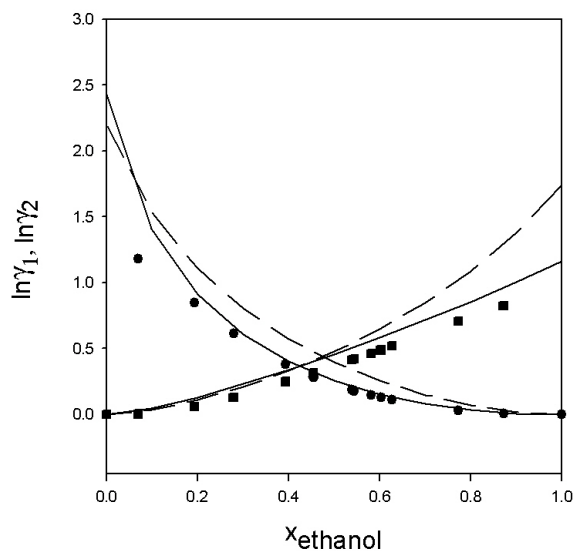


Figure 2. Activity coefficients for ethanol + water at 25 C. Points are experimental data. Dashed lines are activity coefficients based purely on simulations (*sim*). Solid lines are based on simulations and experimental vapour pressures (*sim-P*).

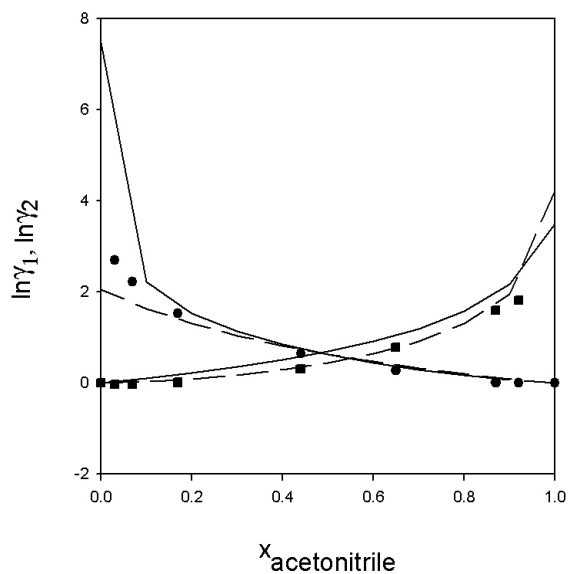


Figure 3. Activity coefficients for acetonitrile + water at 30 C. Points are experimental data. Dashed lines are activity coefficients based purely on simulations (*sim*). Solid lines are based on simulations and experimental vapour pressures (*sim-P*).

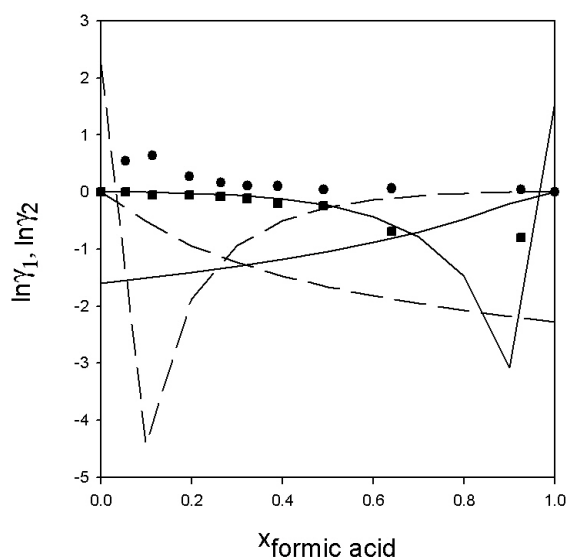


Figure 4. Activity coefficients for formic acid + water at 30 C. Points are experimental data. Dashed lines are activity coefficients based purely on simulations (*sim*). Solid lines are based on simulations and experimental vapour pressures (*sim-P*).

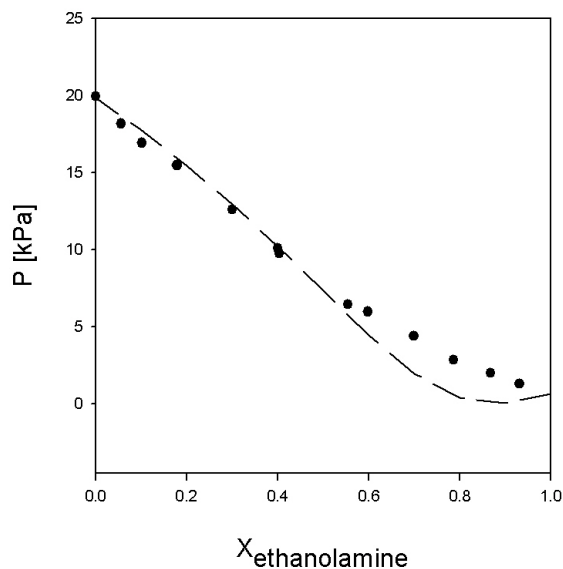


Figure 5. Vapour pressure for ethanolamine + water at 60 C. Points are experimental data. Dashed line is from activity coefficients based purely on simulations (*sim*).

In the fitting process it was found that not all sets of infinite dilution activity coefficients could be fit easily to Wilson's equation. Particularly in the fitting of the ethanolamine system extreme parameters (10^{-74}) were needed, and even this does not produce a perfect fit with the activity coefficients from the simulations. This problem arises because the parameters in Wilson's equation are strongly coupled and the equation is inherently better in fitting to some forms of data.

The pure simulation (*sim*) and simulations in combination with experimental vapour-pressures (*sim-P*) are quite good for methanol + water, ethanol + water and acetonitrile + water. For the formic acid + water system the pure simulation results (*sim*) are wrong while the *sim-P* results are inconclusive. The difference between the *sim* and *sim-P* results are for formic acid dramatic, but this can be easily understood in terms of the uncertainties in the simulations and the use of Wilson's equation to fit the data. Formic acid + water is also a highly non-ideal system and data obtained at infinite dilution might be insufficient to describe the system at all compositions.

For ethanolamine + water there is only limited agreement. Part of the problem might be the issue regarding use of Wilson's equation mentioned previously but the agreement with experimental data at infinite dilution is in this case also poor (Table 6). Further studies are needed for this system.

The methanol + water system has also been studied by Crozier and Rowley [36] using different molecular representation, the results from the present work would appear to be in better agreement with experimental data.

In general the results can be said to be fairly good suggesting that the OPLS force field based on parameterization to density and enthalpy of vaporization is useful in predictions of activity coefficients.

The present simulations do not have the same precision as work by Slusher [33] and by Crozier and Rowley [36], but when comparing the quality of the results it must be kept in mind that the simulations used in the present work are relatively inexpensive in terms of simulation time. Further studies are needed to determine which method can deliver the most precise results for a given amount of CPU time.

For highly non-ideal systems such as formic acid + water it would appear that data at infinite dilution and for pure component are insufficient basis for predicting the full equilibrium. One possibility along the lines of the present work would be to also do free energy perturbations in mixtures of the solvents.

As noted previously there are a number of ways in which a force field can be optimized. While the present work uses TIP4P for water and UA OPLS for methanol, Slusher [8] uses SPC water and a different UA methanol model. The results of the present work suggest that the difference between the models is significant. It is however not clear if any type of force field parameterization is in general superior with respect to obtaining free energies.

It should also be noted that systems involving hydrogen bond forming molecules and water are among the more difficult to model. In work on binary systems with osmotic molecular dynamics Crozier and Rowley [36] in general obtained better results for systems involving alkanes than for systems involving molecules such as methanol and water.

At present it would seem that it is not possible to a priori predict how well a given force field will reproduce experimental data. A semi-qualitative reproduction of experimental data is perhaps what can be expected.

Conclusion

In this paper free energy perturbations have been used to calculate free energies of solvation for pure components and solutes at infinite dilution. The results were used to fit the parameters in Wilson's equation to give overall predictions of activity coefficients for mixtures. Results are shown both for pure simulation results and for simulations used in combination with vapour pressure over pure component. For the systems methanol + water, ethanol + water and acetonitrile + water reasonable agreement was found with experimental data. For formic acid + water the comparison with experimentally based data is ambiguous. For the system ethanolamine + water only partial agreement with experimentally based data was obtained. Apparently the ethanolamine representation used gives too low solvation energies. The present work suggests that the OPLS force field is sufficiently accurate to give useful predictions of overall vapour-liquid equilibrium.

References

- [1] D. M. Austgen, G. T. Rochelle, *Ind. Eng. Chem. Res.*, 28 (1989) 1061.
- [2] A. Fredenslund, J. Gmehling, P. Rasmussen, *Vapour-liquid equilibrium using UNIFAC*, Elsevier, Amsterdam, 1977.
- [3] B. Guillot, *J. Mol. Liq.*, 101 (2002) 219.
- [4] A. K. Sum, S. I. Sandler, *Fluid Phase Equilibria*, 158-160 (1999) 375.
- [5] C. J. Cramer, *Essentials of Computational Chemistry*, John Wiley & Sons, 2002.
- [6] J. Prausnitz, R. Lichtenthaler, E. Gomes de Azevedo, *Molecular Thermodynamics of Fluid-Phase Equilibria*, 3rd ed., Prentice Hall 1999.
- [7] J. Fischer, *Fluid Phase Equilibria*, 10 (1983) 1.
- [8] J. T. Slusher, *J. Phys. Chem. B*, 103 (1999) 6075.
- [9] R. C. Rizzo, W. L. Jorgensen, *J. Am. Chem. Soc.*, 121 (1999) 4827.
- [10] J. T. Slusher, *Fluid Phase Equilibria*, 153 (1998) 45.
- [11] W. L. Jorgensen, D. S. Maxwell, J. Tirado-Rives, *J. Am. Chem. Soc.*, 118 (1996) 11225.
- [12] A. Jakalian, D. B. Jack, C. I. Bayly, *J. Comp. Chem.*, 23 (2002) 1623.
- [13] P. Kollman, *Chem. Rev.*, 93 (1993) 2395.
- [14] G. F. Versteeg, L. A. J. van Dijck, W. P. M. van Swaaij, *Chem. Eng. Commun.*, 144 (1996) 113.
- [15] T. Lazaridis, M. E. Paulaitis, *AIChE J.*, 39 (1993) 1051.
- [16] A. Ben-Naim, Y. Marcus, *J. Chem. Phys.*, 81 (1984) 2016.
- [17] J. Hermans, A. Pathiaseril, A. Anderson, *J. Am. Chem. Soc.*, 110 (1988) 5982.
- [18] M. Mezei, *J. Comp. Chem.*, 13 (1992) 651.
- [19] J. M. Haile, *Fluid Phase Equilibria*, 26 (1986) 103.
- [20] W. L. Jorgensen, C. Ravimohan, *J. Chem. Phys.*, 83 (1985) 3050.
- [21] D. A. Kofke, P. T. Cummings, *Molecular Physics*, 92 (1997) 973.
- [22] W. L. Jorgensen, J. F. Blake, J. K. Buckner, *Chemical Physics*, 129 (1989) 193.
- [23] W. L. Jorgensen, BOSS version 4.3, Yale University, New Haven, CT(1989a)
- [24] W. L. Jorgensen, J. Chandrasekhar, J. D. Madura, R. W. Impey, M. L. Klein, *J. Chem. Phys.*, 79 (1983) 926.
- [25] W. L. Jorgensen, *J. Phys Chem.*, 90 (1986) 1276.
- [26] W. L. Jorgensen, J. M. Briggs, *Molecular Physics*, 63 (1988) 547.
- [27] J. M. Briggs, T. B. Nguyen., W. L. Jorgensen, *J. Phys. Chem.*, 95 (1991) 3315.
- [28] J. A. Riddick, W. B. Bunger, T. K. Sakano, *Organic Solvents*, 4th ed., Wiley, New York, 1986, Vol, II, 360.
- [29] A. Nath, E. Bender, *J. Chem. Eng. Data*, 28 (1983) 370.

- [30] R. M. DiGullio, R.-J. Lee S. T. Schaeffer, L. L. Brasher, A. S. Teja, *J. Chem. Eng. Data*, 37 (1992) 239.
- [31] D. D. Wagman, W. H. Evans, V. B. Parker, R. H. Schumm, I. Halow, S. M. Bailey, K. L. Churney, R. L. Nuttall, *J. Phys. Chem. Ref. Data, Suppl. 2* (1982) 11.
- [32] S.-B. Park, H. Lee, *Korean J. Chem. Eng.*, 14 (1997) 146.
- [33] J. T. Slusher, *Fluid Phase Equilibria*, 154 (1999) 181.
- [34] K. Kojima, S. J. Zhang, T. Hiaki, *Fluid Phase Equilibria*, 131 (1997) 145.
- [35] J. Gmehling, U. Onken, W. Arlt, *Vapour-Liquid Equilibrium Data Collection*, DECHMA, Frankfurt, 1977 and onwards.
- [36] P. S. Crozier, R. L. Rowley, *Fluid Phase Equilibria*, 193 (2002) 53.

Appendix

In the table data are shown for simulations with overlapping double-wide sampling. In such a simulation each perturbation step is covered in both (insertion and deletion) directions. From this total free energies are obtained for insertion and deletion, the average of these two values would correspond to two double-wide sampling calculations. Some of the data are the basis for the averaged results shown in table 5. Results are shown for single simulations.

Table 7 Free Energy of Insertion and Deletion (Results in kcal/mol)

	Solvent	T [°C]	Insertion	Deletion
water ^a → methanol(1)	water ^b	25	2.49 +/-0.21	2.54 +/-0.25
water ^a → methanol(2)	water ^b	25	2.11 +/-0.19	2.11 +/-0.22
water ^a → methanol(3)	water ^b	25	2.12 +/-0.16	2.02 +/-0.15
water ^a → methanol(1)	methanol	25	0.32 +/-0.15	0.23 +/-0.16
water ^a → methanol(2)	methanol	25	0.70 +/-0.12	0.54 +/-0.10
water ^a → methanol(3)	methanol	25	0.82 +/-0.15	0.77 +/-0.16
0 → UC water(1)	water ^b	25	2.22 +/-0.16	2.08 +/-0.17
0 → UC water(2)	water ^b	25	2.73 +/-0.24	2.72 +/-0.22
0 → UC water(3)	water ^b	25	2.57 +/-0.17	2.43 +/-0.16
0 → UC water(1)	methanol	25	1.09 +/-0.09	1.11 +/-0.11
0 → UC water(2)	methanol	25	1.19 +/-0.10	1.17 +/-0.11
0 → UC water(3)	methanol	25	1.02 +/-0.10	0.89 +/-0.10
0 → UC water(1)	ethanol	25	1.20 +/-0.16	1.18 +/-0.15
0 → UC water(2)	ethanol	25	0.99 +/-0.08	0.86 +/-0.10
0 → UC water(3)	ethanol	25	0.66 +/-0.06	0.66 +/-0.08
0 → UC water(1)	acetonitrile	25	1.31 +/-0.12	1.18 +/-0.12
0 → UC water(2)	acetonitrile	25	1.43 +/-0.14	1.24 +/-0.12
0 → UC water(3)	acetonitrile	25	1.12 +/-0.11	1.07 +/-0.12
0 → UC water(1)	formic acid	25	2.04 +/-0.14	1.60 +/-0.12
0 → UC water(2)	formic acid	25	3.45 +/-0.18	2.91 +/-0.15
0 → UC water(3)	formic acid	25	3.30 +/-0.25	2.84 +/-0.18
0 → UC water(1)	ethanolamine	60	2.46 +/-0.12	2.10 +/-0.14
0 → UC water(2)	ethanolamine	60	3.38 +/-0.22	2.85 +/-0.21
0 → UC water(3)	ethanolamine	60	2.64 +/-0.18	2.61 +/-0.15
0 → UC water(1)	water ^b	60	2.71 +/-0.13	2.59 +/-0.13
0 → UC water(2)	water ^b	60	3.38 +/-0.22	2.85 +/-0.21
0 → UC water(3)	water ^b	60	2.84 +/-0.15	2.79 +/-0.16

^a TIP3P. ^b TIP4P.

Paper IV is not included due to copyright restrictions

Paper VI

Molecular Dynamics Study of Ethanolamine as a Pure Liquid and in Aqueous Solution

Eirik Falck da Silva, Tatyana Kuznetsova and Bjørn Kvamme

2005

Molecular Dynamics Study of Ethanolamine as a Pure Liquid and in Aqueous Solution

*Eirik F. da Silva,^{*a} Tatyana Kuznetsova^b and Bjørn Kvamme^b*

^aDepartment of Chemical Engineering, Norwegian University of Science and Technology, N-7491 Trondheim, Norway.

^bDepartment of Physics, University of Bergen, N-5007 Bergen, Norway.

silva@chemeng.ntnu.no

Molecular dynamics simulations have been carried out for ethanolamine as a pure liquid and in aqueous solution at 298.15K and 333K. Two force field representations were utilized for ethanolamine. Results are presented for density, enthalpy of vaporization, radial distribution functions and conformer distributions. The results strongly suggest that the main (O-C-C-N) dihedral tends to stay in its gauche conformers in solution and that the ethanolamine molecules populate conformers with a considerable degree of intramolecular hydrogen bonds. Aqueous ethanolamine shows a preference to be solvated by water molecules, resulting in a liquid structure that is fairly homogeneous at the molecular level. A simulation was also carried out with a CO₂ molecule in an aqueous ethanolamine system, the results suggesting that CO₂ is almost equally attracted to ethanolamine and water.

Introduction

Mixtures of Alkanolamines and water are commonly used to absorb carbon dioxide from natural gas and exhaust gases.¹ This is currently one of the most viable among the available technologies to capture

carbon dioxide.² While alkanolamine based CO₂ capture has received considerable experimental attention little work has been done on the understanding of these systems at the molecular level. Ethanolamine is the simplest of the alkanolamine molecules and some simulation work has been done in recent years to ascertain its liquid structure and properties as well as its behavior in aqueous mixtures.³⁻⁷

Besides being important in gas sweetening and other industrial processes, ethanolamine and other alkanolamines are also of interest for other reasons. Together with 1-2 ethanediol, ethanolamine represents one of the simplest molecules able to form intramolecular hydrogen bonds. Both in pure liquids and aqueous solutions intramolecular hydrogen bonds will compete with the formation of intermolecular hydrogen bonds. This potential for hydrogen bonding also raises questions about the structure of ethanolamine both as a pure liquid and in aqueous solution. The modeling of such small organic molecules is clearly also of relevance to the modeling of more complex biomolecules.

In the parameterization of molecular force fields, ethanolamine and other alkanolamines present an interesting challenge. Two main approaches for parameterization of force fields exist in the open literature. For water and small organic molecules, such as methanol, a number of specially fitted force fields have been presented (Guillot⁸ and Walser et al.⁹ and references therein). These are typically based on reproducing certain experimental properties, such as density, radial distribution functions and enthalpy of vaporization, and each parameter in the force field is often fine-tuned. This approach to force field fitting is not viable in case of larger organic molecules with many atomic sites. For such molecules general transferable force fields such as OPLS¹⁰ have been developed. Ethanolamine is a relatively small molecule, but the number of parameters in a force field will tend to be much higher than for water, and the molecule has not been as rigorously studied experimentally as water or the simple mono-alcohols. There would however appear to be room for more detailed force field parameterization than usually seen for biomolecules.

The intention of the present work has been to look in greater detail at force field parameterization, conformer distribution and other aspects of the system of particular relevance to the gas absorption

process. We were especially interested in understanding the carbamate formation mechanism, which according to da Silva and Svendsen¹¹ can be written in the following way:



Where B is a base molecule (usually a second ethanolamine molecule) and R_1R_2NH is an ethanolamine molecule. The stippled line indicates a hydrogen bond.

Force Field

Two force field representations of ethanolamine were studied in the present work. One is a somewhat adjusted version of the force field presented by Alejandro et al.⁴ while the second force field was based on our own parameterization and analysis. A united atom approach in which methyl group hydrogens are not explicitly represented is utilized for both representations of ethanolamine.

Bond angles are handled by harmonic type potentials:

$$U(\theta) = k_\theta (\theta - \theta_0)^2 \quad (2)$$

where θ is the bond angle and the subscript 0 denotes the equilibrium value. k_θ is the spring constant.

Dihedral angle energies around bonds are given by:

$$U(\phi) = \sum_{i=1}^5 C_i \cos(\phi)^i \quad (3)$$

where ϕ is the dihedral angle and the C_i are constants. In this potential $\phi = 0$ corresponds to the trans form and $\phi = 180$ to the cis form. The potential energy is given by the standard combination of Lennard-Jones and Coulomb potentials:

$$U(r_{ij}) = 4\epsilon \left[\left(\frac{\sigma}{r_{ij}} \right)^{12} - \left(\frac{\sigma}{r_{ij}} \right)^6 \right] + \frac{q_i q_j}{r_{ij}} \quad (4)$$

where q are atomic charges, σ and ϵ are the Lennard-Jones parameters and i and j are any atomic sites. Only intermolecular potential energy is calculated in both the force fields, the intramolecular

potential is represented solely by the dihedral and bond energies. Standard Lorenz-Berthelot mixing rules were applied.

The new representation was based on quantum mechanical calculations to determine geometry and intramolecular potential together with standard Lennard-Jones parameters from the united¹² and all atom^{10, 13} OPLS force field. Atomic charges were fitted to the electrostatic potential from quantum mechanical calculations. The choice of parameters was also guided by our desire to reproduce the experimental enthalpy of vaporization and density. This parameterization combines elements of the approach taken by Jorgensen and coworkers¹⁰ and Cornell and coworkers¹⁴ in their respective force field development.

Conformer notation has been adopted from work by Vorobyov et al.¹⁵ A conformer is represented as xYz. Where x designates the C-C-N- lpN dihedral angle, Y is the O-C-C-N dihedral angle, and z the C-C-O-H dihedral angle. lpN denotes the lone pair on the nitrogen atom. G or g indicates *gauche*(+), G' or g' indicates *gauche*(-) and T or t indicates *trans*.

Vorobyov et al.¹⁵ have published results of quantum mechanical calculations on the ethanolamine geometry more advanced than those presented by Alejandro et al.⁴ In the present work we have replaced the force field geometry presented by Alejandro et al.⁴ with the B3LYP/6-311++G(2d,2p) g'Gg' geometry from this new paper.¹⁵ The resulting force field will be referred to as MEAa, MEA (monoethanolamine) being the common acronym for ethanolamine in chemical engineering.

Gubskaya and Kusilik⁶ observed that the Alejandro et al.⁴ force field has a enthalpy of vaporization significantly lower than the experimental value. In the present work we will use a parametrization procedure similar to that utilized by Alejandro et al.⁴, but making sure that the experimental heat of vaporization is reproduced reasonably well. One of the purposes of the present work is to study the conformer distribution of ethanolamine in greater detail, and for this purpose we performed a more detailed analysis of the intramolecular potential.

For the new force field we again chose geometry from recent quantum mechanical calculations¹⁵ and OPLS Lennard Jones parameters similar to the ones selected by Alejandro et al.⁴ The bond angle

potential was adopted from Alejandro et al.⁴ The approach of deriving the atomic charges from the electrostatic potential taken by Alejandro et al.⁴ seems to us a sensible one, but as their model produces to low heat of vaporization we carried out more detailed analysis of the atomic charges. To calculate the atomic charges from the electrostatic potential the Merz-Kollman¹⁶ (MK) scheme implemented in Gaussian 98¹⁷ was utilized. Calculation on a single molecule in gas-phase will yield only gas-phase charges, while molecules in solution are polarized by the environment and tend to have higher charges. Calculations with a continuum solvent model were carried out to obtain solution phase charges. Different conformer geometries were optimized at the B3LYP/6-311++G(d,p) level and continuum model calculations were carried out as single-point IEFPCM¹⁸ calculations (IEFPCM-B3LYP/6-311++G(d,p)// B3LYP/6-311++G(d,p)). The methyl group charges were added together, and the total charge of these groups were distributed evenly between the two carbon atoms. The amine group hydrogen atom charges were also averaged.

A modified version of the EMP2 model¹⁹ has been utilized to simulate CO₂. The modification consists of adding a flexible bond angle. The spring constant was determined by use of ab initio calculation. B3LYP/6-311++G(d,p) calculations were carried out for unconstrained CO₂ and CO₂ with the bond angle set to 150°. The energy difference between these forms was determined to be 81 kJ/mole, and the spring constant was set to reproduce this energy difference. The model details are given in the supporting information.

Intramolecular Potential

Some simple spread-sheet calculations were performed to study the intramolecular potential for different conformers. The intramolecular distances can be determined from the geometry data for different conformers¹⁵ and the energy of a conformer can be calculated directly for a given force field. The angle energies were neglected in these calculations. Energies were calculated both with ab initio dihedral angles and dihedral values found to be optimal in simulations. Such approximate spread-sheet calculations can provide an immediate picture of relative conformer energies.

Simulations Details

The SPC model²⁰ was chosen to represent water. Simulations were carried out using the constant-temperature, constant-pressure algorithm (nPT) in the MdynaMix package written by Lyubartsev and Laaksonen.²¹ Long-range electrostatic interactions were handled by means of Ewald summation. Lennard-Jones forces and real-space electrostatics were cut off at 11.5Å. A dual time step algorithm was used, with all the forces in the system divided into fast and slow ones. Fast forces included interactions arising from bonds, constrained angles and dihedral angles, as well as Lennard-Jones and real-space electrostatic forces within a cutoff of 5Å. They were recalculated each short time step (0.05 fs), with the rest of the forces recalculated once every 10 short steps. Simulations were carried out with 512 molecules at 298.15 K and 333K and 1 atmosphere of pressure. Two different compositions were studied, one with pure ethanolamine and one with 461 water molecules and 51 ethanolamine molecules. The latter corresponds to 10 mol percent ethanolamine, representative of the composition often used in industrial applications. For comparison purposes simulations we also carried out pure water simulation. Each system was equilibrated over at least 200000 steps (100ps), and sampling was done over 100000 steps (50ps).

The single-molecule simulations (gas-phase) were run for over 20 million steps (20 ns). For these simulations, we followed the approach of Jellinek and Li²² and modified the original MdynaMix package to implement separate temperature controls for each kinetic mode (translation, rotation, and internal).

Results

The relative conformer energies of the MEAa force field are shown together with the relative energies from quantum mechanical calculations in Table 1. Energies for all 14 nonequivalent conformers are shown.¹⁵ The force field results are presented both for quantum mechanical dihedral angles determined by Vorobyov et al.¹⁵ and for the average dihedral angles for each conformer determined from liquid-phase simulations. These were estimated to be 77 for O-C-C-N gauche and 180 for trans, 45 for C-C-O-H gauche and 182 for trans and finally 58 for C-C-N-*lp*N gauche and 180 for trans.

The most stable gas-phase conformer (g'Gg') is shown in Figure 1.

Table 1. Relative conformer energies. Values in [kJ/mole].

	B3LYP ^a	MEAa ^b	MEAa ^c
g'Gg'	0	0	0.0
gGg'	5.5	8.5	0.0
gGt	5.3	5.0	2.6
tGt	5.7	17.0	5.3
tGg	6.6	11.5	2.7
gGg	6.9	-1.4	0.0
tGg'	8.0	9.2	2.7
tTt	9.5	18.2	6.2
tTg	9.7	9.6	3.6
gTt	10.0	9.1	3.5
gTg	10.5	0.5	0.9
g'Tg	10.6	-0.1	0.9
g'Gt	16.2	6.9	2.6
g'Gg	No minima	-1.7	0.0

^a: Sum of electronic and zero-point energies at B3LYP/6-311++G(2d,2p) level from Vorbyov et al.¹⁵ ^b: Conformer energies calculated with dihedral angles determined from ab initio calculations. ^c: Conformer energies calculated with optimal dihedral angles for force field.

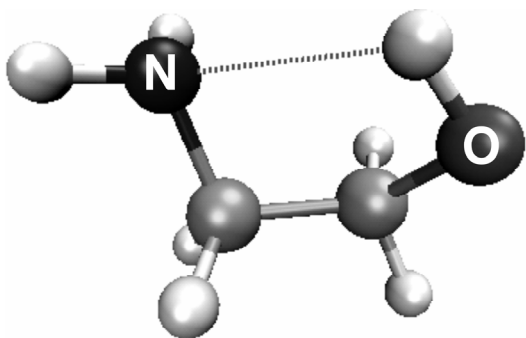


Figure 1. $g'Gg'$ conformer of ethanolamine

The MEAa force field can be seen from the data in Table 1 to be in mostly reasonable agreement with the quantum mechanical results. Some conformers that are not equivalent in the ab initio calculations do however become equivalent in the force field. This is a direct consequence of using a force field with an intramolecular energy only represented by uncoupled dihedral energies. Thus $g'Gg'$, gGg' , gGg and $g'Gg$ become equivalent in terms of energy, the same holds for the $g'Gt$ and gGt pair and gTg and $g'Tg$ as well.

A number of different force fields of ethanolamine were studied in a recent paper by Gubskaya and Kusalik.⁶ They apparently treated the intramolecular potential as a parameter to be set in the overall fitting of liquid properties. It is not clear from their paper if the representations chosen reproduce relative conformer energy differences from quantum mechanical calculations. We believe a more realistic solvent representation is obtained by determining the intramolecular potential from quantum mechanical potential, and that this part of the potential should not be arbitrarily fitted to experimental data. In this we follow the approach taken by Jorgensen et al.¹⁰

Gubskaya and Kusalik⁶ observed, as previously noted, that the MEAa force field had a too low enthalpy of vaporization. Results from our own calculations shown in Table 2 are in agreement with that observation. It should be noted that our density for MEAa is higher than reported by Alejandro et al.⁴ The discrepancy is most probably caused by different ensembles utilized and that, unlike Alejandro et al.⁴, we did not shift or truncate the Lennard-Jones potential.

Table 2. Densities and Heats of Vaporization for ethanolamine.

	MEAa	MEAb	Experimental
$\rho(298.15K)^a$	1.032	1.060	1.012 ^d , 1.008 ^e
$\rho(333K)^a$	1.003	1.037	0.984 ^d , 0.984 ^e
$U_{liq}(298.15K)^a$	-43.04	-62.34	
$U_{gas}(298.15K)^a$	1.90	-1.97	
$\Delta H_{vap}(298.15K)^b$	47.7	63.13	
$U_{liq}(333K)^a$	-37.45	-55.34	
$U_{gas}(333K)^a$	2.59	-1.32	
$\Delta H_{vap}(333K)^b$	42.8	56.80	57.7 ^d

^a Density in g/cm³. ^b Energy in kJ/mole. ^c Enthalpy of vaporization in kJ/mole. ^d Data from da Silva⁵ and references therein. ^e Data from Cheng et al.²⁷

Alejandro et al.⁴ reported a single set of atomic charges for the fitting of charges to the electrostatic potential. Such procedures to fit charges are however known to be ambiguous,²³ and the charges may depend on the conformer form of the molecule.²⁴ In Table 3 results of fitting of the charges to the electrostatic potential in a solvent field (IEFPCM model) for a number of conformer forms are shown.

Table 3. Dipole Moments and Atomic Charges from Fitting the Electrostatic potential.^a

	g'Gg'	tGt	gGt	tTt	gTt
Dipole Moment:	4.110	2.360	1.329	3.607	0.998
N	-1.035	-1.162	-1.163	-1.224	-1.256
H1(N)	0.397	0.423	0.415	0.427	0.436
H2(N)	0.399	0.423	0.436	0.425	0.450
C(N)	0.274	0.402	0.367	0.490	0.448
H1(C(N))	-0.036	-0.016	0.003	-0.008	0.014
H2(C(N))	0.048	0.026	-0.016	-0.004	-0.043
C(O)	0.189	0.161	0.238	0.317	0.312
H1(C(O))	0.021	-0.011	-0.027	-0.028	-0.011
H2(C(O))	0.046	0.034	0.026	-0.030	0.009
O	-0.705	-0.767	-0.756	-0.891	-0.864
H(O)	0.402	0.484	0.477	0.526	0.504

^a MK charges at IEFPCM-B3LYP/6-311++G(d,p)//B3LYP/6-311++G(d,p) level.

It can be seen from Table 3 that there are significant differences in the charges calculated for different conformers. Both the magnitude of charges and (to a lesser extent) their relative distribution between the hydroxyl functional group and the amino functional group vary. The present charges calculated in a solvent field for the g'Gg' conformer are as might be expected higher than the gas-phase charges utilized by Alejandro et al.⁴ It can also be noted that the g'Gg' conformer has the lowest charges of all these conformers. Alejandro et al.⁴ suggested that their choice of charges was validated by the agreement with experimentally-determined dipole moment. The experimental dipole moment is however an average over the conformer population, and as the data in Table 3 suggest that the conformers have widely varying dipole moments, it becomes apparent that this comparison with the experimental value is inconclusive.

We looked at which set of charges that would produce best agreement with the experimental heat of vaporization. A force field based on the g'Gg' charges gave good agreement with the experimental heat

of vaporization and these charges have been adopted. This agreement must be viewed as fortuitous and can not be used to draw conclusions regarding the conformers in solution.

While there is some ambiguity in which charges to choose, the MEAa and MEAb representation are in reasonable qualitative agreement and do not differ too much from the values for ethanolamine in the semi-empirical OPLS force field.^{3, 5}

The MEAb model utilized the same intramolecular potential as in MEAa. In our work we did attempt to apply different intramolecular potentials to get the best possible agreement with the relative conformer energies determined from quantum mechanical calculations. The presence of intramolecular hydrogen bonds in some conformers does mean that the energy dependency of the different dihedral angles is strongly coupled. We have looked into adding intramolecular Coulomb and Lennard-Jones forces interactions as a means to capture this coupling. In such representations there was unfortunately a tendency for the strength of the hydrogen bonds to be overestimated and we were unable to come up with a set of parameters that produced a representation better than the MEAa force field.

The MEAb charges are higher than those used by Alejandro et al.⁴, combined with an otherwise identical force field, this results in increased density. To keep the density from deviating too much from the experimental values, we looked at the possible changes that could be made to the parameters without deviating from geometries derived from quantum mechanical calculations. Alejandro et al.⁴ used the g'Gg' conformer to determine the bond lengths and angles. It is however not clear if this is the best choice when representing a liquid phase were a number of conformer forms are populated. Conformer geometries reported by Vorobyov et al.¹⁵ show that while most bond-lengths change little with conformer, most conformer have a C-O bond of around 1.43 Å, longer than for the g'Gg' conformer (1.42 Å). For MEAb the value of 1.43 Å is therefore chosen. The g'Gg' values are clearly not representative for some of the angles either. We set the C-O-H(O) angle to 108.7 in MEAb, while both the C-C-N and C-C-O angles were set to 112. We also chose to increase the Lennard-Jones σ for Nitrogen to 3.3 Å, which is the standard in the all atom OPLS force field.¹³ The MEAb force field parameters are shown in Table 4, the MEAa parameters are given in the Supporting Information.

Table 4. Potential Parameters of MEAb

Bond	r_0 [Å]				
N-H	1.012				
N-C	1.471				
C-C	1.524				
C-O	1.43				
O-H	0.966				
Angle	θ_0	k_0 [J/mole]			
H-N-H	107.4	269.39			
H-N-C	111.4	316.65			
N-C-C	112	506.21			
C-C-O	112	546.91			
C-O-H	108.8	298.79			
Dihedral	C_1^a	C_2^a	C_3^a	C_4^a	C_5^a
H-N-C-C	-11.05	-2.37	25.30	0.43	-2.02
O-C-C-N	-17.78	23.60	36.81	-16.64	-13.32
C-C-O-H	-19.15	-2.79	13.61	-0.12	1.55
Site	σ [Å]	ϵ [KJ/mole]	q		
H(N)	0	0	0.40		
N	3.3	0.7108	-1.035		
CH ₂	3.905	0.494	0.27		
O	3.07	0.7108	-0.705		
H(O)	0	0	0.40		

^a In kJ/mole.

The density and heat of vaporization of MEAb is shown in Table 1. The ethanolamine force field has a large number of parameters and one could certainly refine the parameters to improve the fit with experimental data. It is however not clear to us at present what kind of parameter adjustment is the most

reasonable, and we have chosen not to deviate from the quantum mechanical representation of the molecule.

The simulated and experimental densities of both MEAa and MEAb as pure component and in mixture with water at 298.15K and 333K are given in Table 5. MEAa reproduces the experimental values quite well, the deviation from experimental values being small and fairly constant. The MEAb is in somewhat worse, but still reasonable, agreement with experimental data. The densities are in general somewhat high, even for SPC water, this would appear to be a result of the type of ensemble and simulation algorithm employed.

Table 5. Densities of ethanolamine-water systems

	MEA	10% MEA ^b	H ₂ O
$\rho(298.15K)^a$ -Exp.	1.008	1.009	0.997
$\rho(298.15K)^a$ -MEAa	1.032	1.040	1.015
$\rho(298.15K)^a$ -MEAb	1.060	1.045	
$\rho(333K)^a$ -Exp.	0.984	0.992	0.983
$\rho(333K)^a$ -MEAa	1.003	1.011	0.994
$\rho(333K)^a$ -MEAb	1.037	1.019	

^a Density in g/cm³, experimental data are from Cheng et al.²⁷ ^b 10 mol percent ethanolamine.

Some of the intermolecular radial distributions for pure ethanolamine at 298.15K and 333K are presented in Figure 2. The MEAa results are mostly in good agreement with those presented by Alejandro et al.⁴ The O-H(N) curve does however show a significantly higher peak in the present calculations. Despite the differences in the force fields utilized most of the radial distribution functions are also in good agreement with results obtained by Gubskaya and Kusilik.⁶

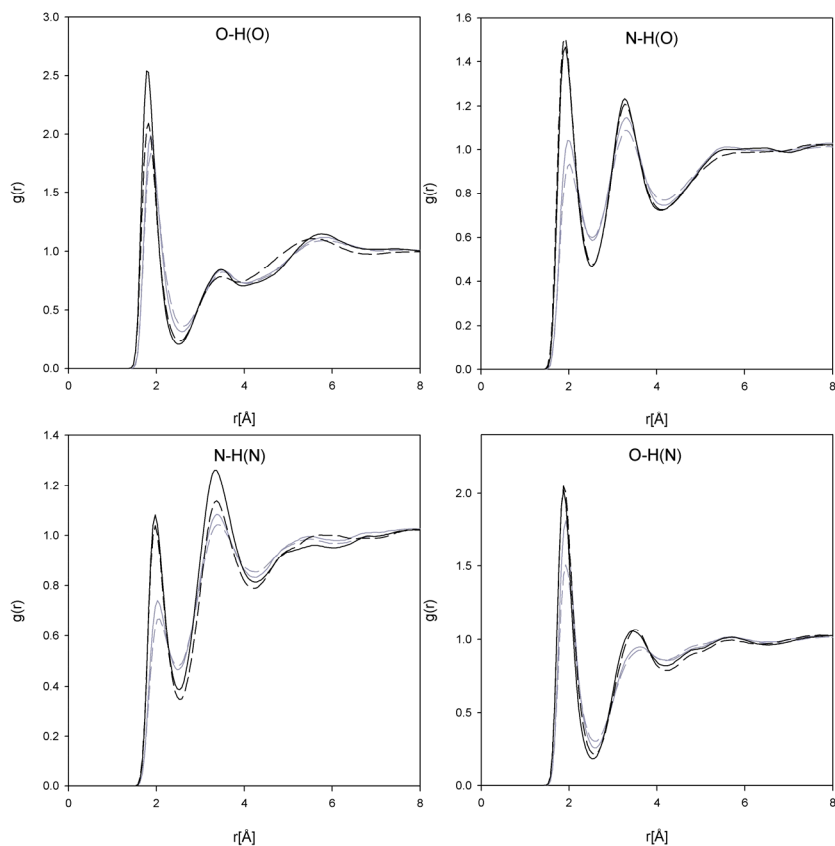


Figure 2. Radial distribution functions for pure ethanolamine. Gray lines are MEAA and black lines are MEAB. Solid lines are for 298.15K while dashed lines are for 333K.

MEAB produces somewhat higher peaks in the radial functions than MEAA, this is consistent with MEAB being the force field with higher atomic charges. The force fields do however appear to produce very similar liquid structures, suggesting that results can be viewed with a high degree of confidence. The results suggest that the strongest bonding takes place between hydroxyl-groups. The second strongest feature is bonding between hydroxyl-group oxygen atoms and amino-group hydrogens. Bonding between the amino groups appear to be somewhat weaker. Both the N-H(O) and N-H(N) curves have second peaks that are higher than first, these reflect bonding taking place at the hydroxyl-functionality of the molecule. The liquid ethanolamine structure is clearly dominated by the hydrogen bonding features. Neither radial distribution functions nor visual inspection of the ensemble suggested any ordered structure.

At 333K the radial distribution functions become somewhat less pronounced, a trend which is common and expected in most liquids. The changes in structure do however appear to be quite small for the temperature range studied.

Radial distribution functions for 10 mol percent MEAa and MEAb in aqueous solution are presented in Figures 3 and 4. Once again we have chosen to display the radial distribution functions that convey information about the hydrogen bonding. In Figure 3 the same ethanolamine-ethanolamine radial distributions as plotted for pure ethanolamine (Figure 2) are shown. All the peaks are lower than in the pure liquid suggesting that ethanolamine molecules have a preference to be surrounded by water molecules, bonding between ethanolamine molecules does however persist. The amino-amino bonding becomes significantly less frequent in the aqueous solution, while the hydroxyl-group interactions change less in their relative prevalence. A fairly homogeneous and random molecular-level structure is suggested by the radial distribution functions and visual inspection of the structure.

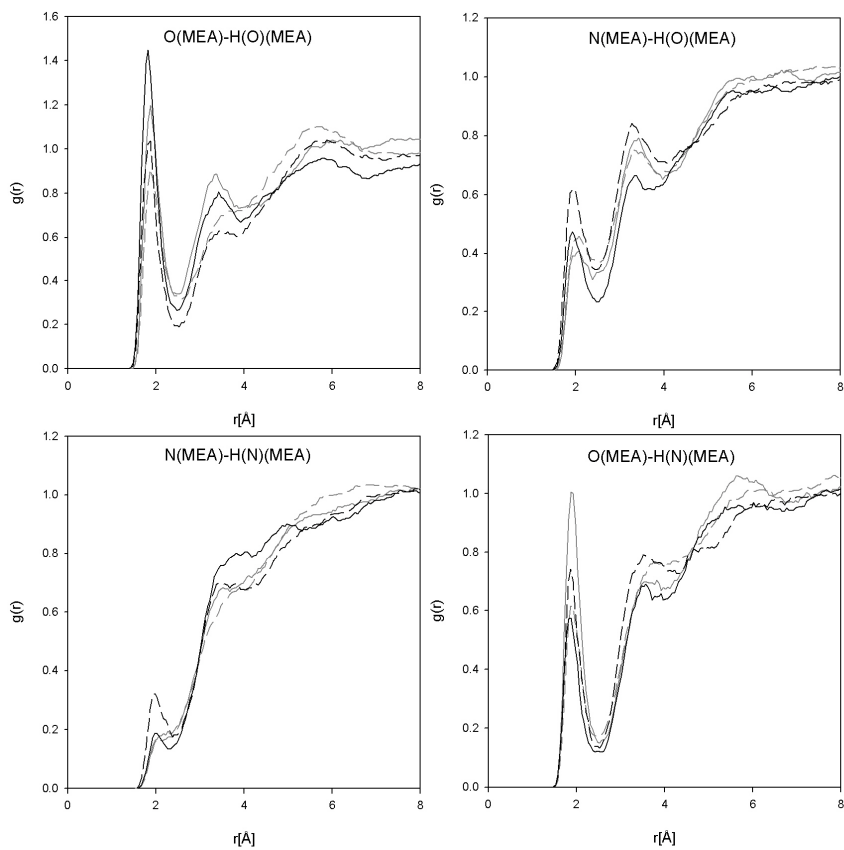


Figure 3. Radial distribution functions for 10 mol percent ethanolamine in water. Gray lines are MEAa and black lines are MEAb. Solid lines are for 298.15K while dashed lines are for 333K.

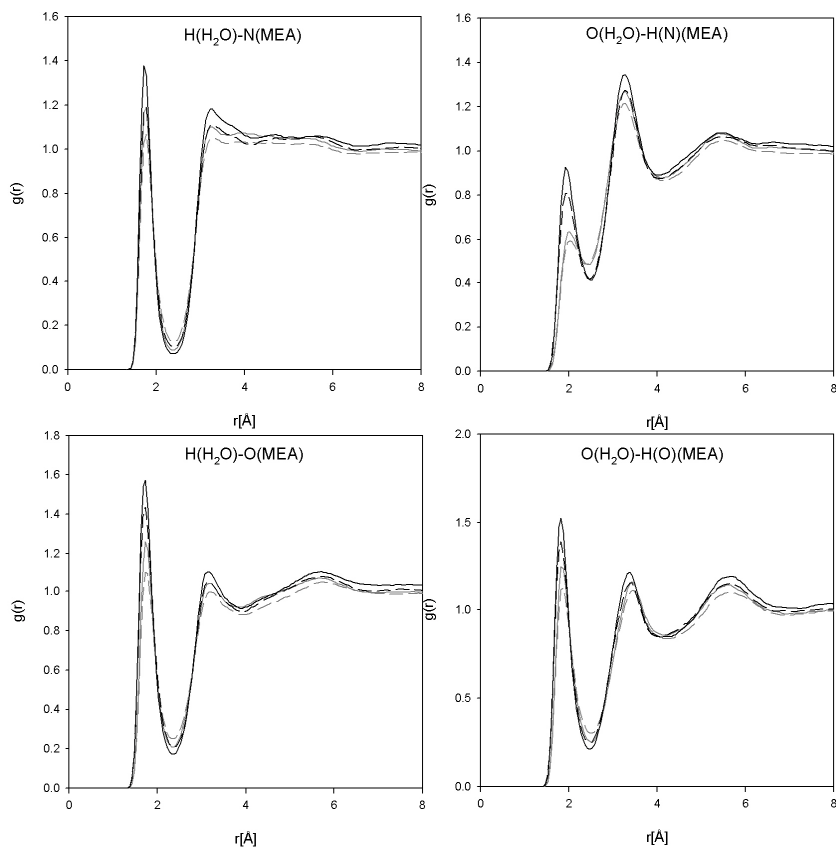


Figure 4. Radial distribution functions for 10 mol percent ethanolamine in water. Gray lines are MEAA and black lines are MEAB. Solid lines are for 298.15K while dashed lines are for 333K.

Radial distributions for the water molecules are shown in Figure 5. The results are for 10 mole percent aqueous ethanolamine and pure water. While the changes are quite small it can be observed that first peaks in the radial distribution functions become somewhat higher in the aqueous ethanolamine system.

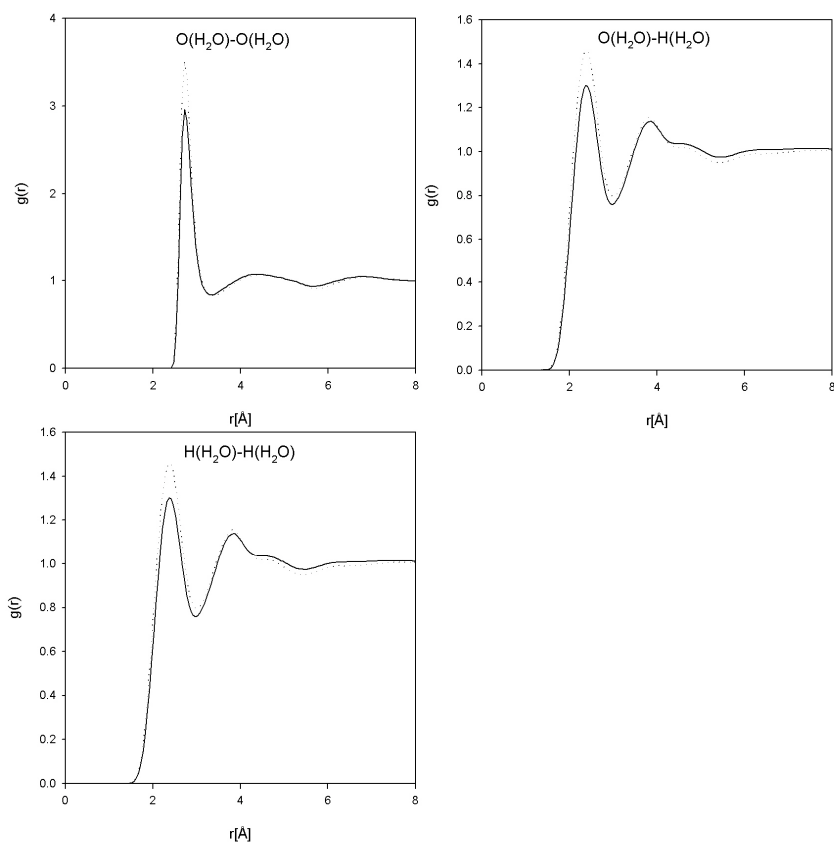


Figure 5. Water-water radial distribution functions at 333K. Stippled lines are from 10 mole percent mixture with MEAb, while solid lines are from pure water simulation.

It has been suggested that ethanolamine forms dimers in aqueous solution.²⁵ The liquid structure and the nature of the bonding in the simulated system is however such that stable dimers would seem unlikely to be formed. The force fields in the present work have however not been parameterized to reproduce dimer formation energies, and more careful studies would be required to draw confident conclusions on this point.

The populations of the various conformers for pure ethanolamine and 10 mol percent aqueous solution of ethanolamine are shown in Table 6. Most of the data pertains to 333K, pure MEAa and MEAb data at 298K are also included.

Table 6. Conformer Populations.

	Ma ^a	Ma ^{a, c}	Ma ^a	Ma ^{a, c}	Mb ^b	Mb ^{b, c}	Mb ^b	Mb ^{b, c}	aH ₂ O ^d	aH ₂ O ^{d, c}	bH ₂ O ^e	bH ₂ O ^{e, c}
	333K	333K	298K	298K	333K	333K	298K	298K	333K	333K	333K	333K
g'Gg'	3.3	13	3.4	11	1.2	1	1.2	9	3.9	27	1	12
gGg'	34.0	43	35.6	37	21	6	22.6	54	22.7	28	14.4	54
gGt	0.1	0	0.1	4	0	0	0	0	0.1	0	0	0
tGt	0.0	0	0.0	0	0	0	0	0	0.0	0	0	0
tGg	0.1	4	0.3	0	1.3	8	0	0	0.0	0	0	0
gGg	40.0	16	37.3	12	16.7	1	16.9	13	55.7	22	20	23
tGg'	0.7	11	1.4	20	16.4	63	0.4	13	0.0	0	0	0
tTt	0.0	0	0.0	0	0	0	0	0	0.0	0	0	0
tTg	0.1	0	0.2	5	2.3	20	0.2	0	0.0	0	0	0
gTt	0.0	0	0.1	0	0.0	0	0	0	0.0	0	0	0
gTg	5.7	3	5.4	2	3.1	0	3	3	3.5	2	0.8	1
g'Tg	13.8	7	13.7	6	6	1	7.4	7	0.1	0	2	3
g'Gt	2.3	3	2.5	3	0.5	0	0.3	1	14.1	21	1.5	7
g'Gg	0.0	0	0.0	11	0	0	0	0	0.0	0	0	0

^a MEAa. ^b MEAb. ^c Values corrected for errors in relative conformer energies of force field. ^d 10 weight percent MEAa in water. ^e 10 weight percent MEAb in water.

We have analyzed the relative conformer populations of both liquid and aqueous MEA at the two temperatures. The dihedral angle distributions for MEAa at 298K are plotted in Figure 6, with the data for the other systems given in the supporting information section. The peaks of MEAa dihedral distributions are located at 77 (gauche) and 180 (trans) in case of the O-C-C-N torsional, 45 (gauche) and 180 (trans) for the C-C-O-H torsional, and finally 58 (gauche) and 180 (trans) for C-C-N-lpN angle. A molecule was classified as a given conformer if its dihedral angles lay within 40 degrees (45 for MEA-water systems) of the corresponding dihedral peaks. Varying the 40 degrees limit did not

significantly alter the relative conformer populations. With this kind of definition a part of the molecules will not be counted as occupying any conformer form, this fraction amounted to between 30 and 60 percent of the ethanolamine molecules. The statistics was worse in case of aqueous solutions, resulting in significantly larger uncertainty in the relative conformer populations.

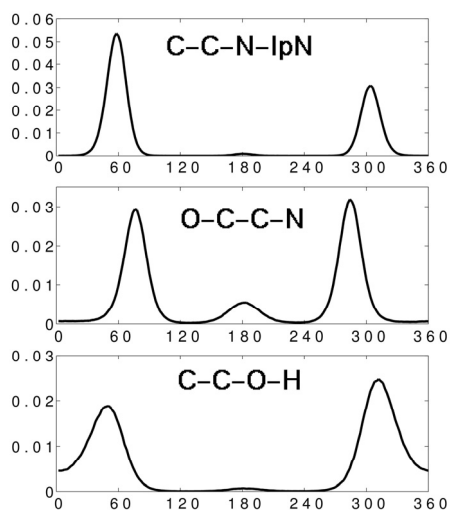


Figure 6. Dihedral angle distribution for pure MEAA at 298K.

The ethanolamine force fields do not fully reproduce the relative conformer energies from ab initio calculations (Table 1). We have therefore done calculations to attempt to correct for this error and give a picture of what the conformer populations would have been if the force field intramolecular potential had accurately reproduced the ab initio energies. The conformer populations were first converted to relative energies. The relative energies were then corrected by the difference between ab initio and force field energies (data in Table 1, second and fourth column). The relative energies were then finally converted back to conformer populations. The results with these corrections provide an approximate estimate of what the conformer population would have been for a more accurate intramolecular potential. Such a correction will however produce uncertain results in case of sparsely populated conformers, therefore no correction was applied and the corrected population values were set to 0 for conformers accounting for less than 0.5 percent of all molecules.

The g'Gg' conformer has a small population in solution, despite being the most stable in the gas-phase. This conclusion holds for both force fields and in aqueous solution as well as in the pure liquid. It can also be seen that the total population for O-C-C-N trans conformers is quite small. While the corrected values for MEAb in aqueous solution in one case shows a significant trans conformer population, the correction was in this case being made to a very small population number and is highly uncertain. Several of the trans conformers in the force field have intramolecular energy differences relative to the g'Gg' conformer that are equal or smaller to the ab initio differences. This would suggest that the force fields overestimate the trans populations, and the total trans (O-C-C-N) population would therefore in general seem to be less than 20 percent. These conclusions are in good agreement with those drawn from experimental work on pure ethanolamine.²⁶ These results strongly suggest that ethanolamine forms a significant amount of intramolecular hydrogen bonds in solution.

In the case of pure ethanolamine the most populated conformers are for MEAa gGg' and gGg, and tGg', gGg' and tTg' for MEAb. Looking at the values corrected for the intramolecular potential there can however be seen to be significant changes. There are also some significant difference between the two force fields. An interesting feature of the MEAb force field is the high tGg' populations for pure component at 333K, at 298K and in aqueous solution this conformer has a much smaller population. The MEAa force field has a very small population for the same conformer. Conformers with the C-C-N-*lp*N dihedral in a trans form can more readily form intermolecular hydrogen bonds to nitrogen atom. Stronger hydrogen bonds to the nitrogen atom in the MEAb force field are therefore the most likely explanation for the high tGg' population.

Silva et al.²⁶ reported the gGt and tGt conformers to be the most common for pure ethanolamine solution. The main difference between their findings and the simulation results would appear to be in the C-C-O-H dihedral angle. All the simulation results (see Figure 6, supporting information and Table 5) suggest that this dihedral remains mainly in the gauche conformers. This might suggest that the atomic charge on the hydroxyl-group hydrogen atom is too low, thereby underestimating the strength of

intermolecular hydrogen bonds formed with the hydroxyl-group hydrogen atom. This observation could perhaps in future work be utilized for further refinement of the force field.

Radial distribution functions for system of a CO_2 molecule in a 10 mole percent ethanolamine (MEAb) in aqueous solution at 333K are shown in Figure 7. The radial distributions shown are for the interactions that are expected to dominate the bonding of CO_2 . The results suggest that the CO_2 molecule is somewhat more attracted to the ethanolamine amino-functionality than to the hydroxyl group. This interaction with the amino group is however somewhat less favored than with the water molecules.

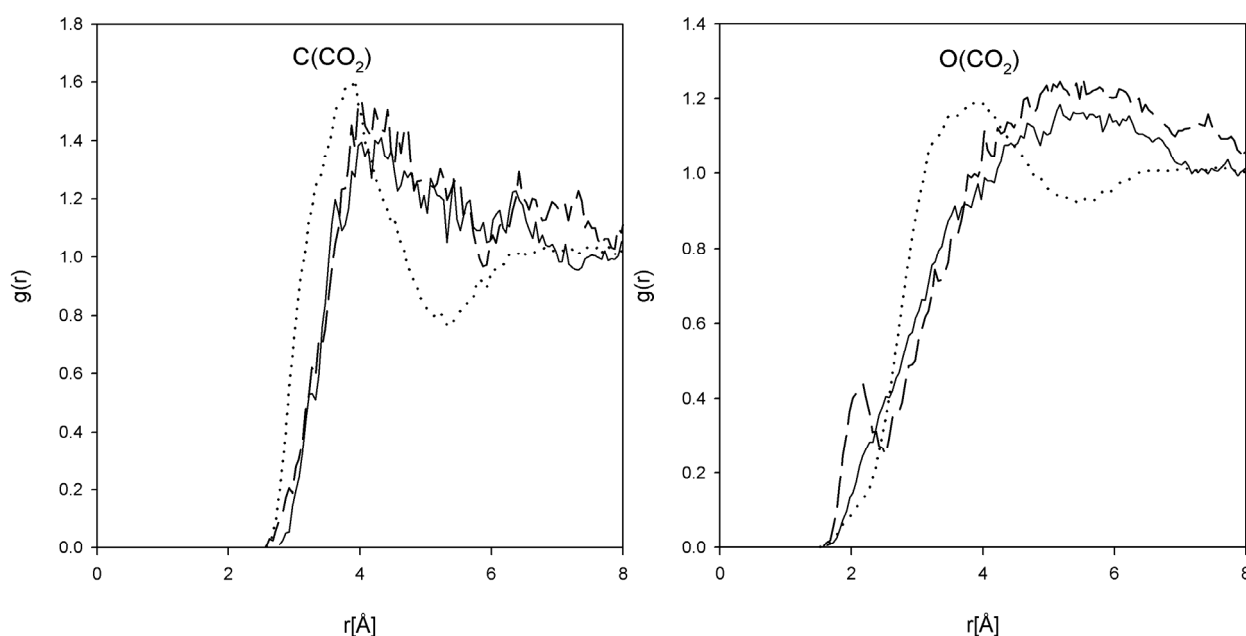


Figure 7. CO_2 -ethanolamine- H_2O radial distribution functions at 333K for 10 mol percent ethanolamine (MEAb) in water. Lines in left plot: Solid line is $\text{C}(\text{CO}_2)$ -N(MEA), dashed line is $\text{C}(\text{CO}_2)$ -O(MEA) and dotted line is $\text{C}(\text{CO}_2)$ -O(H_2O). Lines in right plot: Solid line is $\text{O}(\text{CO}_2)$ -H(N)(MEA), dashed line is $\text{O}(\text{CO}_2)$ -H(O)(MEA) and dotted line is $\text{O}(\text{CO}_2)$ -H(H_2O).

CO_2 is known to react with ethanolamine according to equation 1 in an aqueous alkanolamine system. da Silva and Svendsen¹⁰ concluded that the reaction mechanism had no intrinsic barrier. They also suggested that the barrier could either arise from the CO_2 molecule needing to displace the water molecules around the amino group before reacting or from the need for two amine molecules to

approach each other sufficiently for a proton transfer to take place. Such a reaction can not readily be studied with the classical simulations in the present work. The picture of the liquid structure from the present work can nevertheless further the understanding of the reaction mechanism. Since the CO₂ molecule bonds readily to the amino group it would appear that there is not a significant barrier to the approach of the ethanolamine amino group and CO₂. The low degree of direct interaction between amino-functionalities on different molecules would on the other hand suggest that the low likelihood of such interactions may be a significant barrier to reaction.

Conclusions

Two different force fields were used to perform simulations of ethanolamine. The general agreement in results between the two parameterization suggest that the results can be viewed with a high degree of confidence. The results suggest that the ethanolamine O-C-C-N dihedral tends to stay in a gauche conformer and that there is a significant degree of intramolecular hydrogen bonding. These findings holds for ethanolamine as a pure liquid as well as in aqueous solution. While the simulation results are in broad general agreement with conclusions drawn from experimental work on conformer populations, it would appear that the force fields are not sufficiently accurate to predict relative conformer energies in solution. In aqueous solution ethanolamine is preferentially solvated by water molecules, producing an aqueous solution that is homogeneous on the molecular level.

Simulations in aqueous solution suggest that CO₂ has a comparable level of affinity to ethanolamine molecules and water.

Supporting Information Available: Force field parameters for MEAA and CO₂ and dihedral angle distribution figures.

REFERENCES

- (1) Versteeg, G. F.; Van Dijck, L. A. J.; Van Swaaij, W. P. M. *Chem. Eng. Comm.* 1996, 144, 113.
- (2) Rao, A. B.; Rubin, E. S. *Environ. Sci. Technol.* 2002, 36, 4467.
- (3) Button, J. K.; Gubbins, K. E.; Tanaka, H.; Nakanishi, K. *Fluid Phase Equilib.* 1996, 116, 320.
- (4) Alejandro, J.; Rivera, J. L.; Mora, M. A.; de la Garza, V. J. *Phys. Chem. B* 2000, 104, 1332.
- (5) da Silva, E. F. *Fluid Phase Equilib.* 2004, 220, 239.
- (6) Gubskaya, A. V.; Kusilik, P. G. *J. Phys. Chem. A* 2004, 108, 7151.
- (7) Gubskaya, A. V.; Kusilik, P. G. *J. Phys. Chem. A* 2004, 108, 7165.
- (8) Guillot, B. J. *Mol. Liq.* 2002, 101, 219.
- (9) Walser, R.; Mark, A. E.; van Gunsteren, W. F. *J. Chem. Phys.* 2000, 112, 10450.
- (10) Jorgensen, W. L.; Maxwell, D. S.; Tirado-Rives, J. J. *Am. Chem. Soc.* 1996, 118, 11225.
- (11) da Silva, E. F.; Svendsen, H. F. *Ind. Eng. Chem. Res.* 2004, 43, 3413.
- (12) Jorgensen, W. L.; Tirado-Rives, J. J. *Am. Chem. Soc.* 1988, 110, 1657.
- (13) Jorgensen, W. L.; Rizzo, R. C. *J. Am. Chem. Soc.* 1999, 121, 4827.
- (14) Cornell, W. L.; Cieplak, P.; Bayly, C. I.; Gould, I. R.; Merz, K. M.; Ferguson, D. M.; Spellmeyer, D. C.; Fox, T.; Caldwell, J. W.; Kollman, P. A. *J. Am. Chem. Soc.* 1995, 117, 5179.
- (15) Vorobyov, I.; Yappert, M. C.; DuPre, D. B. *J. Phys. Chem. A*, 2002, 106, 668.
- (16) Singh, U. C.; Kollman, P. A. *J. Comp. Chem.* 1984, 5, 129.

- (17) M. J. Frisch, G. W. Trucks, H. B. Schlegel, G. E. Scuseria, M. A. Robb, J. R. Cheeseman, V. G. Zakrzewski, J. A. Montgomery, Jr., R. E. Stratmann, J. C. Burant, S. Dapprich, J. M. Millam, A. D. Daniels, K. N. Kudin, M. C. Strain, O. Farkas, J. Tomasi, V. Barone, M. Cossi, R. Cammi, B. Mennucci, C. Pomelli, C. Adamo, S. Clifford, J. Ochterski, G. A. Petersson, P. Y. Ayala, Q. Cui, K. Morokuma, D. K. Malick, A. D. Rabuck, K. Raghavachari, J. B. Foresman, J. Cioslowski, J. V. Ortiz, A. G. Baboul, B. B. Stefanov, G. Liu, A. Liashenko, P. Piskorz, I. Komaromi, R. Gomperts, R. L. Martin, D. J. Fox, T. Keith, M. A. Al-Laham, C. Y. Peng, A. Nanayakkara, M. Challacombe, P. M. W. Gill, B. Johnson, W. Chen, M. W. Wong, J. L. Andres, C. Gonzalez, M. Head-Gordon, E. S. Replogle, and J. A. Pople, Gaussian 98, Revision A.9, Gaussian, Inc., Pittsburgh PA, 1998.
- (18) Cancès, M. T.; Mennucci, V.; Tomasi, J. *Chem. Phys.* 1997, 107, 3032.
- (19) Harris, J. G.; Yung, K. H.; *J. Phys. Chem.* 1995, 99, 12021.
- (20) Jorgensen, W. L.; Chandrasekhar, J.; Madura, J. D.; Impey, Klein, M. L. *J. Chem. Phys.* 1983, 79, 926.
- (21) Lyubartsev, A. P.; Laaksonen, A. *Comput. Phys. Commun.* 2000, 128, 565.
- (22) Jellinek, J.; Li, D. H. *Phys. Rev. Lett.* 1989, 62, 241.
- (23) Franckl, M. M.; Chirlian, L. In *Reviews in Computational Chemistry* Lipkowitz, K. B.; Boyd, D. B.; Ed.; Volume 14, Wiley-VCH, 2000, 1-31.
- (24) Bayly, C. I.; Cieplak, P.; Cornell, W. D.; Kollman, P. A. *J. Phys. Chem.* 1993, 97, 10269.
- (25) Mate-Divo, M.; Barcza, L. *Zeit. Physicalische Chemie* 1995, 190, 223.
- (26) Silva, C. F. P.; Duarte, M. L. T. S.; Fausto, R. *J. Mol. Struct.* 1999, 482-483, 591.
- (27) Cheng, S.; Meisen, A., Chakma, A. *Hydrocarbon Processing*, 1996, February, 81.

Supporting Information for:
Molecular Dynamics Study of Ethanolamine as a Pure Liquid and in Aqueous Solution

Eirik F. da Silva, Tatyana Kuznetsova and Bjørn Kvamme

Potential Parameters of MEAa

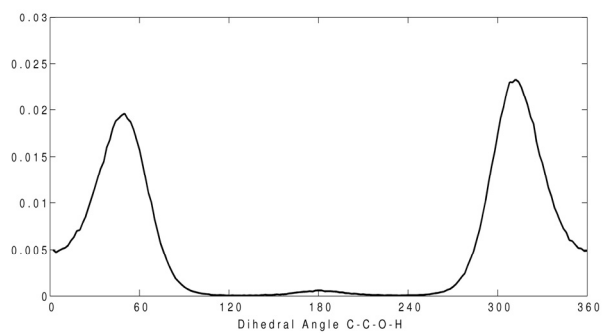
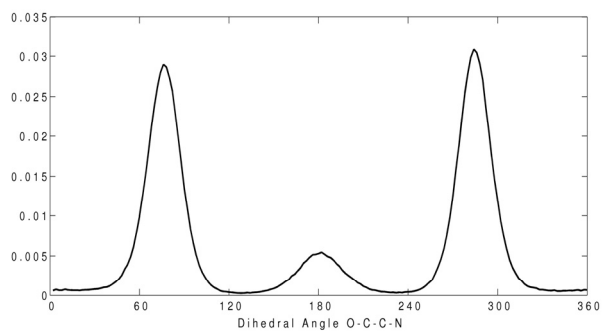
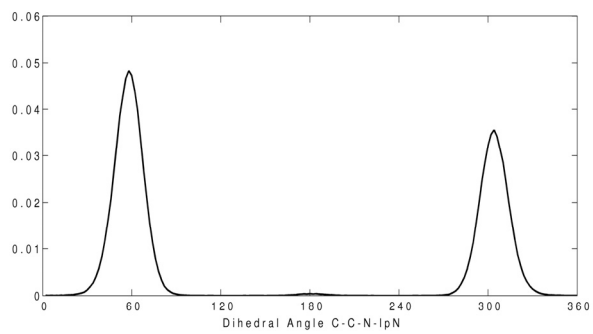
Bond	r_0 [Å]				
N-H	1.012				
N-C	1.471				
C-C	1.524				
C-O	1.419				
O-H	0.966				
Angle	θ_0	k_θ [J/mole]			
H-N-H	107.4	269.39			
H-N-C	111.4	316.65			
N-C-C	109	506.21			
C-C-O	111.4	546.91			
C-O-H	105.8	298.79			
Dihedral	C_1^a	C_2^a	C_3^a	C_4^a	C_5^a
H-N-C-C	-11.05	-2.37	25.30	0.43	-2.02
N-C-C-O	-17.78	23.60	36.81	-16.64	-13.32
C-C-O-H	-19.15	-2.79	13.61	-0.12	1.55
Site	σ [Å]	ϵ [J/mole]		q	
H(N)	0	0		0.347	
N	3.25	0.7108		-0.938	
CH ₂	3.905	0.494		0.257	
O	3.07	0.7108		-0.644	
H(O)	0	0		0.374	

^a In KJ/mole.

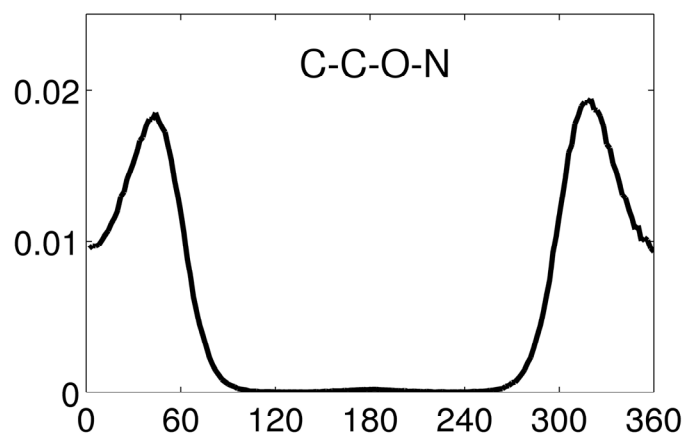
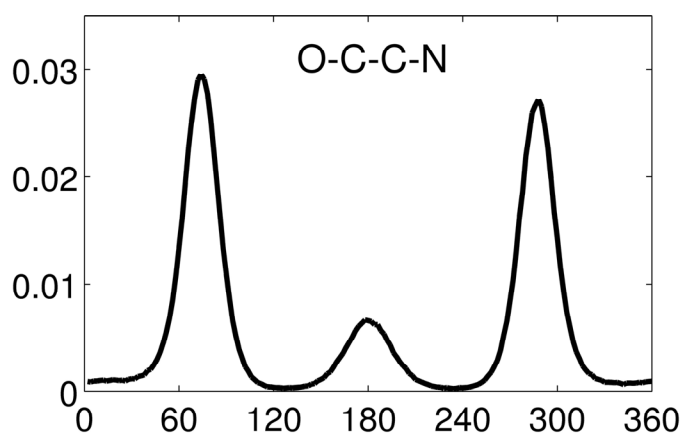
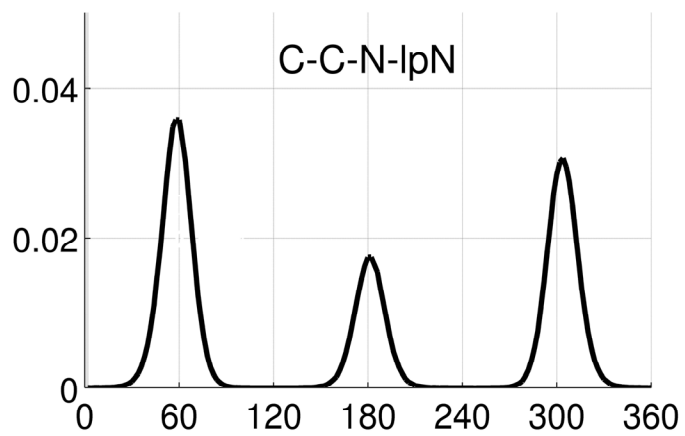
Potential Parameters of CO₂

Bond	r_0 [Å]		
C-O	1.149		
Angle	θ_0	k_θ [J/mole]	
O-C-O	180	236.3	
Site	σ [Å]	ϵ [J/mole]	q
C	2.757	0.2334	0.6512
O	3.033	0.6694	-0.3256

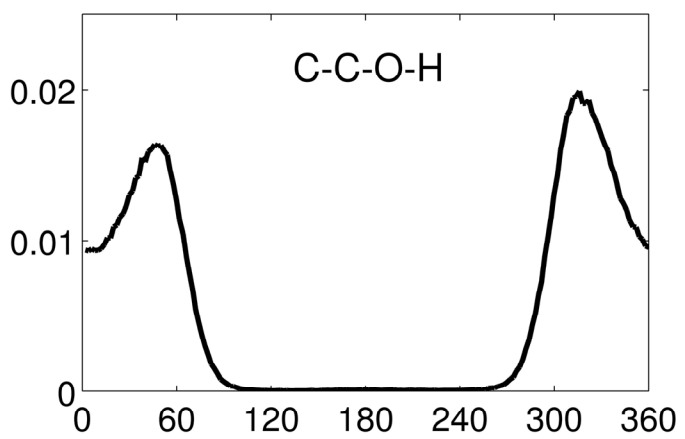
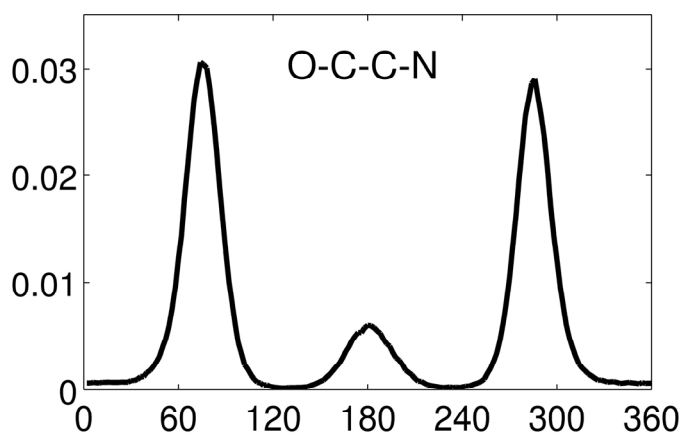
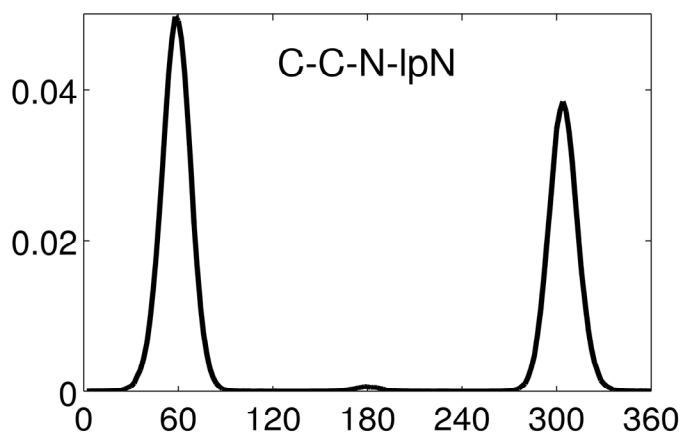
^a In kJ/mole.



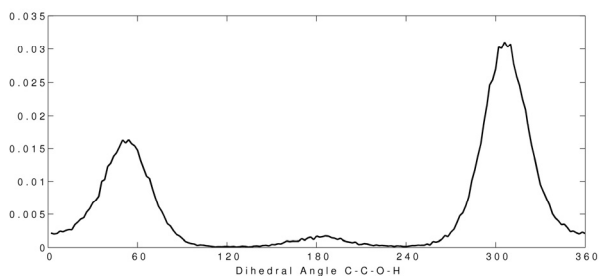
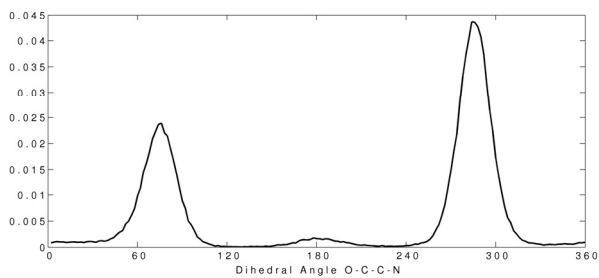
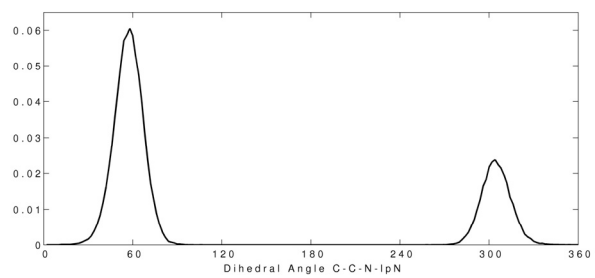
Dihedral angle distribution for pure MEAa at 333K.



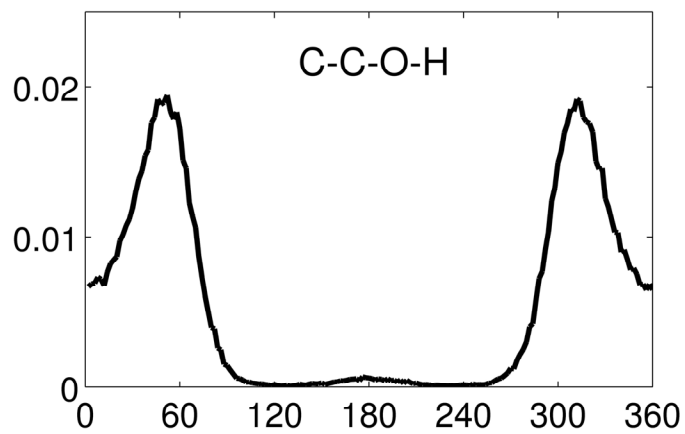
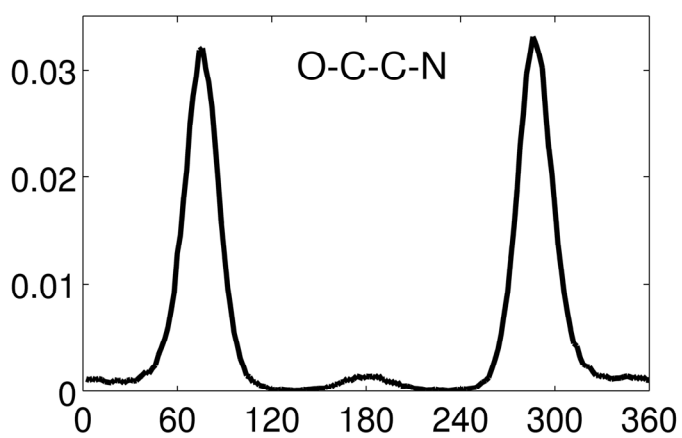
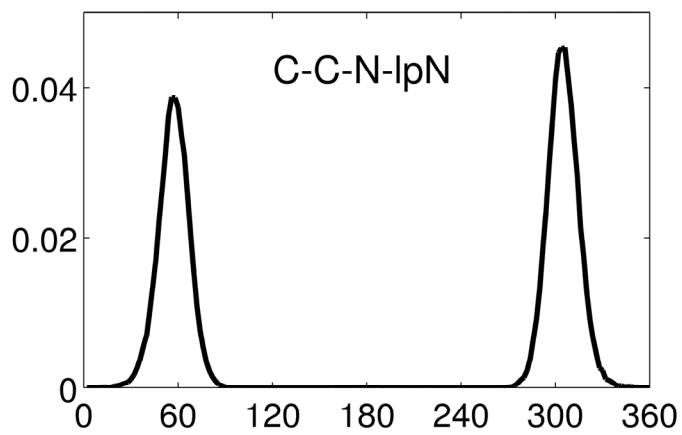
Dihedral angle distribution for pure MEAb at 333K.



Dihedral angle distribution for pure MEAb at 298K.



Dihedral angle distribution for 10 mol percent MEAa in aqueous solution at 333K.



Dihedral angle distribution for 10 mol percent MEAb in aqueous solution at 333K.

Paper VII

Comparison of Solvation Models in the Calculation of Amine Basicity

Eirik Falck da Silva, Takeshi Yamazaki and Fumio Hirata

2005

Theoretical Study of Amine Basicity in Solution with RISM-SCF Calculations and Free Energy
Perturbations

*Eirik F. da Silva**, Takeshi Yamazaki and Fumio Hirata

Contribution from the Department of Chemical Engineering, Norwegian University of Science and
Technology, Trondheim, Norway and the Institute of Molecular Science, Okazaki, Japan

silva@chemeng.ntnu.no

Abstract

The relative basicity of a series of 10 amines in aqueous solution was calculated with three separate sets of solvation energies and gas phase basicities calculated at the B3LYP/6-311++G(d,p) level. The solvation energies were calculated with RISM-SCF and two sets of Monte Carlo simulations. RISM-SCF is a method combining ab initio solute description with the reference interaction site method in statistical mechanics to describe solvation. The simulations were free energy perturbations with classical force fields and charges derived from ab initio calculations. Two different types of charges were studied. Both the RISM-SCF calculations and simulations produced results in reasonable agreement with experimental data. The level of agreement between RISM-SCF and free energy perturbations is consistent with the similarity in solute and solvent representation. Explicit solute polarization, included in RISM-SCF but not simulations, did have a significant effect on relative solvation energies. Solvation energies were found to be sensitive to the scheme utilized to determine atomic charges.

Introduction

Many important chemical processes take place in solution and the effects of the solvent are often of crucial importance. Solution phenomena are therefore of interest in many fields of chemistry, from chemical engineering to biochemistry. Considerable effort has also gone into the study of solution phenomena in computational chemistry, and while various methods in computational chemistry have contributed to the understanding of solvation phenomena it is also clear that the modeling of solvation effects remains challenging.

One of the solvation properties of greatest interest is the free energy of solvation. It is key both to modeling chemical equilibrium in the solution and vapor-gas equilibrium. A fairly large number of schemes have been developed to calculate the free energy of solvation. The most common forms of solvation models in the context of computational chemistry are simulations and continuum models. Some reviews offer general coverage of most schemes¹⁻⁴ while others focus on continuum models.⁵⁻⁶

In the present work the RISM-SCF method and simulations were used for the calculation of solvation energy. RISM-SCF⁷⁻⁸ is a method developed from the statistical mechanics of molecular liquids. While various forms of RISM have successfully been applied to a number of issues in the modeling of liquids⁹ it has still not received much attention as a general solvation model. The simulations were Monte Carlo free energy perturbations (FEP). The RISM-SCF calculations and FEP were carried out with similar, but different, solute and solvent representation. Comparison of the results serves to validate the methodologies, and at the same time this can give insight into what effect differences in solute and solvent representation have on calculated solvation energies.

The solvation energies obtained from RISM-SCF and simulations were used to calculate basicities of a series of amine molecules. While estimates of free energy of solution can be made directly from experimental data for neutral species, this is much more difficult for ionic species. Calculation of base, or acid, strength offers an indirect route to testing the ability of a method to calculate the energy of both

neutral and ionic species. For base strength fairly accurate experimental data are available for a large number of molecules.

It should be noted that both RISM-SCF and simulations can be used to acquire a microscopic picture of solvation effects, for example in terms of radial distribution functions. In the present work we will however focus on solvation energies and solute atomic charges.

The dissociation of the conjugate base of a molecule can be written as



assuming the molfraction based activity of water to be 1 and writing H_3O^+ as H^+ the following equilibrium constant is obtained:

$$K_a = \frac{a_B a_{H^+}}{a_{BH^+}} \quad (2)$$

The definition of pK_a is:

$$pK_a = -\log K_a \quad (3)$$

The free energy of protonation in aqueous solution (ΔG_{ps}) is related to K_a by the following equation:

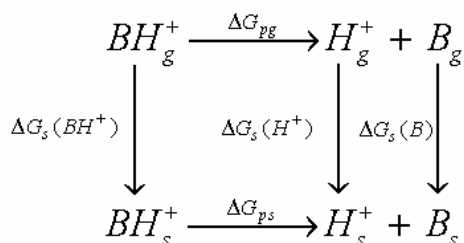
$$\Delta G_{ps} = -2.303RT \log K_a \quad (4)$$

This gives us the relation between pK_a and ΔG_{ps} .

$$pK_a = \frac{1}{2.303RT} \Delta G_{ps} \quad (5)$$

Model predictions for ΔG_{ps} should therefore give a linear correlation with the pK_a .

The general approach for calculating ΔG_{ps} is to use a thermodynamic cycle:¹⁰



where ΔG_{pg} is the gas phase basicity and the ΔG_s 's are the solvation energies of the different species involved.

In the present work the relative basicity in solution, will be studied. The relative basicity is defined as:

$$\Delta\Delta G_{ps} = \Delta G_g(B) - \Delta G_g(B^{ref}) \quad (6)$$

Ammonia will be used as reference base (B^{ref}). The energy of the proton itself (H^+) is not needed to determine relative basicity and is not included in the calculations. Based on the thermodynamic cycle, $\Delta\Delta G_{ps}$ can be divided into the relative gas phase basicity ($\Delta\Delta G_{pg}$) and contributions from solvation:

$$\Delta G_{pg} = [G_g(B) - G_g(NH_3)] - [G_g(BH^+) - G_g(NH_4^+)] \quad (7)$$

and

$$\Delta\Delta G_{ps} = \Delta\Delta G_{pg}(B) + [\Delta G_s(B) - \Delta G_s(NH_3)] - [\Delta G_s(BH^+) - \Delta G_s(NH_4^+)] \quad (8)$$

This can be written as:

$$\Delta\Delta G_{ps} = \Delta\Delta G_{pg}(B) + \Delta\Delta G_s(B) - \Delta\Delta G_s(BH^+) \quad (9)$$

Given a reasonably accurate model for the calculation of relative gas phase basicity the challenge is reduced to calculating the relative solvation energies.

Methods

Gas Phase Basicity

The theoretical basicity of a series of amines at B3LYP/6-311++G(d,p) level with thermal corrections to the free energy and the zero point energies (ZPE) calculated at HF/6-31G(d) level have recently been published.¹¹ It was in the same publication shown that basicities calculated at this level are in good agreement with experimental values. For 2,2,6,6-Tetramethyl-4-piperidinol (TMP) we have performed calculations at the same theoretical level as these published values. Gas phase energy calculations were performed with Gaussian 98.¹²

Solvent Phase Geometry

Amine geometries were optimized in gas phase and the same geometries were used for all calculations in solution. The RISM-SCF calculations were performed on gas phase HF/6-31G(d,p) geometry, similar to what was utilized in a previous study.¹³ Simulations were carried out on HF/6-31G(d) gas phase geometries. The RISM-SCF calculations were performed without optimization of solute geometry. Optimization of solute geometry is in general expected to have a limited effect on calculated energies,^{14,15} something that should hold true for the fairly rigid molecules studied in the present work. We have chosen to carry out calculations on a widely used and not particularly large basis set. In this work we chose to calculate gas phase energies and geometry at a different level from the solution phase calculations. While it might seem more consistent to use the same level of theory for calculations in gas phase and in solution, it must be noted that the relationship between level of theory and quality of results is not the same in the two phases. In gas phase a level of theory that is accurate in calculating basicities is desired. For the solvation energy calculations partial atomic charges and geometry are required as input, and the level of theory should be selected keeping these properties in mind.

RISM-SCF

The Reference Interaction Site Model (RISM) is a method originally developed by Chandler and Anderson¹⁶ in statistical mechanics for the description of interactions in molecular liquids. RISM-SCF^{7,8,17} (Self-Consistent Field) is an extension that allows the simultaneous calculation of distribution of solvent molecules and the electronic structure of the solute molecule. For the calculation of free energy of solvation, the equation derived by Singer and Chandler is employed.¹⁸ In the present work the focus will be on the molecular representation, for description of theory and method we refer the reader to previous work.⁹

In the RISM-SCF framework, the solute molecule is described by ab initio electronic structure theory and the solvent is represented by a classical force field. The interaction between the solute and solvent is described as a sum of classical Coulomb and Lennard-Jones potentials. The Coulomb potential is the potential between the partial charges of the solvent and partial charges of solute sites derived from the electronic wave function of the solute molecule. In the present RISM-SCF calculations Hartree-Fock theory is utilized. The contribution of the solvent reaction-field is introduced in the Fock operator of the solute:^{8,17}

$$F_i^{solv} = F_i^{vacuum} - f_i \sum_{\lambda \in u} V_\lambda b_\lambda \quad (9)$$

where F_i^{vacuum} is the Fock operator in vacuum, f_i is the occupation number of orbital i and b_λ is the population operator that determines the partial charge on site λ in the solute molecule (subscript u). V_λ is obtained as the electrostatic potential on site λ in the solute molecule generated by the atomic charges on the solvent molecules (subscript v):

$$V_{\lambda \in u} = \rho \sum_{\alpha \in v} q_\alpha \int_0^\infty 4\pi r^2 \frac{h_{\lambda\alpha}(r)}{r} dr \quad (10)$$

where $h_{\lambda\alpha}$ is the pair correlation function between site λ on the solute molecule and site α on the solvent molecule. The pair correlation function is determined from the RISM equations.¹⁹ The solvent effect is in this calculation represented by the microscopic distribution of the charges on the solvent molecules. A RISM-SCF calculation begins with deriving solute partial atomic charges from the gas phase electronic structure in a quantum mechanical calculation. From these partial atomic charges the solute-solvent interactions are tabulated. The solvent structure around the solute is then calculated using the RISM equation. The solute electronic structure and partial atomic charges are then recalculated from the solvated Fock operator. These calculations proceed in an iterative cycle until the electronic structure of the solute and solvent distribution converge.

Atomic charges are in the present RISM-SCF calculations represented with MK* charges described in the following section. The solute Lennard-Jones parameters are from the all-atom OPLS force field.^{20,21} The choice was made to use the same Lennard-Jones parameters for the neutral and protonated forms of the amines. The solvent was represented with the TIP3P²² water model. Hydrogen atom sites with zero Lennard-Jones parameters in the OPLS force field are augmented with a small core to facilitate the RISM calculations.⁸ Calculations were performed at 298.15K and a density of 0.997 g/cm³ (0.03334 molecules/Å³). To improve convergence the modified-DIIS method for RISM was utilized.²³ In the present work the RISM equations were solved with the hyper-netted chain (HNC) approximation.²⁴ It should be noted that the use of RISM with the HNC closure produces results that are known to overestimate the effect of solute size on solvation energy.²⁵ In the present work where the focus is on calculating the relative solvation energies this effect is expected to cancel out.

Simulations

Monte Carlo FEP simulations were carried out in a NPT ensemble at 298.15K and 1 atmosphere pressure. These calculations were performed with BOSS version 4.1²⁶ using procedures developed by Jorgensen et al.^{20, 27} A single solute molecule was placed in a periodic cube with 267 TIP4P²² water molecules. Periodic boundary conditions were applied. A number of water molecules corresponding to

the number (n) of non-hydrogen atoms in the amine molecule were removed, giving 267 - n water molecules. The perturbations were carried out over 10 windows of double-wide sampling giving 20 free energy increments that are summed up to give the total change in the free energy of solvation. Each window had 500000 steps for equilibration and another 500000 for sampling. FEPs were used to calculate the relative free energies between neutral species and in a separate series the relative free energies of the protonated forms. Simulations were carried out between the amines closest in size.

The Lennard-Jones potential parameters from the all-atom OPLS force field^{20,21} (same as used for the RISM-SCF calculations) were utilized. These were used together with two different types of charges derived from quantum mechanical calculations. The description of the charges is given in the following section. These simulations are very similar in form to what has been presented by Wiberg et al.,²⁸ the main difference being the choice of routines to calculate the atomic charges.

The simulations, unlike the RISM-SCF calculations, are not deterministic and each perturbation has a statistical uncertainty. This was by the batch means procedure²⁰ determined to be between 0.1 to 0.5 kcal/mol for each simulation. While this uncertainty is significant it will be seen in the results that energy differences are in general larger than these uncertainties.

In the present study the focus is on the description of solute partial atomic charges. The main difference between the RISM-SCF and simulations lies in the schemes to calculate the atomic charges and the use of a polarizable solute representation, in which the energy to polarize the solute is also accounted for, in the RISM-SCF calculations.

Atomic Charges

In the RISM-SCF and the simulations atomic charges are used together with a Lennard-Jones potential both in the solute and solvent representation. Intermolecular energies between molecules a and b are then written in the following well-known form:

$$\Delta E_{ab} = \sum_i^{\text{on a}} \sum_j^{\text{on b}} \left\{ \frac{q_i q_j e^2}{r_{ij}} + 4\epsilon_{ij} \left[\left(\frac{\sigma_{ij}}{r_{ij}} \right)^{12} - \left(\frac{\sigma_{ij}}{r_{ij}} \right)^6 \right] \right\} \quad (11)$$

Where q is the atomic charge, ϵ and σ are the Lennard-Jones potential parameters. In both RISM-SCF calculations and simulation, solute partial atomic charges derived from quantum mechanical calculations were utilized. Atomic charges are not uniquely defined and a number of different schemes for their calculation have been proposed. These are often based on reproducing some form of observable quantities or properties from quantum mechanical calculations. One of the more common schemes is to reproduce the electrostatic potential around the solute. Even for this approach there are however a number of different implementations.²⁹⁻³³ Singh and Kollmann²⁹ developed a procedure based on reproducing the electrostatic potential on gridpoints distributed spherically around each solute atom center, outside the van der Waals volume of the solute. This scheme will in the present work be referred to by its common acronym MK. In the RISM-SCF calculations a procedure similar to the one proposed by Singh and Kollmann is utilized. A grid was set up with nine spherical layers around each atom center. Layers with equal thickness were utilized, the inner having a radius of 1.5 Å and the outer a radius of 2.4 Å. For each layer 36 gridpoints were evenly distributed. Any gridpoints within the van der Waals radii of the solute atoms were disregarded. The atomic charges were then fitted to optimize the agreement, as measured by the mean square error, with the electrostatic potential at these gridpoints. Charges calculated by this procedure will be referred to as MK*. In the first cycle of the RISM-SCF calculation the gas phase charges are calculated, the (converged) solution phase charges are obtained in the final step of the iterative loop.

It has been observed by Besler, Merz and Kollman³⁴ that the Hartree-Fock 6-31G(d) procedure overestimate gas phase dipole moments by 10-20%. The same authors suggest that charges calculated at this level therefore implicitly account for solvation effects. This approach has later been implemented by Cornell et al.³⁵ in a simulation force field. In the RISM-SCF calculation polarization is added to such charges, and there might be a risk of overestimation of polarization in solution.

Simulations were carried out with charges derived from two different schemes. One scheme is reproduction of the electrostatic potential in the gas phase. Here the standard Gaussian 98¹¹ version of the MK²⁹ scheme was utilized. Charges were calculated at the HF/6-31G(d) level. Here gas phase values were chosen. As noted above gas phase Hartree-Fock level charges are believed to be inherently high, and we adopt the approach suggested by Besler et al.³⁴ of using these gas phase charges without modification in solution. Free energy perturbations carried out with the combination of these charges and the OPLS force field will be referred to as FEP-MK.

The second type of charges utilized in the simulations is CM2³⁶ charges calculated at the HF/6-31G(d) level. While this model is also based on the quantum mechanical description of the solute, it involves semi-empirical corrections to reproduce experimental gas phase dipole moments. With the CM2 charges there is no implicit polarization present, and the charges should be adjusted to the levels one would expect in solution. Here we chose to do the calculations with a continuum solvent model to obtain solution phase charges. CM2 charges were therefore calculated with the SM 5.42R solvent field model³⁷ in Gamesol.³⁸ Free energy perturbations carried out with the combination of these charges and the OPLS force field will be referred to as FEP-CM2.

While atomic charges are not uniquely defined some criteria have been presented for when they can be considered reasonable.^{32, 33} In the present work the purpose is to calculate solvation energies and in this context we argue that the best charges are those that produce free energies of solvation closest to experimental values. Charges should also take on values that are not unreasonably large and should reflect molecular symmetry.

Molecules

In Figure 1 are shown the amine molecules studied. The purpose of the present study was to look at how RISM-SCF and simulations perform in general prediction of solvation energies. The set of amines was therefore chosen to include varied forms of molecular geometry. A second consideration in selecting the amines has been to use molecules for which experimental gas phase and solution phase

basicity data are available. No gas phase value has however been reported for 2,2,6,6-Tetramethyl-4-piperidinol (TMP). Finally the set has been limited to molecules with no conformers or known conformers (piperazine). For piperazine calculations have been done on the chair-conformer.

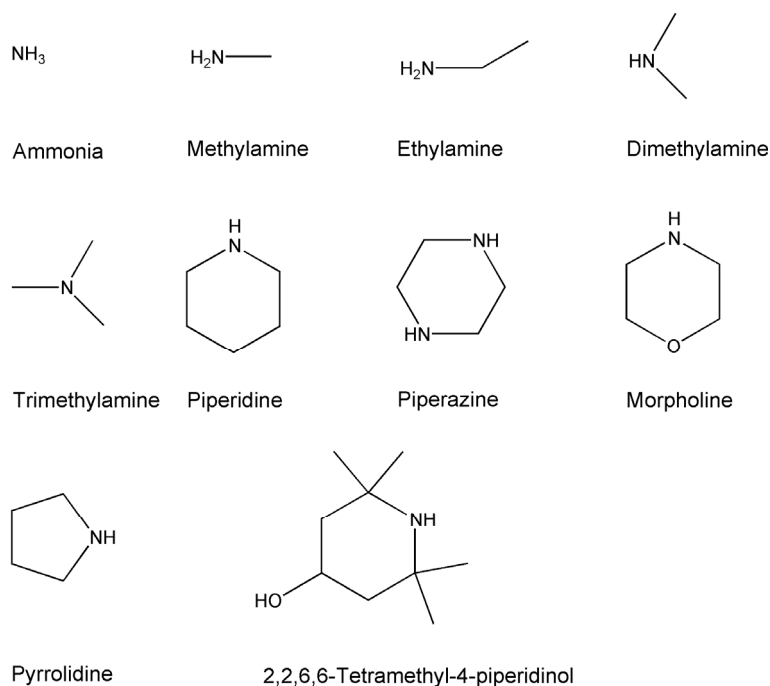


Figure 1. Amine molecules studied.

Results

In Table 1 calculated and experimental gas phase basicity for the amines are shown. All data are given relative to ammonia, a convention that will be used for all basicity results presented. While neither experimental nor calculated gas phase basicities are likely to be completely accurate, the agreement between the data offers a level of mutual validation. While no experimental data is available for TMP, the agreement between theoretical and experimental results for the other molecules would suggest that the level of theory is adequate for this molecule too. It should be noted that the present values differ significantly from what have been used in previous studies^{13,14} on ammonia, methylamine, dimethylamine and trimethylamine. The present values are in better agreement with currently accepted experimental values (Table 1) and are likely to be the more accurate.

Table 1. Relative Gas Phase Protonation Energies. Data in [kcal/mol].

Molecule	Theoretical ^a	Experimental ^b
Ammonia	0.0	0.0
Methylamine	10.2	10.9
Ethylamine	14.3	14.1
Dimethylamine	17.9	18.5
Trimethylamine	22.2	23.7
Piperidine	24.2	24.4
Piperazine	23.3	22.9
Morpholine	17.0	17.3
Pyrrolidine	23.6	23.0
2,2,6,6-Tetramethyl-4-piperidinol (TMP)	29.7	

^a B3LYP/6-311++G(d,p) energy with thermal correction and ZPE calculated at HF/6-31G(d), TMP data are from present work, other data from da Silva.¹¹ ^b Data from Hunter and Lias.³⁹

In Table 2 the atomic charges of the amine functionalities for the neutral amines are given and in Table 3 data for the protonated forms are given. MK* charges are given both for gas phase and solution (from RISM-SCF calculation). MK charges are in gas phase and CM2 charges are in solution (SM 5.42R solvation model). These are the same form of the charges as utilized in the energy calculations. The MK* gas phase charges are however only used as a starting point for the RISM-SCF calculations.

Table 2. Partial Atomic Charges of Neutral Amines.

Molecule	MK*		MK*		MK		CM2	
	gas phase		solution ^a		gas phase		solution ^b	
	N	H ^c	N	H ^c	N	H ^c	N	H ^c
Ammonia	-1.02	0.34	-1.28	0.43	-1.11	0.37	-0.86	0.29
Methylamine	-1.01	0.35	-1.18	0.45	-1.03	0.38	-0.75	0.33
Ethylamine	-1.02	0.35	-1.33	0.46	-1.06	0.37	-0.72	0.32
Dimethylamine	-0.75	0.35	-0.96	0.44	-0.72	0.38	-0.55	0.28
Trimethylamine	-0.41	----	-0.55	----	-0.23	----	-0.41	----
Piperidine	-0.83	0.37	-1.17	0.52	-0.80	0.36	-0.54	0.28
Piperazine(1)	-0.73	0.34	-0.94	0.43	-0.74	0.37	-0.53	0.27
Piperazine(2)	-0.80	0.36	-1.07	0.47	-0.75	0.39	-0.54	0.28
Morpholine	-0.82	0.38	-1.16	0.53	-0.77	0.37	-0.54	0.28
Pyrrolidine	-0.81	0.30	-0.98	0.45	-0.75	0.35	-0.53	0.33
TMP	-1.14	0.37	-1.67	0.52	-1.06	0.38	-0.52	0.35

^a RISM-SCF method. ^b SM 5.42R solvation model. ^c Amine functionality hydrogen atoms, average value for amine group with more than one hydrogen atom.

Table 3. Partial Atomic Charges of Protonated Amines.

Molecule	MK*		MK*		MK		CM2	
	gas phase		solution ^a		gas phase		solution ^b	
	N	H ^c	N	H ^c	N	H ^c	N	H ^c
Ammonia	-0.78	0.44	-0.81	0.45	-0.87	0.47	-0.52	0.38
Methylamine	-0.21	0.31	-0.26	0.33	-0.30	0.32	-0.44	0.37
Ethylamine	-0.65	0.39	-0.72	0.43	-0.69	0.40	-0.69	0.40
Dimethylamine	-0.05	0.29	-0.06	0.33	-0.05	0.30	-0.34	0.35
Trimethylamine	0.17	0.31	0.14	0.37	0.08	0.34	-0.25	0.34
Piperidine	-0.25	0.31	-0.29	0.35	-0.28	0.32	-0.32	0.35
Piperazine(1) ^d	-0.23	0.33	-0.32	0.39	-0.22	0.33	-0.32	0.35
Piperazine(2)	-0.83	0.42	-1.09	0.52	-0.81	0.42	-0.53	0.29
Morpholine	-0.24	0.32	-0.33	0.38	-0.32	0.36	-0.32	0.36
Pyrrolidine	-0.23	0.30	-0.28	0.35	-0.34	0.33	-0.53	0.33
TMP	-0.13	0.22	-0.31	0.31	-0.93	0.45	-0.34	0.34

^a RISM-SCF method. ^b SM 5.42R solvation model. ^c Amine functionality hydrogen atoms, average value for amine group with more than one hydrogen atom. ^d Protonated site.

It can be observed that in the RISM-SCF results polarization is significantly higher for the neutral (unprotonated) amines than for the protonated forms. For the neutral species charges on the amine functionalities can be seen to increase with 20-40% over the gas phase values, while the increase for the protonated forms are around 10-20%. The same observation was made in previous RISM-SCF work.¹³ It was in that work suggested that this was caused by the (uncharged) amines producing an anisotropic field in the solvent, which again causes an anisotropic reaction field on the solute giving additional electrical polarization. The protonated amines will on the other hand produce a more isotropic field and the same effect will not be seen. Most of the amines show comparable level of increases in charges in solution, but particularly large increases can be observed for neutral (uncharged) TMP, piperidine and morpholine. For TMP the value would appear to be greater than what can be considered physically reasonable.

The amine functionalities and their representation are expected to be the most important in determining the solvation behavior of the molecules. Some observations will however be made on the other charges, the full set of data is given in the supporting information.

In most cases neutral amine gas phase MK* and MK were in reasonable agreement. Carbon charges were mostly in a range between 0 to 0.4, while hydrogen charges were close to zero. For trimethylamine the average MK carbon charge was however -0.29 while the average MK* value was 0.07. In some cases MK and MK* charges took on unreasonable high values. For TMP the MK carbon charges varied between 0.87 and -0.53, while the MK* charges varied between 0.88 and -0.41. In most cases MK and MK* charges were quite similar for atoms in symmetrically equivalent positions. Both MK and MK* charges were however somewhat different for carbons in equivalent positions in morpholine.

The CM2 charges for the alkane functionalities were much more stable, reflecting the different nature of the model. Carbon charges stayed mostly in a range of 0 to -0.3 for neutral amines. Alkane-hydrogens mostly had charges around 0.1. The CM2 charges did in general display values that would appear not to be unreasonable in terms of the dimension of the charges.

In summary it can be observed that MK* and MK charges are quite similar, which is reassuring since they are only variations of fittings to the same electrostatic potential. The trends in charges for different molecules would seem to be similar for the MK and CM2 charges. The CM2 charges are however systematically lower than the MK charges, despite the fact that CM2 charges have been scaled up from their gas phase values with the use of a continuum model. The MK/MK* charges also tend to fluctuate more than the CM2 charges, this being particularly true for *sp*³ carbon atoms.

In Table 4 the relative solvation energies are shown, while in Table 5 the experimental p*K*_a values and relative basicity in solution calculated from these are shown together with the basicity in solution derived from RISM-SCF and simulations.

Table 4. Total Relative Solvation Energy Contribution. Data in [kcal/mol].

Molecule	$\Delta\Delta G_s(B) - \Delta\Delta G_s(BH^+)$		
	RISM-SCF	FEP-MK	FEP-CM2
Ammonia	0	0.0	0.0
Methylamine	-8.7	-10.4	-8.2
Ethylamine	-9.3	-12.0	-9.1
Dimethylamine	-14.0	-14.6	-14.8
Trimethylamine	-17.4	-18.3	-22.4
Piperidine	-23.7	-23.0	-17.9
Piperazine	-19.3	-21.6	-17.2
Morpholine	-19.3	-15.2	-14.4
Pyrrolidine	-18.5	-18.4	-20.9
TMP	-33.2	-21.1	-24.0

Table 5. Relative Basicity in solution. Data in [kcal/mol].

Molecule	exptl pK_a	$\Delta\Delta G_{ps}^a$			
		exptl	RISM-SCF	FEP-MK	FEP-CM2
Ammonia	9.24 ^b	0.00	0.0	0.0	0.0
Methylamine	10.65 ^b	1.92	1.5	-0.2	2.1
Ethylamine	10.78 ^b	2.10	5.0	2.3	5.3
Dimethylamine	10.8 ^b	2.13	3.9	3.3	3.1
Trimethylamine	9.80 ^b	0.90	4.8	3.9	-0.2
Piperidine	11.12 ^c	2.56	0.5	1.2	6.3
Piperazine	9.83 ^c	0.80	4.0	1.7	6.1
Morpholine	8.49 ^c	-1.02	-2.3	1.7	2.6
Pyrrolidine	11.30 ^c	2.81	5.1	5.2	2.7
TMP	10.05 ^c	1.10	-3.5	8.6	5.7

^a Energies relative to ammonia. ^b Data from Jones and Arnett.¹⁰ ^c Data from Perrin.⁴⁰

In Figure 2 the calculated gas phase basicities are plotted against the experimental pK_a of the amines, the low correlation in this plot shows how important the solvation energies are in determining basicity in solution. In Figure 3 the relative pK_a values calculated from RISM-SCF and FEP-MK are plotted against the experimental pK_a . In Figure 4 the pK_a values determined from FEP-MK and FEP-CM2 are plotted against experimental pK_a . The stippled line in the figures indicates the theoretical ratio between pK_a and protonation energy from equation 5. All data are relative to ammonia.

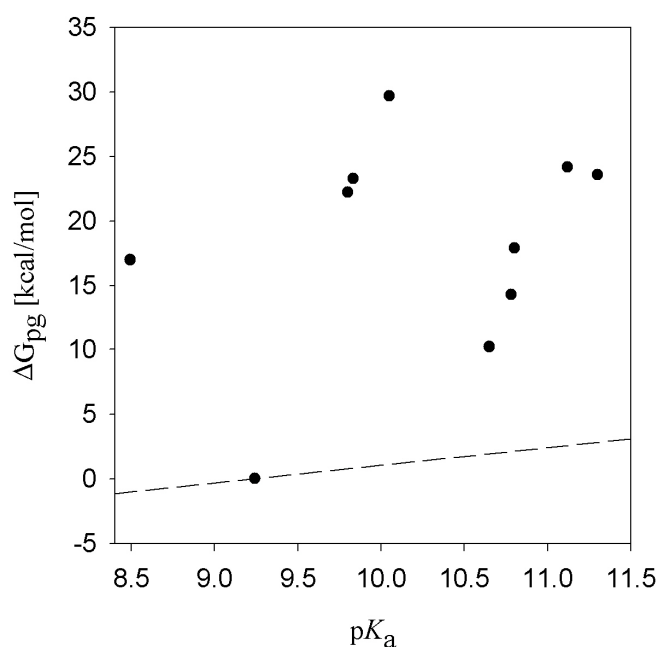


Figure 2. Calculated gas phase basicity versus experimental pK_a . The stippled line indicates the theoretical trend relative to ammonia.

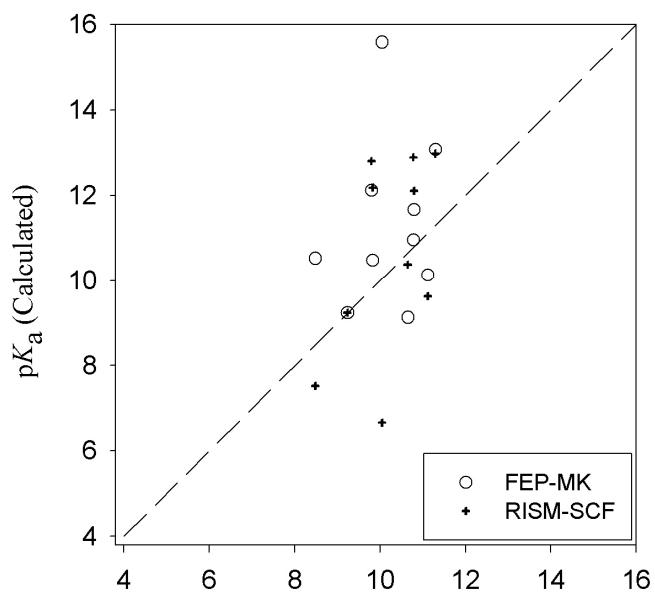


Figure 3. Calculated pK_a versus experimental pK_a . Crosshairs are RISM-SCF and Open circles are FEP-MK. The stippled line indicates the theoretical trend relative to ammonia.

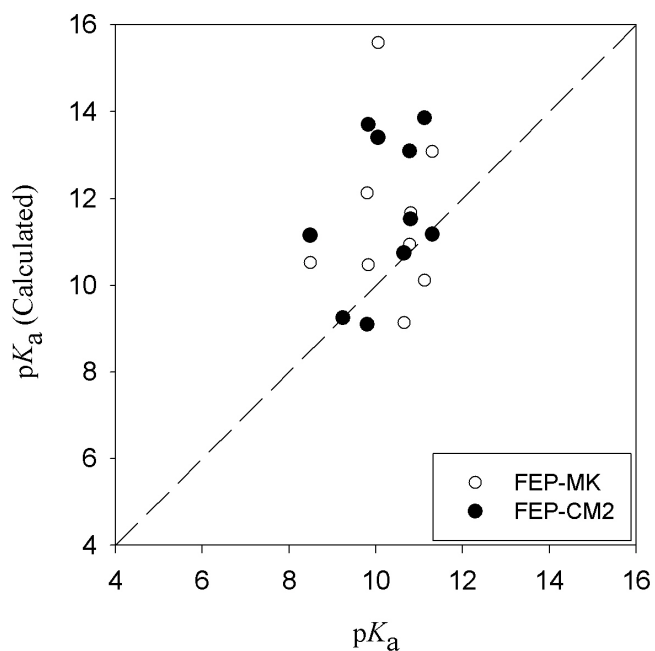


Figure 4. Calculated pK_a versus experimental pK_a . Open circles are FEP-MK and black circles are FEP-CM2. The stippled line indicates the theoretical trend relative to ammonia.

In Figure 5 the contributions to the RISM-SCF solvation energy are shown together with the FEP-MK solvation energies. The contributions to the RISM-SCF solvation energy are the solute polarization and excess chemical potential from interactions with the solvent. The plot shows the solute polarization to have a relatively small, but significant, effect on relative solvation energies. The figure also illustrates the good overall agreement between RISM-SCF and FEP-MK solvation energies.

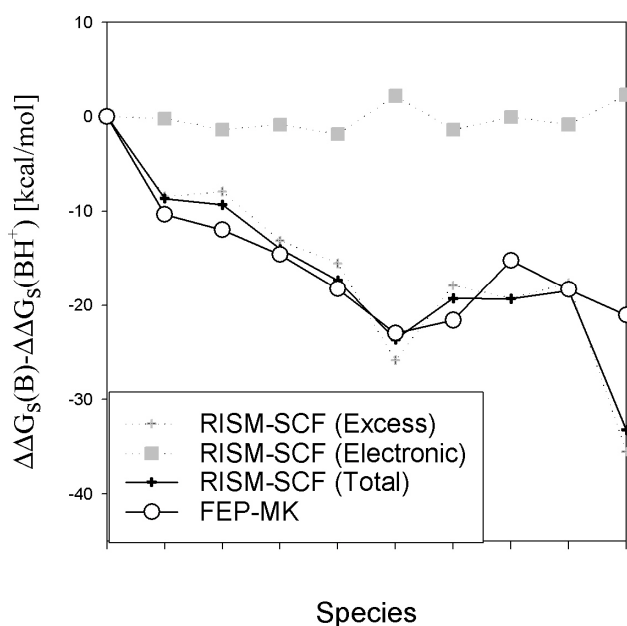


Figure 5. Contributions to RISM-SCF solvation energies. RISM-SCF (Electronic) refers to the solute polarization energy. RISM-SCF (Excess) refers to the excess chemical potential from interactions with the solvent.

Discussion

Basicity

Looking at Figures 3 and 4 it can be seen that neither RISM-SCF nor simulations produce full quantitative agreement with experimental data. Comparing the solvation models results with the gas phase energies in Figure 2 it can however be seen that the large gap between relative energies in the gas phase and solution is closed. It must also be kept in mind that this set of amines contains large variations in geometry and that the experimental energy differences to be reproduced are relatively small.

The RISM-SCF results are mostly in reasonable agreement with the experimental data. The largest error was for TMP. As noted in the Results section the MK* charges for this molecule were very high. These charges are most likely the cause of the inaccurate solvation energies.

The present results differ somewhat from previous RISM-SCF results¹³ for ammonia, methylamine, dimethylamine and trimethylamine. This is due to changes in the scheme to calculate atomic charges, illustrating the sensitivity of the results to the choice of scheme.

The FEP-MK simulations and RISM-SCF calculations utilize similar charges, same Lennard-Jones potential and similar solvent representation (TIP4P and TIP3P respectively). The agreement between the results (Figure 3 and Figure 5) is consistent with the underlying similarities in solute and solvent representation. For TMP the FEP-MK results and RISM-SCF results differ strongly from each other and neither is close to the experimental value. In this case the MK and MK* charges were quite different, both taking on unreasonable values. For morpholine the RISM-SCF result was in better agreement with the experimental data than the FEP-MK result. This difference is probably due to the increase of solute charges from solvent polarization in the RISM-SCF model. In this particular case this contribution would appear to be necessary to predict the basicity relative to ammonia.

The FEP-MK and FEP-CM2 simulations only differ in the scheme to calculate atomic charges. Comparing the two sets of results in Figure 4 one can see that the choice of scheme for calculating atomic charges has a considerable effect on the solvation energies.

Some previous studies^{13,14} have looked at the irregular trend in basicity for the series ammonia, methylamine, dimethylamine and trimethylamine. Both the RISM-SCF and simulations give a decreasing trend in solvation energy of the protonated forms of these amines and stable values for the neutral forms. If this trend in the solvation energies is taken together with the increasing trend in gas phase basicities the irregular order in basicity is readily accounted for. The models can therefore be said to capture this in a qualitative sense. At a quantitative level none of the models is however accurate enough to confidently reproduce the small energy differences involved.

Atomic Charges

It can clearly be seen from the results, both for RISM-SCF and simulations, that the free energies are sensitive to the scheme for calculating atomic charges. Some examples are also seen in the present study of MK and MK* charges taking on unphysical values resulting in unreasonable solvation energies. This is related to a known issue⁴¹ with fitting charges to the electrostatic potential: if an atomic center is far away from the grid points in the fitting its value becomes ill-determined and the charges can fluctuate dramatically without significantly altering the quality of the fit. This is often the case for *sp*³-carbons, in the fitting they can become buried behind the atoms they are bonded to. In the present work the problem was particularly large for TMP. This is not surprising given the structure of the molecule. Because of the methyl substituents there are few gridpoints close to the amine functionality. Several atoms are almost completely buried. This can result in charges that fluctuate widely. In the RISM-SCF calculations polarization effects are added and ill-determined charges can fluctuate even more.

It has been suggested that this problem can be handled by adding constraints on the fitting. In the RESP⁴¹ procedure the carbon-charges are constrained. This approach should resolve some of the problems seen in the present work, but further work is perhaps needed to determine what are the best constraining conditions for free energy calculations. A hybridization between fitting to the electrostatic potential and semi-empirical corrections to reproduce different properties has also been proposed.⁴² Another modification that might improve the fitting is to include Boltzmann-weighting of the points

being fitted.³² It is clear that fitting atomic charges to the electrostatic potential is difficult and with the scheme used in the present work not entirely reliable. The proposals to improve the fitting schemes do however suggest that this approach to determine atomic charges can be developed further.

As noted in the Methods section the addition of solvent polarization to already high Hartree-Fock level charges in the RISM-SCF calculations might result in too high charges. In future work the RISM-SCF calculations should perhaps be performed at another level of theory or with some form of scaling of charges to correct for the overestimation.

RISM-SCF

Improvement of the schemes to calculate the atomic charges are likely to lead to a more accurate RISM-SCF model. Work has also been done on directly calculating the interaction between solvent molecules and the electrostatic field of the solute,⁴² an approach that eliminates the task of determining atomic charges.

One important approximation in the present work, and most simulations, is the use of a solvent model with fixed charges. It has been suggested⁴⁴ that introduction of polarizable solvent models have a significant effect on solvation energies. This is an issue that should be explored further.

All together this would suggest that there is room for further refinement of the RISM-SCF method to produce a general and accurate solvation model. It should also be noted that the present implementation of RISM-SCF is fairly robust in terms of convergence.

Simulations

As with the RISM-SCF calculations the main issue with the simulations is the calculation of atomic charges. In the simulations it is however less clear how polarization effects should be incorporated. In the present work a continuum model and inherently high Hartree-Fock level charges have been used to obtain charges in solution. In the literature other schemes can also be found such as scaling up gas phase values and calculating the polarization from the average electrostatic potential of the solvent in

QM/MM simulations.⁴⁵ Charges derived from RISM-SCF calculations could also be an interesting option in simulations, particularly as they are derived in the context of the same solvent representation. The choice of scheme to calculate charges is clearly of great importance and is likely to remain an area of active research.

In RISM-SCF the charges include polarization effects and the energy to polarize the solute is included when determining the solvation. It remains to be determined if and how this contribution should be accounted for in simulations.

Conclusions

In the present work RISM-SCF and simulations have been used to calculate the relative basicity of a series of 10 amine molecules. Results showed mostly reasonable agreement between experimental data and calculated values. The results were however found to be sensitive to the scheme for calculation of atomic charges. None of the methods used for determining charges in the present work were found to be completely satisfactory. There would however appear to be a number of ways in which such schemes can be improved upon. Comparison between results with (RISM-SCF) and without (simulations) polarizable solute representation suggests that polarization can have a significant effect on relative solvation energies.

Acknowledgment

Gratitude is expressed to the Japan-Norway Sasakawa foundation for supporting a visit by Eirik F. da Silva to the Institute for Molecular Science.

Supporting Information Available:

Atomic charges for alkane and alcohol groups, Lennard-Jones force field parameters and data utilized in Figure 5 are given in the supporting information. This material is available free of charge via the Internet at <http://pubs.acs.org>.

References

- 1 Cramer, C. J. *Essentials of Computational Chemistry*, John Wiley & Sons, 2002.
- 2 Orozco, M.; Javier Luque, F. *Chem. Rev.* 2000, 100, 4187.
- 3 Tomasi, J.; Menucci, B.; Cammi, R. In *Handbook of Molecular Physics and Quantum chemistry* Wilson, S. Ed.; Volume 3, John Wiley & Sons, 2002, 299.
- 4 Bacskay, G. B.; Reimers, J. R. In *Encyclopedia of computational chemistry*, Schleyer, P. R. Ed.; John Wiley & Sons, 1998, 2620.
- 5 Cramer, C. J.; Truhlar, D. G. *Chem. Rev.* 1999, 99, 2161.
- 6 Tomasi, J.; Persico, M. *Chem. Rev.* 1994, 94, 2027.
- 7 Ten-no, S.; Hirata, F.; Kato, S. *Chem. Phys Lett.*, 1993, 214, 391.
- 8 Ten-no, S.; Hirata, F.; Kato, S. *J. Chem. Phys.* 1994, 100, 7443.
- 9 Hirata, F. Ed. *Molecular Theory of Solution*, Kluwer Academic Publishers, 2003.
- 10 Jones, F. M.; Arnett, E. M. *Prog. Phys. Org. Chem.* 1974, 11, 263.
- 11 da Silva, E. F. *J. Phys. Chem. A*, 2005, 109, 1603.
- 12 M. J. Frisch, G. W. Trucks, H. B. Schlegel, G. E. Scuseria, M. A. Robb, J. R. Cheeseman, V. G. Zakrzewski, J. A. Montgomery, Jr., R. E. Stratmann, J. C. Burant, S. Dapprich, J. M. Millam, A. D. Daniels, K. N. Kudin, M. C. Strain, O. Farkas, J. Tomasi, V. Barone, M. Cossi, R. Cammi, B. Mennucci, C. Pomelli, C. Adamo, S. Clifford, J. Ochterski, G. A. Petersson, P. Y. Ayala, Q. Cui, K. Morokuma, D. K. Malick, A. D. Rabuck, K. Raghavachari, J. B. Foresman, J. Cioslowski, J. V. Ortiz, A. G. Baboul, B. B. Stefanov, G. Liu, A. Liashenko, P. Piskorz, I. Komaromi, R. Gomperts, R. L. Martin, D. J. Fox, T. Keith, M. A. Al-Laham, C. Y. Peng, A. Nanayakkara, M. Challacombe, P. M. W. Gill, B. Johnson, W. Chen, M. W. Wong, J.

- L. Andres, C. Gonzalez, M. Head-Gordon, E. S. Replogle, and J. A. Pople, Gaussian 98, Revision A.9, Gaussian, Inc., Pittsburgh PA, 1998.
- 13 Kawata, M.; Ten-no, S.; Kato, S.; Hirata, F. *Chem. Phys.*, 1996, 203, 53.
- 14 Tunon, I.; Silla, E. Tomasi, J. *J. Phys. Chem.*, 1992, 96, 9043.
- 15 Liptak, M. D.; Gross, K. C.; Seybold, P. G.; Feldgus, S.; Shields, G. C. *J. Am. Chem. Soc.* 2002, 124, 6421.
- 16 Chandler, D.; Andersen, H. C. *J. Chem. Phys.* 1972, 57, 1930.
- 17 Sato, H.; Hirata, F.; Kato, S. *J. Chem. Phys.* 1996, 105, 1546.
- 18 Singer, S. J.; Chandler, D. *Mol. Phys.* 1985, 55, 621.
- 19 Hirata, F.; Rossky, P. J.; Pettitt, B. M. *J. Chem. Phys.* 1983, 78, 4133.
- 20 Rizzo, R. C.; Jorgensen, W. L. *J. Am. Chem. Soc.* 1999, 121, 4827.
- 21 Jorgensen, W. L.; Maxwell, D. S.; Tirado-Rives, J. *J. Am. Chem. Soc.* 1996, 118, 11225.
- 22 Jorgensen, W. L.; Chandrasekhar, J.; Madura, J. D.; Impey, R. W.; Klein, M. L. *J. Chem. Phys.* 1983 79, 926.
- 23 Kovalenko, A. Ten-No, F.; Hirata, F. *J. Comp. Chem.* 1999, 20, 928.
- 24 Hansen, J. P.; McDonald, I. R. *Theory of Simple Liquids*, AP Academic Press, 1986.
- 25 Kovalenko, A.; Hirata, F. *J. Chem. Phys.* 2000, 113, 2793.
- 26 Jorgensen, W.L. BOSS version 4.3, Yale University, New Haven, CT(1989a)
- 27 Jorgensen, W. L.; Ravimohan, C. *J. Chem. Phys.* 1985, 83, 3050.
- 28 Wiberg, K. B.; Clifford, S.; Jorgensen, W. L.; Frisch, M. J. *J. Phys. Chem. A* 2000, 104, 7625.

- 29 Singh, U. C.; Kollman, P. A. *J. Comp. Chem.* 1984, 5, 129.
- 30 Chirlian, L. E.; Franckl, M. M. *J. Comp Chem.* 1987, 8, 894.
- 31 Breneman, C. M.; Wiberg, K. B. *J. Comp. Chem.* 1990, 11, 361.
- 32 Sigfridsson, E.; Ryde, U. *J. Comp. Chem.* 1998, 19, 377.
- 33 Franckl, M. M.; Chirlian, L. In *Reviews in Computational Chemistry* Lipkowitz, K. B.; Boyd, D. B.; Ed.; Volume 14, Wiley-VCH, 2000, 1.
- 34 Besler, B. H.; Merz, K. M.; Kollman, P. A. *J. Comp. Chem.* 1990, 11, 431.
- 35 Cornell, W. L.; Cieplak, P.; Bayly, C. I.; Gould, I. R.; Merz, K. M.; Ferguson, D. M.; Spellmeyer, D. C.; Fox, T.; Caldwell, J. W.; Kollman, P. A. *J. Am. Chem. Soc.* 1995, 117, 5179.
- 36 Li, J.; Zhu, T.; Cramer, C. J.; Truhlar, D. G. *J. Phys. Chem. A* 1998, 102, 1820.
- 37 Hawkins, G. D.; Zhu, T.; Li, J.; Chambers, C. C.; Giesen, D. J.; Liotard, D. A.; Cramer, C. J.; Truhlar, D. G. *Universal Solvation Models in Combined Quantum Mechanical and Molecular Mechanical Methods*, Gao, J.; Thompson, M. A. Eds. American Chemical Society: Washington DC, 1998, 201.
- 38 Xidos, J.D.; Li, J.; Zhu, T.; Hawkins, G. D.; Thompson, J. D.; Chuang, Y.-Y.; Fast, P. L.; Liotard, D. A.; Rinaldi, D.; Cramer, C. J.; Truhlar, D. G. *Gamesol-version 3.1*, University of Minnesota, Minneapolis 2002, based on the General Atomic and Molecular Electronic Structure System (GAMESS) as described in Schmidt, M. W.; Baldridge, K. K.; Boatz, J. A.; Elbert, S. T.; Gordon, M. S.; Jensen, J. H.; Koseki, S.; Matsunaga, N.; Nguyen, K. A.; Su, S. J.; Windus, T. L.; Dupuis, M.; Montgomery, J. A. *J. Comp. Chem.* 1993, 14, 1347.
- 39 Hunter, E. P.; Lias, S.G.; *Proton Affinity Evaluation*, National Institute of Standards and Technology, Gaithersburg, MD, 2003, <http://webbook.nist.gov>.

- 40 Perrin, D. D. *Dissociation Constants of Organic Bases in Aqueous Solution*. Butterworths, London, 1965; Supplement, 1972.
- 41 Bayly, C. I.; Cieplak, P.; Cornell, W. D.; Kollman, P. A. *J. Phys. Chem.* 1993, 97, 10269.
- 42 Jakalian, A.; Jack, D. B.; Bayly, C. I. *J. Comp. Chem.* 2002, 23, 1623.
- 43 Sato, H.; Kovalenko, A.; Hirata, F. *J. Chem. Phys.* 2000, 112, 9463.
- 44 Meng, E. C.; Cieplak, P.; Caldwell, J. W.; Kollman, P. A. *J. Am. Chem. Soc.* 1994, 116, 12061.
- 45 Gao, J.; Luque, F. J.; Orozco, M. *J. Chem. Phys.* 1993, 98, 2975.

Appendix 1

OPLS Lennard Jones Parameters

	[Å]	[kcal/mol]	q electron units
N-Amine	3.3	0.17	
N-Ammonia	3.42	0.17	
H(N)-Amine	0.0 (1.0) ^a	0.0 (0.056) ^a	
C-Carbon	3.5	0.066	
H(C(N))-Hydrogen on carbon bonded to amine	2.5	0.015	
H(C) Alkane	2.5	0.030	
O-Alcohol	3.12	0.17	
H(O) Alcohol	0.0 (1.0) ^a	0.0 (0.056) ^a	
O-Morpholine	2.9	0.14	
O-TIP3P	3.15061	0.1521	-0.834
H-TIP3P	0.0 (1.0) ^a	0.0 (0.015) ^a	0.417
O-TIP4P	3.15365	0.155	0.0
H-TIP4P	0.0	0.0	0.52
M-TIP4P	0.0	0.0	-1.040

^a Parameters utilized in RISM-SCF calculations that differ from the standard values are given in parenthesis.

Appendix 2

Partial Atomic Charges of Alkane and Oxygen/Alcohol in Neutral Amines

Molecule site ^a	MK*		MK*		MK		CM2	
	gas phase		solution ^b		gas phase		solution ^c	
	C/O ^d	H ^d	C/O ^d	H ^d	C/O ^d	H ^d	C/O ^d	H ^d
Methylamine-C	0.58	-0.09	0.69	-0.10	0.38	-0.04	-0.35	0.15
Ethylamine-C1	0.58	-0.07	0.69	-0.07	0.54	-0.06	-0.22	0.14
Ethylamine-C2	-0.27	0.07	-0.36	0.08	-0.33	0.08	-0.43	0.15
Dimethylamine-C	0.23	-0.02	0.26	0.00	0.05	0.04	-0.10	0.08
Trimethylamine-C	0.07	0.03	0.07	0.04	-0.29	0.12	-0.10	0.08
Piperidine-C1,C5	0.24	0.01	0.27	0.04	0.20	0.01	-0.01	0.09
Piperidine-C2, C4	-0.12	0.03	-0.23	0.07	-0.13	0.01	-0.16	0.09
Piperidine-C3	0.12	-0.01	0.13	0.00	0.11	0.02	-0.16	0.09
Piperazine-C2, C5	0.21	-0.02	0.23	0.00	0.00	0.06	-0.19	0.08
Piperazine-C3, C4	0.27	-0.03	0.35	-0.02	0.12	0.06	-0.20	0.08
Morpholine-C2	0.21	0.00	0.25	0.04	0.12	0.04	-0.02	0.08
Morpholine-C5	0.27	-0.01	0.33	0.02	0.20	0.02	-0.02	0.08
Morpholine- C3, C4	0.10	0.04	0.07	0.07	0.06	0.07	0.00	0.08
Morpholine-O	-0.41		-0.52		-0.40		-0.33	
Pyrrolidine-C1	0.26	-0.03	0.25	0.00	0.16	0.01	-0.20	0.14
Pyrrolidine-C4	0.26	-0.03	0.25	0.00	0.22	0.00	-0.20	0.14
Pyrrolidine-C2	0.03	-0.01	0.01	0.00	-0.04	0.03	-0.28	0.15
Pyrrolidine-C3	0.03	-0.01	0.01	0.00	-0.08	0.03	-0.28	0.15
TMP-C1,C5	0.88		1.15		0.82		0.13	
TMP-C2,C4	-0.37	0.06	-0.39	0.05	-0.44	0.11	-0.16	0.08
TMP-C3	0.69	-0.13	0.72	-0.11	0.59	0.02	0.07	0.08
TMP-CH ₃	-0.41	0.08	-0.42	0.07	-0.53	0.11	-0.25	0.08
TMP-O	-0.70	0.42	-0.90	0.51	-0.75	0.43	-0.49	0.27

^a For symmetric sites average charges are given except when they diverge significantly. The carbon given the number 1 is bonded to the amine, the carbon bonded to C1 is given the number C2 and so on.

^b RISM-SCF method. ^c SM 5.42R solvation model. ^d Average value in case of more than atom.

Partial Atomic Charges of Alkane and Oxygen/Alcohol in Protonated Amines

Molecule ^a	MK*		MK*		MK		CM2	
	gas phase		solution ^b		gas phase		solution ^c	
	C/O ^d	H ^d	C/O ^d	H ^d	C/O ^d	H ^d	C/O ^d	H ^d
Methylamine-C	-0.14	0.14	-0.13	0.13	-0.02	0.11	-0.09	0.14
Ethylamine-C1	0.42	0.06	0.57	0.02	-0.22	0.26	-0.19	0.20
Ethylamine-C2	-0.84	0.26	-1.07	0.30	-0.52	0.22	-0.43	0.17
Dimethylamine-C	-0.23	0.15	-0.23	0.14	-0.37	0.26	-0.09	0.20
Trimethylamine-C	-0.32	0.17	-0.33	0.16	-0.35	0.25	-0.10	0.13
Piperidine-C1,C5	0.04	0.08	0.06	0.08	0.01	0.10	-0.01	0.11
Piperidine-C2, C4	-0.03	0.05	-0.03	0.04	-0.08	0.07	-0.01	0.11
Piperidine-C3	0.01	0.03	0.02	0.02	-0.04	0.06	-0.01	0.13
Piperazine-C2, C5	-0.12	0.13	-0.14	0.14	-0.13	0.14	-0.16	0.16
Piperazine-C3, C4	0.22	0.05	0.28	0.06	0.19	0.07	-0.15	0.15
Morpholine-C2	-0.07	0.12	-0.01	0.11	0.12	0.14	-0.02	0.14
Morpholine-C5	-0.07	0.12	-0.01	0.11	-0.11	0.10	-0.02	0.14
Morpholine-C3	0.19	0.07	0.22	0.07	-0.08	0.13	-0.01	0.10
Morpholine-C4	0.19	0.07	0.22	0.07	0.14	0.10	-0.01	0.10
Morpholine-O	-0.41		-0.53		-0.41		-0.33	
Pyrrolidine-C1,C4	0.06	0.08	0.09	0.08	0.08	0.08	-0.17	0.26
Pyrrolidine-C2,C3	-0.04	0.07	-0.07	0.06	-0.03	0.06	-0.27	0.23
TMP-C1,C5	0.45		0.61		0.66		0.14	
TMP-C2,C4	-0.34	0.11	-0.39	0.11	-0.50	0.16	-0.16	0.10
TMP-C3	0.50	-0.04	0.61	-0.04	0.58	0.06	0.06	0.09
TMP-CH3	-0.44	0.13	-0.50	0.13	-0.56	0.16	-0.26	0.11
TMP-O	-0.69	0.44	-0.85	0.51	-0.71	0.45	-0.48	0.35

^a For symmetric sites average charges are given except when they diverge significantly. The carbon given the number 1 is bonded to the amine, the carbon bonded to C1 is given the number C2 and so on.

^b RISM-SCF method. ^c SM 5.42R solvation model. ^d Average value in case of more than atom.

Appendix 3

RISM-SCF Relative Solvation Energy Contributions. Data in [kcal/mol].

	excess chemical potential	solute polarization energy
Ammonia	0.00	0.00
Methylamine	-8.46	-0.21
Ethylamine	-7.94	-1.38
Dimethylamine	-13.14	-0.85
Trimethylamine	-15.53	-1.82
Piperidine	-25.84	2.19
Piperazine	-17.90	-1.39
Morpholine	-19.29	-0.04
Pyrrolidine	-17.65	-0.84
TMP	-35.52	2.30